Dissertation zur Erlangung des Doktorgrades

der Fakultät für Chemie und Pharmazie

der Ludwig-Maximilians-Universität München

Water-based Spider Silk Films

Elisa Agostini

aus

Trient, Italien

2017

Erklärung

Diese Dissertation wurde im Sinne von §7 der Promotionsordnung vom 01. Dezember 2010 von Herrn Prof. Dr. Gerhard Winter betreut.

Eidesstattliche Versicherung

Diese Dissertation wurde eigenständig und ohne unerlaubte Hilfe erarbeitet.

München, 03/05/2017

…….

Elisa Agostini

Dissertation eingereicht am: 03/05/2017

1. Gutachter: Prof. Dr. Gerhard Winter

2. Gutachter: PD Dr. Julia Engert

Mündliche Prüfung am: 02/06/2017

Ai miei amati Genitori

"Many times an obstacle is only a message. You need to find another way,

it doesn´t mean that you won't achieve your goal"

- *Samantha Cristoforetti*

Astronaut, Air Force pilot, engineer, first Italian woman in space, record longest single space flight by a woman, *first person who made an espresso coffee in space*

ACKNOWLEDGMENTS

Prof. Dr. Winter is here gratefully acknowledged for giving me the opportunity to work in his group and for the extremely interesting topic of this research work. I especially appreciated his scientific guidance, the fruitful discussions and the enthusiastic and challenging ways of working. I would like to thank him for the excellence team atmosphere and for supporting my participation on different conferences both in Europe and in U.S.

I would like to express my sincere gratitude to my supervisor PD Dr. Julia Engert for her great supervision, encouragement, and for taking the time to carefully reviewing all my work. In particular, I appreciated her many scientific inputs and I would like to thank her for keeping her door always opened for me. Furthermore, I am deeply thankful for her advices and guidance on my personal development over the last years.

Thanks to AMSilk GmbH for kindly providing the spider silk proteins and to Michael Bergfeld (AMSilk GmbH, Martinsried, Germany) for performing the mechanical properties measurements. Scientific support by Dr. Ute Slotta and Dr. Nathalie Maksimovikj and Lin Römer (AMSilk GmbH, Martinsried, Germany) is here gratefully acknowledged.

Furthermore, I would like to thank Dr. Stephan Reschauer for helping us preparing our patent application, Dr. Thomas Luxbacher (AntonPaar) for performing the zeta-potential measurements, and Christian Minke for his help in SEM analysis.

Special thanks go to my colleagues in the spider silk lab Markus Hofer and Matthias Lucke for the amazing time we spent together, all the jokes (Markus) and the funny noises (Matthias).

My gratitude goes also to the “older” student generation: Raimund Geidobler, Thomas Bosch, Angelika Freitag, Elsa Kis, Sebastian Hertel, Christian Hildebrandt, Matthaeus Noga, Yibin Deng, and Elisabeth Härtl. Thank you so much for your scientific support, you made me feel very welcome in your group from day one. Big thanks go to Cihad Anamur, Laura Engelke, Robert Liebner, Roman Mathäs, and Christian Neuhofer for spicing up these exciting years. Many thanks to Alice

Hirschmann and Ayla Tekbudak for their help and support.

I would like to thank Prof. Frieß and his group for the nice atmosphere provided in the department and for the many activities outside the lab that made this experience so enjoyable! Thanks to Kerstin Hoffmann, Stefanie Funke, Verena Saller, and especially to Kay Strüver for his undeniable BBQ skills.

Special thanks go to Marie-Paul Even and Madeleine Witting, the best friends you could wish for, and to the "Queen-Tour Committee"…hurra!

This is the place where I need to thank a special partner in this journey: thank you Chiara for sharing this experience with me, I will never forget the years we spent together in Haderner Stern! Big thanks go also to Norbert (only Chiara will understand here what I mean).

Walter Kamm, Nils Poth, Melanie Hofmann, Riccardo Torosantucci, Dieter Kadereit, Ahmed Youssef, Susanne Neschen, and my cat Ivy, are here also acknowledged for their important moral support during the writing of this thesis.

I would like to write my immense gratitude to my parents Franco and Lucia for giving me roots and wings. Thanks for your unconditional love.

Last but not least, I want to say thanks to Toby for his patience during the last phase of the thesis, for his love and endless support.

This thesis was supported by m^4 Munich Biotech Cluster, grant number 01EX1022P.

TABLE OF CONTENT

I. LIST OF ABBREVIATIONS

AA	Amino Acid
ADF	Araneus Diadematus Fibroin
A.U.	Arbitrate Unit
ACN	Acetonitrile
BSA	Serum Bovin Albumine
c	Concentration
Da	Dalton
DDS	Drug Delivery System
DSC	Differential Scanning Calorimetry
EtOH	Ethanol
EPO	Erythropoietin
FD04	FITC-dextran 4 kDa
FD10	FITC-dextran 10 kDa
FD20	FITC-dextran 20 kDa
FITC	Fluorescein Isothiocyanate
FT-IR	Fourier Transform Infrared Spectroscopy
Gly	Glycerol
GudmSNC	Guanidinium thyocyanate
h	Hour

HFPI	Hexafluor-2-propanol
HMW	High Molecular Weight
HPLC	High Performance Liquid Chromatography
HPW	Highly Purified Water
M	Molar
MeOH	Methanol
mM	Millimolar
mg	Milligram
Mbp	Million base pairs
min	Minute
mL	Milliliter
NGF	Nerve Growth Factor
PEG	Polyethylene glycol
PEI	Polyetherimide
PES	polyether sulfone
PET	Polyethylene terephthalate
PBS	Phosphate Buffered Saline
pI	Isoelectric point
PLGA	poly(lactic-co-glycolic acid)
2-Pyrr	2-Pyrrolidone

RH	Relative Humidity
RP	Reverse Phase
rpm	Rounds per minute
RSSP	Recombinant Spider Silk Protein
SDS	Sodium dodecyl sulfate
SDS-PAGE	Sodium dodecyl sulfate polyacrylamide gel electrophoresis
SEC	Size Exclusion Chromatography
SEM	Scanning Electron Microscopy
SMW	Small Molecular Weight
SSP	Spider Silk Protein
TFA	Trifluoroacetic acid
T_g	Glass Transition Temperature
TRIS	Tris(hydroxymethyl)aminomethane
UV	Ultraviolet

II. LIST OF FIGURES

III. LIST OF TABLES

IV. PATENT, PUBLICATIONS AND POSTERS ASSOCIATED WITH THIS THESIS

Patent

- Elisa Agostini, Julia Engert, Gerhard Winter

  Patent Application WO/2015/117888, Coated Silk Films, Methods for the Production thereof and uses thereof

Publications

- Elisa Agostini, Gerhard Winter, Julia Engert

  Water-based preparation of spider silk films as drug delivery matrices

  Journal of Controlled Release, 2015, Volume 213, Pages 134–14

- Elisa Agostini, Gerhard Winter, Julia Engert

  Scale-up of water-based spider silk film casting

  Submitted to International Journal of Pharmaceutics

Posters

- Elisa Agostini, Gerhard Winter, Julia Engert

  Water-based Spider silk films for controlled drug delivery

  9th World Meeting on Pharmaceutics, Biopharmaceutics and Pharm. Technology, Lisbon, 31th March - 3rd April, 2014

- Elisa Agostini, Gerhard Winter, Julia Engert

  Spider silk films as pharmaceutical protein drug delivery matrix

  AAPS National Biotechnology Conference, San Diego (CA), May 20th-22nd, 2013

- Elisa Agostini, Gerhard Winter, Julia Myschik

  Preparation and investigation of water-based spider silk films

  8th World Meeting on Pharmaceutics, Biopharmaceutics and Pharmaceutical Technology, Istanbul, March 19th-22nd, 2012

- Markus Hofer, Elisa Agostini, Gerhard Winter, Julia Myschik

  Recombinant spider silk proteins as new biomaterial for innovative drug delivery systems

1. Introduction

1.1. Biomaterials in Drug Delivery

A biomaterial as by definition is „*a material intended to interface with biological systems to evaluate, treat, augment or replace any tissue, organ or function of the body*"[1]. Biocompatibility is the essential characteristic of a biomaterial, and it is described as "*the ability of a material to perform with an appropriate host response in a specific situation*" [1]. Biomaterials in general have attracted increasing interest in the pharmaceutical industry, and a wide range of their applications have been described in the past decades [2]. One of the most remarkable applications is a controlled drug delivery system (DDS) using biocompatible polymers [3, 4]. In these DDS, drugs are incorporated into a polymeric material with the release rate of the drug being determined by the properties of the drug-polymer system and by the surrounding environment [5].

In the past, constant rate release kinetics were obtained by incorporating the drug in polymeric matrices like poly(ethylen-co-vinyl acetate) (Ocusert®, Progestesert®) and silicone rubbers (Norplant®, Vaginal Ring®) [6]. Another strategy was the use of a rate controlling polymeric membrane (Implanon®[7], Oros®[8], Duros®[9]). Furthermore, most of the transdermal therapeutic systems (TTS), are designed to release the drug at a constant rate [10]. The above mentioned DDS are able to release the drug in an almost zero order release kinetic, which is particularly interesting due to its capacity to control the plasma drug concentration. In addition to this, they can reduce the administration frequency improving patient compliance.

When a DDS is implanted, the biomaterial that composes it should not react adversely with the biological surrounding and the functionality of the tissue should not be compromised [11-13]. On top of this, it should also fulfil the requirements described by ISO 10993 (Biological evaluation of medical devices [14]). Another desired characteristic in designing an implantable DDS is the biodegradation of the polymer that composes it. Two important examples of biodegradable materials used in drug release technology are poly(lactic-co-

glycolic acid) (Zoladex® [15], Enantone Depot®) and polyanhydrides (Gliadel® Wafer [16]). Since the launch of Zoladex® (1989) less than ten clinical products able to deliver peptides and proteins have been developed [17].

Poly(lactic-co-glycolic acid) (PLGA) polymers have been extensively investigated [18-20]. Their drug release profile is often described as a three-phase profile [21-23]. Phase I is characterized by a burst where the non-encapsulated drug or the drug loaded on the surface of the DDS is released. Phase II consists of a slow constant release, where the drug needs to diffuse through the polymeric matrix before being released. Phase III is considered as a second burst, where the drug is released quickly due to the erosion of the PLGA matrix. In general, the encapsulated drug can diffuse out of the PLGA polymeric matrix due to: (I) diffusion through water-filled pores, (II) diffusion through the polymer, (III) osmotic pumping, and finally (IV) erosion [23]. The tissue reaction to the presence of this family of polymers has been covered substantially in literature [24-26]. PLGA particles can cause a body inflammation response that mainly depends on particle size, tissue type, and finally the nature of the polymer [13, 25, 27].

In spite of the frequent use of PLGA co-polymers in the pharmaceutical industry, some negative aspects of this material have been reported in the past years, especially with regards to the encapsulation and delivery of peptides and protein [19, 28]. The manufacturing process of PLGA-based DDS has a major impact on the drug delivery system characteristics [28, 29]. For instance, during the process the biologic active ingredient can undergo denaturation and aggregation due to its instability at the water to organic solvent interface [28, 30, 31]. Moreover, the shear force applied to homogenize the primary emulsion during preparation of the particles can denature proteins and peptides as well [32]. Protein and peptide stability is particularly important, since aggregation not only decreases the drug's activity but it can also lead to toxicity [33, 34]. Another reported negative aspect of PLGA drug delivery systems is the drug release profile, where often an incomplete release [35-38] or high bursts [39-42] can be observed. DDS that are made of PLGA which are currently available commercially are listed in Table 1.

Table 1: Marketed PLGA-based products, November 2016.

Commercial Name	Form	Active Ingredient	Application	Company
Lupron Depot®	Particles	Leuprolide	1-, 3-, 4-, 6-Month	Takeda, Abbott
Suprecur® MP	Particles	Buserelin	Monthly	Sanofi
Enantone®	Particles	Leuprorelin	Monthly	Takeda
Zoladex®	Implant	Goserelin	1-, 3-Month	Astra Zeneca
Sandostatin LAR®	Particles	Octreotid	Monthly	Novartis
Profact® Depot	Implant	Buserelin	2-, 3-Month	Sanofi
Decapeptyl® SR	Particles	Triptorelin	1-, 3-Month	Debiopharm
Arestin™	Particles	Minocyclin	2-Week	OraPharma
Risperdal® Consta™	Particles	Risperidon	2-Week	Janssen
Eligard®	Liquid	Leuprorelin	1-, 3-, 4-, 6-Month	Astellas
Vivitrol™	Particles	Naltrexon	Monthly	Alkermes
Leuprone®	Implant	Leuprorelin	3-Month	Hexal
Somatuline® LA	Particles	Lanreotide	2-Week	Ipsen
Trelstar™ Depot	Particles	Triptorelin	Monthly	Debiopharm
Bydureon®	Particles	Exenatide	Weekly	Astra Zeneca
Salvacyl®	Particles	Triptorelin	3-Month	Ipsen
Ozurdex®	Implant	Dextamethasone	Monthly	Allergan

For these reasons, despite the extensive use of biomaterials in medical care, the research on polymers capable to minimize the negative foreign body reaction induced by its implantation is still a relevant topic [43, 44]. Moreover, obtaining the desired drug release profile remains a particular challenge. Even though there are many drug delivery systems already in the market, the incorporation of therapeutic biomolecules and their controlled release from a DDS is still a demanding task. Biologics represent a new therapeutic drug class and are particularly difficult to formulate into a stable drug product [45]. This is why the research of new biomaterials and new product designs can be considered a necessary focus for the development of next generation drug delivery systems.

1.2. Rational for Investigating Spider Silk as Biomaterial

Among all the above mentioned polymers, spider silk proteins are exceptional natural materials when it comes to their mechanical properties [46-48], biocompatibility, and hypoallergenicity [49-52]. Spider silk has been used for medical purposes since ancient history. For instance, it was applied in Roman and medieval dermatological practices to facilitate open wound healing and halt bleeding [53, 54]. In the past, natural spider silk fibres have been tested as alternative microsurgical suture [55, 56]. Furthermore spider silk proteins were investigated as scaffold for nerve regeneration [57, 58]. In the modern ages the use of this outstanding material has been limited to research purposes. Product development has been disregarded due to the many difficulties encountered in farming spiders [59, 60]. This specific drawback has been addressed in the past years, through a method able to efficiently produce different recombinant spider silk proteins in *Escherichia coli* [61-63]. Recombinant spider silk proteins (RSSPs) are hydrophobic and slowly biodegrading biopolymers that unify the required properties for a drug delivery system [64]. RSSPs can be used to encapsulate and release a various range of active molecules including genes for tumor targeted delivery, enzymes and drugs [65-70]. One of the most interesting recombinant spider silk proteins is the protein eADF4(C16) [46]. This engineered protein composes primarily the natural spider protein ADF-4 produced by the spider *Araneus diadematus* (the common European garden spider). In one recent study [71], medical grade silicone implants have been coated with this recombinant spider silk protein. During an in *vivo* study using Sprague-Dawley rats as models, it was reported that eADF4(C16) coatings were able to reduce post-operative inflammation after inserting medical grade silicone implants in the animals [71]. As a consequence of inhibiting fibroblast proliferation and the synthesis of collagen I, the capsular fibrosis formation was reduced. Hence, the biocompatibility of eADF4(C16) was proven. The use of eADF4(C16) proteins as a polymeric matrix offers several advantages. Among these are its biocompatibility

[71], as well as the ability to be naturally degraded in the human body by proteases, leading to non-toxic degradation products (amino acids), and avoiding any additional surgery to remove the DDS [72].

1.3. Spider Silk Proteins

In nature, over 34000 species of spiders have been identified [73]. Each of them is able to produce several task specific silks with diverse mechanical properties [50, 74-76]. Spider silk is characterized by outstanding mechanical properties [50, 77]. For instance major ampullate silk has a tensile strength comparable with the one of Kevlar fibers (4 x 10^9 N/m^2 [73]). Furthermore, one single spider can produce and store up to seven different silk proteins in as many glands [78]. Spiders are notorious for their talent in building spider webs, which are composed by various silk proteins. The two main types of silk are the ones produced in the major and minor ampullate glands [49]. The first silk type is called dragline silk and it is characterized by high tensile strength since it is used by the spider to get away from potential enemies and furthermore it composes the frame of the spider web [73].

Minor ampullate silk supports the web during its manufacture [79]. Other web threads are composed by flagelliform silk. These particular threads are covered by additional silk and other material in order to become sticky and are used for catching prays in the capture core threads of the spider web [80]. Finally, spiders produce specific silks to wrap their eggs and to conserve the food [80].

The primary amino acid structure of spider silk proteins is characterized by repetitive units. Within the amino acid sequence it is possible to identify the following functional parts:

1) The unit GPGXX, which is forming the β-turn spiral that is responsible for the outstanding elasticity properties of flagelliform silk [73, 81]

2) A_n or GA_n are alanine rich motifs, which contain 6-9 alanine amino acids forming crystalline β-sheets, fundamental for tensile strength [82, 83]. Proteins composing dragline threads present alanine rich motives. leading to the high strength that characterizes draglines [84, 85]. On the contrary, flagelliform silk does not contain this unit

3) GGX is a glycine rich element which forms 3_1-helical units connecting the different crystalline regions (the β-sheet stacks) with each other. This particular structure is responsible for the elasticity proprieties of the dragline and flagelliform silks [86-88]

4) Spacers: contain charged groups and separate the repetitive peptide units into cluster [73]

5) NR: non repetitive regions at the amino- and carboxyl-termini of the proteins [61, 89]

One of the most studied dragline thread is the one produced by the spider *Araneus Diadematus* (the common European garden cross spider). This dragline is mainly composed by two silk proteins: ADF-4 and ADF-3 (ADF stands for Araneus Diademaus Fibroin) [90, 91]. The molecular ratio between ADF-4 and ADF-3 is 3 to 2 [92]. ADF-3 and ADF-4 have a similar amino acid sequences, but different water solubility. ADF-3 is soluble at high concentrations [93], in contrast, ADF-4 is almost water insoluble [94].

The natural spider silk assembly process (into thread) is characterized by a liquid-solid phase transition and structural changes of the proteins [48].

Spider dragline silk proteins are produced by cells located in the epithelium of spider´s glands [95]. The proteins are then stored in the dope of the gland at high concentrations (up to 50% w/w without aggregation [73]). It is assumed that due to the amphiphilic nature of silk proteins, these are not arranged in a defined secondary structure inside the gland, but they are mostly organized into micelles [96, 97]. The auto-assembly process takes place in the spinning duct. The final fibers are rich in β-sheet crystallites aligned in parallel to the long axis of the fiber. The following physical and biochemical factors are responsible for the assembly process:

1) pH changes from 7.2 in the glands to 6.3 in the spinning duct [98, 99]

2) Ionic composition changes inside the duct: the chaotropic ions such as sodium and chloride are exchanged by the more kosmotropic ions like phosphate and potassium [98]

3) The protein concentration increases in the distal part of the duct [100]

4) At the end the viscous protein solution is subjected to increasing elongational flow and shear forces [96, 101]

It has been suggested that the formation of colloidal aggregates is fundamental for the formation of the fiber in the spinning duct [102]. These particles are in the micrometre range and assemble together due to the applied shear forces. This is in accordance with the model described for assembly process of silks produced by the *bombix mori* worm [97, 103].

1.4. The Recombinant Spider Silk Protein eADF4(C16)

The production of recombinant spider silk proteins is complicated by several aspects such as the highly repetitive units of the genes, the length of the constructs (silk genes are very large, up to 15 Mbp) and finally the specific codon usage of spiders [104]. AMSilk GmbH (Martinsried, Germany) was one of the first company that successfully produced recombinant spider silk proteins.

AMSilk has developed a unique process for producing spider silk proteins in industrial scale. This technology is based on the research of Prof. Thomas Scheibel. His group created engineered synthetic spider DNA leading to the production of spider silk-like proteins in *E. coli* [105, 106]. The production of recombinant spider silk proteins opened a new range of possibilities, including the opportunity to specifically modify the primary structure of these biopolymers and design a new protein with an enlarged functionality portfolio [46]. For instance, cell binding motifs (such as the integrin recognition sequence RDG) can be incorporated increasing cell adhesion and proliferation on scaffolds containing the modified recombinant spider silk protein [107-111]. Another example is the incorporation of a silver binding peptide or the human antimicrobial peptide NHP-2, leading to hybrid silk films showing antimicrobial activities [112-114]. Ultimately, this technology enables the design of tailor-made recombinant spider silk proteins.

Today AMSilk is the first industrial supplier of synthetic silk biopolymers, with a distribution network across Europe and South Korea. Recently (November 2016) the sport company Adidas announced a new performance shoe using Biosteel® fiber from AMSilk.

Spider silk proteins can assemble in several stable morphological shapes, including particles, hydrogels, foams, films, and non-woven meshes [101, 107, 109, 115-121].

One of the most promising spider silk proteins produced from AMSilk is the recombinant protein eADF4(C16) (also called C_{16} or SSP1). Its protein structure is based on the natural spider protein ADF-4 and comprises 16 repeats of the following sequence:

$(GSSAAAAAAAASGPGGYGPENQGPSGPGGYGPGGP)_{16}$

It is possible to identify the same amino acid clusters described in paragraph 1.3 within the primary structure. These units are correlated with the formation of distinct secondary structures which are ultimately responsible for the mechanical properties of the recombinant silk protein [61, 73, 81-89]. Figure 1 shows these amino acid clusters and their functionality.

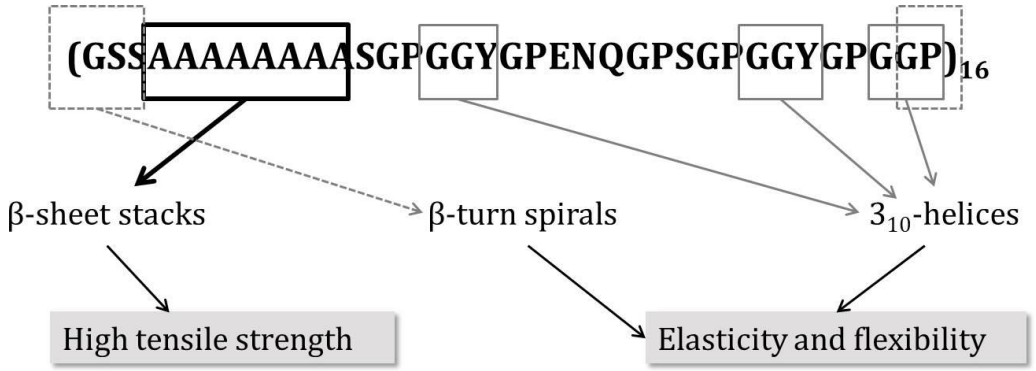

Figure 1: Primary structure of the recombinant protein eADF(C16). Highlighted with a dotted line is the functional group GPGXX, in black the group A_n, and finally in grey the unit GGX.

The following table is intended to highlight the differences between the recombinant spider silk protein eADF4(C16) and the natural spider silk protein ADF4.

Table 2: Selected characteristics of the natural spider silk protein ADF4 and the engineered recombinant spider silk protein eADF4(C16) [61].

	ADF-4	**eADF4(C_{16})**
Molecular mass (kDa)	34.9	47.7
Extinction coefficient$_{276\ nm}$ ($M^{-1}cm^{-1}$)	nd	46400
No. of charged amino acid residues (positive/negative)	2/6	0/16
Mean hydropathicity	-0.075	-0.464
Solubility (% w/v)	<1	8

The recombinant protein eADF4(C16) has a higher molecular mass and solubility than the natural protein ADF-4. Furthermore, the number of negatively charged amino acid residues is more than duplicated in comparison to the native protein ADF-4.

The assembly process of the protein eADF4(C16) into fibrils has been recently investigated [122-124]. According to the described model, the polyalanine motifs within the primary structure are the key that triggers the auto-assembly process. The conversion from intrinsically disordered protein monomers to partially folded β-sheet rich monomers takes place after defined stimuli (such as: kosmotropic ions, temperature, or high protein concentration). These partially folded monomers further assemble into nuclei which lead to fibril formation after addition of other disordered monomers. The nucleation-step is considered to be the rate-limited one. Hydrogen bonds formation during β-sheet rearrangement and hydrophobic interactions are the major forces involved [122].

1.5. Spider Silk Films

Spider silk matrices can be produced through a large number of different techniques as recently reported by Borkner et al. [125]. The list of technologies that can be employed include: dip or spin coating [71, 126-128], layer-by-layer deposition [129], Langmuir-Blodgett deposition [130, 131], electrospinning [132-137], electrophoretic deposition [138-140], and finally lithography [141, 142]. However, the most adopted method to cast spider silk films remains the solvent evaporation technique [46, 72, 143-147]. Evaporation of the solvent yields a silk film that is formed via non-covalent intermolecular interactions [48]. The properties of the resulting film are mainly determined by two components: the secondary structure of the assembled protein and the macroscopic structure, which provides the material's interface with its environment [59]. The secondary structure is determined or influenced by the primary structure of the protein, the solvent and the type of post-treatment. Silk films can be structurally or chemically modified by subsequent post-treatments [146]. Spider silk protein films are commonly formed by a protein solution in water, hexafluoro-2-propanol (HFIP), formic acid, or trifluoroacetic acid [73, 107].

Films casted from aqueous solution mainly consist of random coil structures [148], whereas films from HFIP solutions show α-helix rich structures [147, 149], and films from formic acid solutions are mainly composed of β-sheet structures [107, 150]. Films rich in β-sheet structure are water insoluble [107]. Post-treatments of water soluble films with dehydrating agents like alcohols, or kosmotropic ions, can result in water-insoluble films [107]. These post-treatments allow a transition from random coil/α-helical structures to higher content of β-sheet crystals of about 70-80 Å [146].

In a recent work, the influence of the substrate whereon the film is cast was investigated [151]. It was shown that a glass template surface leads to less content of β-sheets in comparison to polystyrene (PS) and polytetrafluorethylen (Teflon). Furthermore it was observed that it was easier to peel off spider silk films from

hydrophobic surfaces. Microphase separation has been already described for dragline silk and RSSPs [102, 115]. In this case the authors reported different microphase separations related to the nature of the template. Hydrophobic surfaces led to coatings with high amount of β-sheet structures where the hydrophilic areas (random coil and helical units) were distributed in the hydrophobic matrix. On the contrary, in the case of films cast on a hydrophilic surface, the matrix was mostly composed by random coil and helical structures while the hydrophobic areas (β-sheets) were dispersed within the matrix [151].

Solubility of HFIP-based spider silk films, was investigated by Slotta et al. [147]. In this work films were incubated respectively in water, 8 M urea, 6 M guanidinium chloride (GdmCl) and finally 6 M guanidinium thiocyanate (GdmSCN). Films were soluble in water, but after post-treatment with methanol they became water insoluble. Furthermore, methanol-processed eADF4(C16) films were also insoluble in urea and GdmCl. Only GdmSCN was able to unfold the proteins composing the film matrix and therefore dissolve the spider silk films again.

Junghans et al. [126] analyzed the properties of several silk layers composed respectively by: recombinant spider silk-ELP fusion protein SO1-ELP, recombinant spider silk protein AQ24NR3, and eADF4(C16). After microhardness testing, they concluded that only the eADF4(C16) films combined high hardness with elasticity comparable to technical plastics (PET and PEI).

Spiess at al. [145] cast spider silk films using buffers, formic acid and HFIP. After investigating these films by thermal gravimetric analysis (TGA) and differential scanning calorimetry (DSC), they concluded that the thermal stability was not affected by the solvent used in the casting solution. On the contrary, mechanical properties were different. Films cast with formic acid showed a higher tensile strength, while HFIP-based films showed the higher elongation at break. Buffer-based films were the most delicate. Moreover, they observed different β-sheet content in different areas of the same water-based film.

After film processing it is possible to covalently couple small and large molecules on the film surface. In one example, spider silk films were activated with 1-ethyl-

3-(3-dimethylaminopropyl)carbodiimide (EDC) and N-hydroxysulfosuccinimide (NHS). Films were then incubated with a solution of fluorescein or β-galactosidase [152].

Alternatively, it is also feasible to produce a variation of the protein eADF4(C16) containing a single cysteine residue in the primary structure [107]. Films cast with this engineered silk protein showed similar properties compared to films cast with the original protein [107]. This specific functionalization can be used for controlled coupling using the free thiol groups presented on the film surface.

In the past, drug loading and release of both small molecules and proteins have been studied for spider silk particles [65-67, 69]. In a recent work, films composed by eADF4(C16) or eADF4(C16) blended with a polymer, polycaprolactone (PCL) or thermoplastic polyurethane (TPU), were prepared using a HFIP-based casting solution [143]. Films were then post-treated with methanol to achieve water insolubility. These silk layers were loaded with small molecules (methyl violet or ethacridine lactate), and the described release profiles where affected by the film composition and by the presence of elastase. Films composed only by spider silk released more model drug and in general the presence of the enzyme slightly increased the release [143].

More recently, using the same manufacturing process new films were obtained by blending eADF4(C16) proteins with polybutylene terephthalate (PBT) or poly(butylene terephthalate-co-poly(alkyleneglycol) terephthalate) (PBTAT) [153]. These films were mineralized with calcium ions and tested as scaffolds for bone tissue regeneration. In this study the biocompatibility of the films with both fibroblasts and human mesenchymal stem cells was assessed. Fibroblast adhesion was observed to be higher on blended films than on pure eADF4(C16) films. In addition, calcium mineralized PBTAT-50 and PBTAT-75 films showed the best biocompatibility with stem cells where the higher alkaline phosphatase (ALP) activity was measured [153].

Cell adhesion was further investigated on different spider silk coated catheter polymers: polyurethane, polytetrafluoroethylene, and finally silicone [154]. In this

study, several cell types were taken into consideration, such as: keratinocytes, neuronal cells, myoblasts, and fibroblasts. In accordance with the previous work, Borkner at al. observed poor or no cell adhesion on RSSP coatings suggesting good biocompatibility of spider silk and its use in biomedical applications.

As discussed in this chapter, in a near future spider silk films could be successfully employed as scaffolds for tissue engineering, artificial nerve construct, delivery system, diagnostics, biocompatible coating for biomedical device and implants [46, 125].

1.6. Aim of the Thesis

The aim of this research project was the development and characterization of water-based spider silk films composed of eADF4(C16) protein. When this work started, spider silk films were normally produced using organic solvents and little was known about casting films from a water solution. Furthermore their potential as a drug delivery system had not been yet investigated. Most of the interesting studies presented in paragraph 1.5 on spider silk films were done in parallel to this project by the Scheibel group. This thesis focused in the investigation of the application of water-based eADF4(C16) films as DDS for both small molecular weight drugs and protein pharmaceuticals. Different loading methods were taken into consideration and different film designs were investigated. For instance multilayer films had not been described yet, as well as coated films. The characterization of the obtained films was a crucial part of the project as well. The analytical information collected will help in the future when choosing the right medical application as well as suitable drugs for a successful loading and release process. The last part of this project addresses the need to automate the film casting process using a film applicator. Spider silk protein films could be used for several pharmaceutical and medical purposes, especially in situations where the mechanical strength of a drug eluting device is of high relevance. Benchmarking of this new material against standard implant polymers like PLGA and novel full

synthetic polymers will allow positioning the new material in the field.

The aims of this work can be defined as:

1. Development of a reproducible all-aqueous protein film production process
2. Manufacturing of water-based spider silk films having superior mechanical properties compared to marketed films
3. Evaluation of spider silk films as novel carrier for various pharmaceuticals

2. Materials

2.1. Reagents and Chemicals

The reagents and chemicals used during this work are listed in the following table:

Table 3: Reagents and chemicals

Description	Description/Purity	Provider
Acetonitrile	HPLC grade	VWR Chemicals, Germany
Bromophenol blue solution	Ph. Eur.	Merck, Germany
Di-potassium hydrogen phosphate	≥ 98.0%	Sigma-Aldrich, Germany
Di-sodium hydrogen phosphate	≥ 99.5%	AppliChem, Germany
Ethanol	70% v/v	VWR Chemicals, Germany
Ethacridine-lactate	Ph. Eur.	Fagron GmbH, Germany
FITC-Dextran	Average molecular weight: 21 kDa	Sigma-Aldrich, Germany
Glycerol	Ph. Eur.	Ceaser & Loretz, Germany
Guanidinium thiocyanate	For molecular biology	AppliChem, Germany
Hydrochlorid acid	1 M	AppliChem, Germany
Mark 12™	-	Invitrogen, USA
Methanol	HPLC grade	VWR Chemicals, Germany
Nipagin	Ph. Eur.	Fagron GmbH, Germany
Paracetamol	Ph. Eur.	Fagron GmbH, Germany
Phenol red	Suitable for cell culture	Sigma-Aldrich, Germany
Polyethylene glycol	Molecular weight range: 16-24 kDa	Sigma-Aldrich, Germany

Potassium chloride	≥ 99.5%	AppliChem, Germany
Potassium di-hydrogen phosphate	≥ 98.0%	Sigma-Aldrich, Germany
2-Pyrrolidone	≥ 99.0%	Sigma-Aldrich, Germany
Sodium Azide	≥ 99.5%	Sigma-Aldrich, Germany
Sodium chloride	≥ 99.9%	AppliChem, Germany
Sodium di-hydrogen phosphate	≥ 99.0%	AppliChem, Germany
Sodium dodecyl sulphate	≥ 99.0%	Sigma-Aldrich, Germany
Sodium hydroxide	1 M	AppliChem, Germany
Tetracaine-HCl	Ph. Eur.	Fagron GmbH, Germany
Trizma® base	≥ 99.9%	Sigma-Aldrich, Germany

2.2. Proteins

The following proteins have been used in this work:

Table 4: Proteins

Description	Description/Purity	Provider
eADF4(C16)	Spray dried	AMSilk, Germany
Lysozyme from chicken egg	≥ 90.0%	Sigma-Aldrich, Germany
Albumin–fluorescein isothiocyanate conjugate	-	Sigma-Aldrich, Germany
Nerve growth factor	0.5 mg/mL, 100 mM acetate buffer pH 6.0	From stock
Erythropoietin	0.65 mg/mL, 20 mM phosphate buffer pH 7.2	From stock

2.3. Buffers

The following buffer compounds were used in this work. All buffers were prepared using demineralized water.

Table 5: Buffers

Tris/HCl buffer, 5 mM, pH 8	
Tris trisma® base	5 mM
Hydrochlorid acid	to pH 8.0
PBS 10 mM, pH 7.4	
KH_2PO_4	1 mM
Na_2HPO_4	10 mM
NaCl	137 mM
KCl	2.7 mM
Sodium azide	0.05% w/v
HPLC-RP Buffer	
Mobile Phase I	HPW + ACN 10% + TFA 0.1%
Mobile Phase II	ACN 100% + TFA 0.1%
SEC buffer A, pH 7.0 (NGF)	
Potassium phosphate buffer	200 mM
KCl	450 mM
SEC buffer B, pH 7.0 (eADF4(C16))	
Potassium phosphate buffer	50 mM
Sodium chloride	300 mM
Laemmli Buffer	
Tris(hydroxymethyl)-aminomethane	250 mM
Glycerol	23%

Bromophenol blue 0.1% solution	1%
Sodium dodecyl sulphate	4%

2.4. Kit used for SDS-Page

Table 6: Kit

Description	Provider
SilverXpress®	Invitrogen, USA

2.5. Software

Table 7: Software

Description	Provider
Origin 8G	OriginLab Corporation, USA
Opus 6.5	Bruker, USA
Chromeleon	Dionex, Germany
Microsoft Office 2010	Microsoft, USA

3. Preparation and Analysis of Water-based SSP Films

3.1. Introduction

This Chapter focuses on the investigation of water-based spider silk film physical- and chemical-characteristics. Before starting to consider any biomedical application for this new biomaterial, it is mandatory to understand first the film´s properties. Prior casting the film, the spider silk protein solution was analyzed by SDS-PAGE and HPLC-SEC in order to gain information on the protein eADF4(C16) in solution. Additionally the viscosity and the surface tension of the casting solution were measured to identify important properties which will become relevant during the manufacturing process. In this Chapter all films were cast manually by solvent evaporation technique. The resulting water-based eADF4(C16) films were characterized in terms of protein secondary structure, thermal stability, zeta-potential, solubility in water, mechanical properties, and finally, water absorption and desorption. Furthermore changes in the protein structure were investigated in the film matrix after a methanol post-treatment.

3.2. Methods

3.2.1. Preparation of the Spider Silk Casting Solution

Spray-dried eADF4(C16) protein was dissolved in 6 M guanidinium thicynate GdmSNC and subsequently dialyzed against 5 mM Tris/HCl buffer, pH 8 at 4°C. The pH of the protein solution was determined using a pH meter MP 220 (Mettler Toledo, Giessen, Germany). The protein solution was centrifuged for 15 min at 10000 rpm and filtered through a 0.45 µm cellulose acetate filter. The protein concentration was determined UV-photometrically using a NanoDrop 2000 system from peqlab (Erlanger, Germany). Spider silk solution was finally diluted with 4°C cooled Tris buffer to 2.5% w/v.

3.2.2. Analysis of the Protein Casting Solution

3.2.2.1. Viscosity and surface tension of the protein casting solution

The viscosity of the eADF4(C16) water solution was measured at 24°C using a

viscometer m-VROC chip A (RehoSense, Inc.). The tensiometer K100 (Krüss, Hamburg, Germany) was used to define the surface tension of the casting solution. The device was equipped with a Krüss standard plate, the velocity was set as 6 mm/min, the immersion depth was 2 mm, and the measurements were carried out at 25°C as triplicate.

3.2.2.2. SDS-PAGE of the Casting Solution

After dialysis, eADF4(C16) solution was mixed 1:1 with Laemmli buffer. The Laemmli buffer consisted in Tris(hydroxymethyl)-aminomethane 250 mM, 23% glycerol, 4% sodium dodecyl sulphate, and 1% of a bromphenol blue 0.1% solution. The final concentration of the spider silk protein was 12 µg/mL. A thermostat Grant QBT (Grant Instruments, Cambridgeshire, UK) was used to heat the mixture to 95°C for 20 minutes. After equilibrating the sample at room temperature, the mixture was pipetted into a well of a Novex NuPAGE 12% Bis–Tris gel (Life Technologies, Carlsbad, USA). Mark12 (Life Technologies, Carlsbad, USA) was used as protein standard as a reference to evaluate the size of the components. Gel electrophoresis was performed using a chamber (Bio-Rad Munich, Germany). The module was filled with a 20 fold diluted Novex NuPAGE MES SDS-Running buffer (Life Technologies, Carlsbad, USA). Electrophoresis was carried out applying 100 V for 10 min followed by 160 V for 30 min. After the separation step, the gel was treated following the Silver Xpress® protocol [155]. Finally, imaging of the gel was obtained by scanning the gel (Epson Perfection V370, Epson, Japan).

3.2.2.3. Size Exclusion High Performance Liquid Chromatography of the Casting Solution

The casting solution was diluted with Tris buffer to 1.5 mg/mL. This solution was then further diluted in order to create a calibration curve (from 96.4 µg/mL to 1.5 mg/mL). Finally, samples were placed in the autosampler ASI-100 (Dionex Softron GmbH, Germering, Germany). Size exclusion high performance liquid chromatography was performed using a Dionex HPLC system (ASI 100, P 680, RF 2000, Dionex Softron GmbH, Germering, Germany) equipped with a column YMC-

Pack Diol-120 (YMC Europe GmbH, Dinslaken, Germany). The mobile phase used was a potassium phosphate buffer 50 mM pH 7.0 containing 300 mM sodium chloride. Flow rate was set to 0.5 mL/min, and 50 µL of each sample were injected. Protein detection was carried out using a fluorescence detector RF 2000 (Dionex Softron GmbH, Germering, Germany) at an excitation wavelength of 288 nm and an emission wavelength of 344 nm.

3.2.3. Manual Film Casting of Spider Silk Films

Each film was cast using 1 mL of the silk solution. The silk solution was dropped on a plastic foil A5 22/5B from mtv-messtechnik (Cologne, Germany, Figure 2), and using the pipette tip it was spread into a rectangular shape. Films (2.5x3 cm; 3.33 mg/cm^2) were cast and dried in a laminar flow cabinet at room temperature overnight at 45% relative humidity. The humidity was controlled placing 5 L of a saturated solution of potassium carbonate bihydrate [156] in the laminar flow cabinet. Spider silk films containing the plasticizer glycerol or 2-pyrrolidone were prepared dissolving 1% w/v of the plasticizer in the eADF4(C16) casting solution, and finally films were cast as described above.

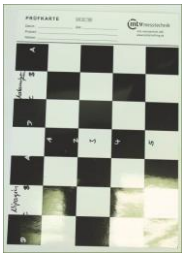

Figure 2: Plastic foil A5 22/5B from mtv-messtechnik (Cologne, Germany) used as substrate to cast spider silk films

3.2.4. Spider Silk Film Morphology

Photographs of eADF4(C16) films were obtained using a digital camera DSC-S75 (Sony Corporation, Tokyo, Japan), or a digital microscope Keyence VHX-500F (Keyence Corporation, Osaka, Japan). Scanning electron micrographs of film surface were collected after the films were immobilized on Leit-Tabs (Plano GmbH, Wetzlar, Germany) to a sample holder. Samples were carbon sputtered

under vacuum and analyzed by Joel JSM-6500F field emission scanning electron microscope (Joel Inc., Peabody, USA). Samples were viewed at a magnification of X 1000, X 5000, X 30000 and X 40000. SEM pictures were collected with the support of Christian Minke.

3.2.5. Diffusion of Different Molecules through the Spider Silk Film Matrix

The diffusion of different model molecules (paracetamol, FITC-dextrans and FITC-BSA) through eADF4(C16) film matrices was studied *via* a Franz-Cell setup. The water jacket of each Franz Cell was connected to a water bath to maintain the temperature constant at 37°C. The acceptor compartment was filled with PBS buffer. A magnetic bar stirrer was placed in the acceptor unit. Spider silk films were placed between two hydrophilic polypropylene filters (pore size 0.45 µm, Pall Corporation, Ann Arbor, Michigan). Both film and membranes were previously immersed in PBS buffer to allow them to adhere closely together removing any possible air bubbles. Membranes and film were placed over the acceptor compartment in contact with the buffer. Afterwards, the donor unit was mounted on the top of the acceptor compartment and the two compartments were fixed together by a clamp. The donor compartment was additionally sealed with parafilm®M roll (Bemis Company, Inc., Bonn, Germany) and finally, the complete Franz Cell system was left to equilibrate overnight at 300 rpm. The day after, the donor compartment was filled with 2 mL PBS buffer containing 5 mg/mL of the model substance. At the defined time points of: 30, 60, 120, 180, 240, 300 and 390 min, the concentration of the model molecule was measured in the acceptor compartment. Paracetamol samples were analyzed UV-photometrically using a Nanodrop 2000 at the wavelength of 242 nm, while FITC-dextran and FITC-BSA samples were measured by a fluorescence spectrophotometer Cary Eclipse Varian (Agilent technology, Böblingen, Germany) applying an excitation wavelength of 490 nm and an emission of 520 nm. Film integrity was checked before and at the end of the experiment. Blank samples were considered studying the diffusion of the model substances through two polypropylene membranes 0.45 µm (Pall Corporation, Ann Arbor, Michigan) without spider silk films.

3.2.6. Protein Secondary Structure of Water-based Spider Silk Films

Fourier transform infrared (FT-IR) spectra were collected using a Hyperon microscope from Bruker Optik (Bruker, Germany) using a 20x attenuated total reflectance objective (ATR). The spectra were averaged with 120 scans at the resolution of 4 cm^{-1}. All measurements were performed in the range of 600 and 4000 cm^{-1}. In one case, four different films were considered and the measurements were carried out for each film in three different areas: in the middle, next to the border and between the middle and the border. In a second case, seven different areas of the same spider silk film were analyzed with this technique.

3.2.7. Mechanical Properties of Spider Silk Films

Measurements were performed using a Zwick tensile tester Z0.5 (Zwick GmbH & Co. KG, Ulm, Germany), equipped with a 5 N capacity load cell. The length gauge was 10 mm. All spider silk films were tested in a dry state. The measurements were carried out on different days. For these reasons, both temperature and relative humidity (RH) was recorded for each measurement. Films were cut into strips of 2x120 mm. The thickness was determined using a Mitutoyo pen (Mitutoyo Deutschland GmbH, Neuss, Germany). Tensile test of spider silk films (n=5) were carried out at 24°C and 43% RH; spider silk films containing 1% w/v glycerol (n=5) were measured at 25°C and 29% RH; and finally, spider silk films containing 1% w/v 2-pyrrolidone (n=5) were analyzed at 26°C and 41% RH. Spider silk films mechanical properties were compared with three standard films made from Nylon 66, Poly-L-lactic-acid (PLLA) and ultra-high-molecular-weight polyethylene (LMWPE) respectively. The mechanical properties of these films were measured with the method described above. Nylon measurements (n=10) were performed at 42% RH at 24°C; while PLLA (n=10) and LMWPE (n=5) measurements were performed at 40% RH at 25°C. All these standard films were purchased from GoodFellow (Bad Nauheim, Germany). The mechanical properties measuraments were carried out by Michael Bergfield from AmSilk.

3.2.8. Thermal Analysis of Water-based Spider Silk Films

Thermograms of spider silk films were obtained by differential scanning calorimetry (DCS 204 Netzsch, Selb, Germany). Spider silk films were loaded in aluminum pans and a small hole was punched in the pan covers. Samples were heated under nitrogen flow at 10 K/min up to 110°C, then cooled to -40°C, followed by heating to 400°C [145].

3.2.9. Solubility Test for Spider Silk Films

At least three films (3 x 2.5 cm) were weighed and placed in a 6-well plate. Each film was covered with 2 mL of highly purified water. The well plate was positioned on a shaking plate at 2 rpm at room temperature. After 1 h, 24 h, three days and six days, the water was removed and analysed by spectrophotometer Agilent 8453 (Boeblingen, Germany). Protein concentration in solution was determined UV-photometrically. The amount of the dissolved spider silk was compared with the initial mass of the film obtaining the percentage of the loss in mass of the film in water. The same experiment was performed in 0.01 M PBS buffer pH 7.4 at 37°C.

3.2.10. Methanol Post-treatment of Spider Silk Films

A MeOH post-treatment was performed incubating water-based spider silk films in 5 mL of MeOH (HPLC quality) for 30 min, 1 h, 24 h and 72 h. Six films were treated for every time conditions. Three of them were analyzed by FT-IR (Method 3.2.6) followed by DSC measurements (Method 3.2.8), and three of them were used for studying their water solubility (Method 3.2.9).

3.2.11. Water Absorption and Desorption of Spider Silk Films

Measurements were performed according to the method previously published [157] using a Moisture Analyzer IGASorp (Hiden Analytical, Germany) with a microbalance resolution of 0.1 μg and a minimal humidity step change of 0.2%. Briefly, eADF4(C16) films were incubated at constant temperature of 25°C and a nitrogen flow rate of 200 mL min^{-1}, while the relative humidity was increased from 0 to 90%. Three absorption and desorption cycles were performed assuming an absorption of zero at 0% relative humidity.

3.2.12. Zeta-potential Measurements of Spider Silk Films

The zeta-potential measurements were performed using a SurPass electrokinetic analyser, having an integrated titration unit and equipped with the adjustable gap cell (Anton Paar GmbH, Graz, Austria). These experiments were carried out by Thomas Luxbacher from Anton Paar.

3.3. Results and Discussion

3.3.1. Water-based Casting Solution

The primary structure of the recombinant spider silk protein eADF4(C16) is rich in alanin, glycin and prolin [146]. The high content of these hydrophobic amino acids leads to low water solubility of the protein [94]. In order to prepare a water-based casting solution (Method 3.2.1) the protein needs to be dissolved at first in a solvent containing a high concentration of guanidinium thiocyanate, a protein unfolding agent. After that, a slow dialysis needs to take place to remove the unfolding agent. For the purpose of this project, a buffer of 5 mM Tris/HCl was used as dialysis buffer. It was chosen due to its pH range and its inertia towards the spider silk protein, since for instance high concentration of phosphate ions can trigger the aggregation of eADF4(C16) [65]. The molar concentration of Tris in the buffer was defined as low as possible, with the intention to avoid the formation of salt crystals in the film matrix after the evaporation of the solvent during film preparation. After dialysis, a transparent, colorless, spider silk protein buffer solution having a final concentration of 30 mg/mL eADF4(C16) was obtained. It has been reported by Huemmerich et al., that the recombinant protein eADF4(C16) is characterized by random coiled structures when dissolved in aqueous solution [152]. In this work, the casting solution was analyzed by SDS-PAGE (Method 3.2.2.2) and HPLC-SEC (Method 3.2.2.3). The SEC chromatogram (Figure 3) showed the presence of aggregates (peak 11.5 min and peak 12.7 min) followed by the main eADF4(C16) peak (at 14.7 min). The protein main peak is characterized by a large tailing (from 14.7 to 29 min), suggesting the presence of

different eADF4(C16) fragments, which was also confirmed by SDS gel analysis (Figure 4). Here, the main protein signal was present at around 67 kDa, followed by numerous smaller molecules bands of 66-37 kDa.

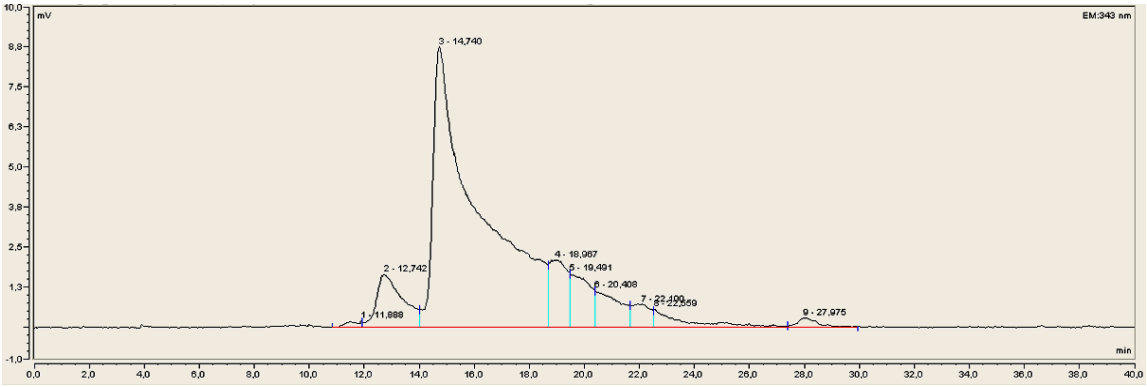

Figure 3: Example of HPLC-SEC chromatogram of the recombinant spider silk protein eADF4(C16) in the casting solution before film casting.

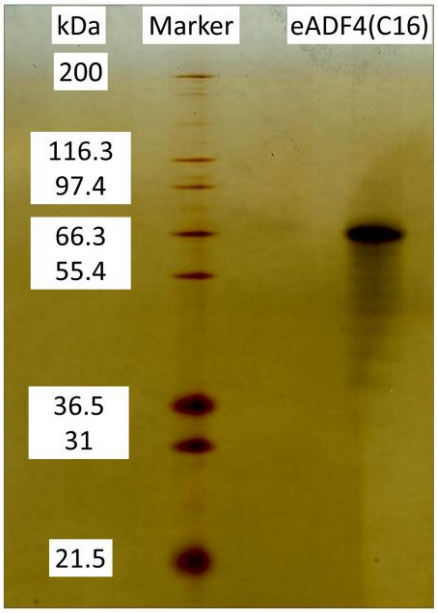

Figure 4: SDS-Page gel of the recombinant spider silk protein eADF4(C16) in the casting solution before film casting.

The physical characteristics of the spider silk casting solution will play an important role in the industrialization of the manufacturing process. In Table 8, the viscosity and the surface tension of the casting solution are listed.

Table 8: Physical properties of the spider silk casting solution

Protein casting solution Composition	Viscosity (mPa-s)	Surface tension (mN/m)
eADF4(C16) 25 mg/mL Tris/HCl buffer 5 mM pH 8	2.33 ± 0.75	48.14 ± 0.04

3.3.2. Morphology and Surface of SSP Water-based Films

The casting solution was always processed into films the same day after completing the dialysis process. By casting (Method 3.2.1) spider silk films from aqueous solvents, transparent films having a homogeneous morphology and a smooth surface were obtained.

The average thickness of the films was about 29 ± 4 μm. Films prepared with this method were easy to handle, and the process was found to be reproducible.

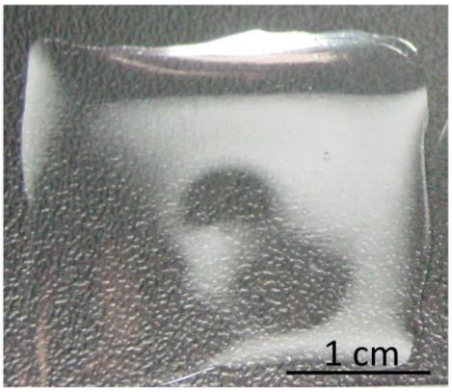

Figure 5: Photograph of eADF4(C16) films cast by solvent evaporation technique, film dimensions: 2.5 x 3 x 0.03 cm. Bar = 1 cm

The film surface was analyzed using a digital microscope (Method 3.2.4). Overall, the surface was observed to be smooth, compact and homogeneous. Although, it is possible to observe different brighter and darker spots, those could refer to the presence of pores and/or protuberances. A closer analysis of the surface by SEM (Figure 7) highlights the absence of pores and the presence of minor extrusions, caused from the spider silk protein aggregation process. The high resolution of the

micrographs C and D reveal the presence of microglobular structures which compose the film matrix network. Those structures have been described previously by Yucel et al. as the final stage of silk self-aggregation [103].

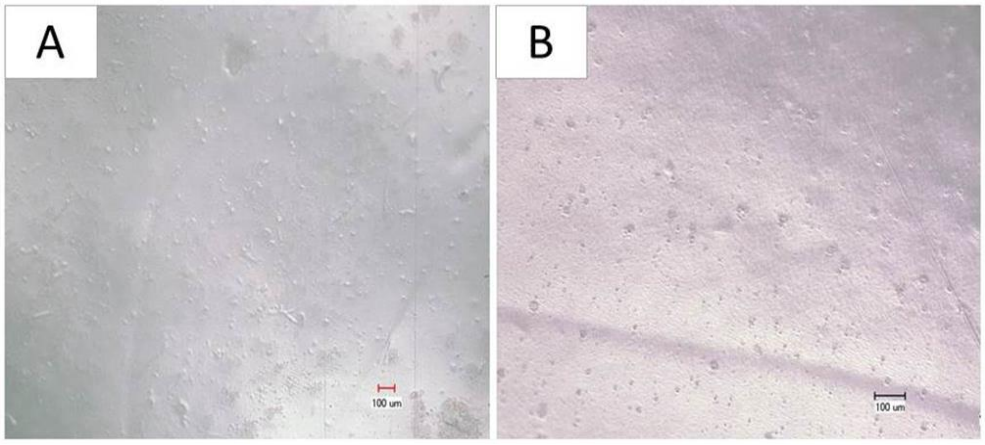

Figure 6: Images of the surface of spider silk films obtained using a digital microscope (Method 3.2.4). A: magnification 100x, bar = 100 µm; B: magnification 200x, bar = 100 µm

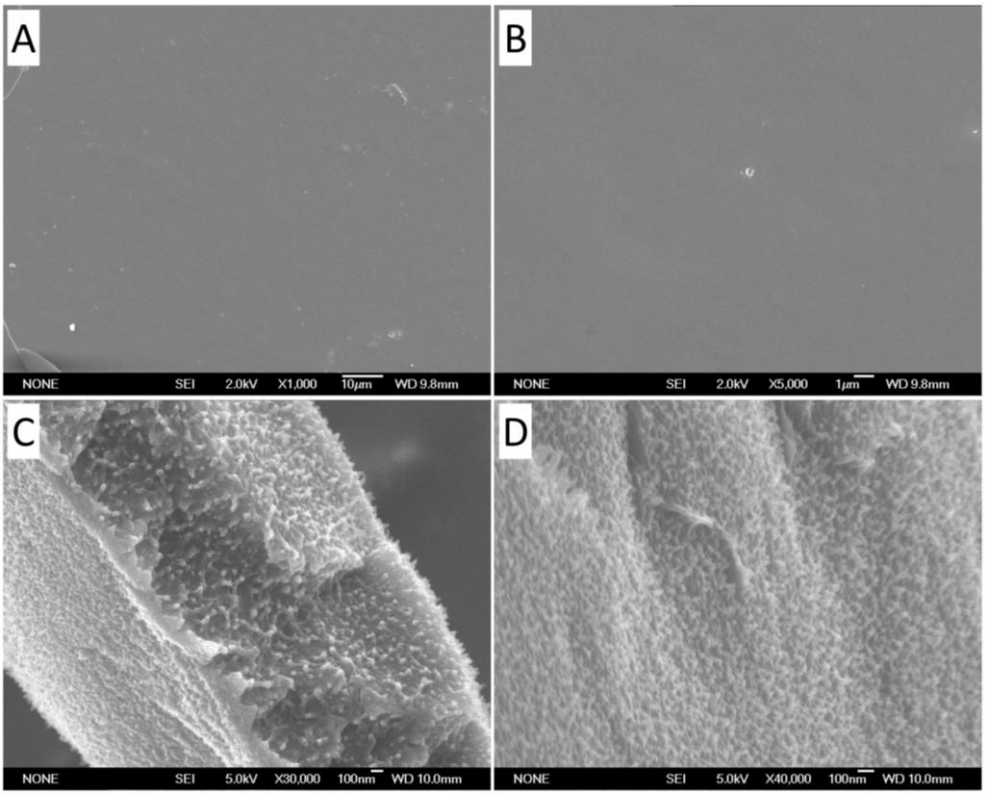

Figure 7: Scanning electron micrographs of water-based spider silk films cast by solvent evaporation technique. A: Surface of a spider silk film, magnification of 1000x, bar = 10 µm; B: Surface of a spider silk film, magnification of 5000x, bar = 1 µm; C: Cross section of a spider silk film, magnification of 30000x, bar = 100 nm; D: Surface of a spider silk film, magnification of 40000x, bar = 100 nm.

To further examine spider silk film, a diffusion test *via* Franz Cells was performed (Method 3.2.5). The scope of the experiment was to evaluate the diffusion of molecules having different molecular weights through the spider silk matrix.

Figure 8 shows the results obtained. Since the calculated isoelectric point of eADF4(C16) is 3.48 [67], spider silk films are assumed to be negatively charged in the experiment conditions (pH 7.4). Paracetamol, a small and neutrally charged molecule was able to diffuse through the film matrix. On the contrary, larger neutrally charged molecules like dextran 4, 10, and 20 kDa, did not pass through the film matrix to reach the acceptor compartment during the time considered. The control showed that when the spider silk was not included between the two polyethylene membranes, dextran molecules diffused to the acceptor compartment.

In the case of BSA, a globular protein negatively charged at pH 7.4 with a size of 66.5 kDa, the molecule was not able to pass through the film to the acceptor compartment during the time considered. Since both film and protein (BSA) are negatively charged, the diffusion of the large molecule was additionally challenged by repulsive forces. On the other hand, BSA was able to reach the acceptor donor in the control during the time considered.

In conclusion, the film surface resulted to be tight and compact; it appears that the film surface can act as a functional mechanical barrier for large molecules since it prevents their migration from the donor to the acceptor compartment.

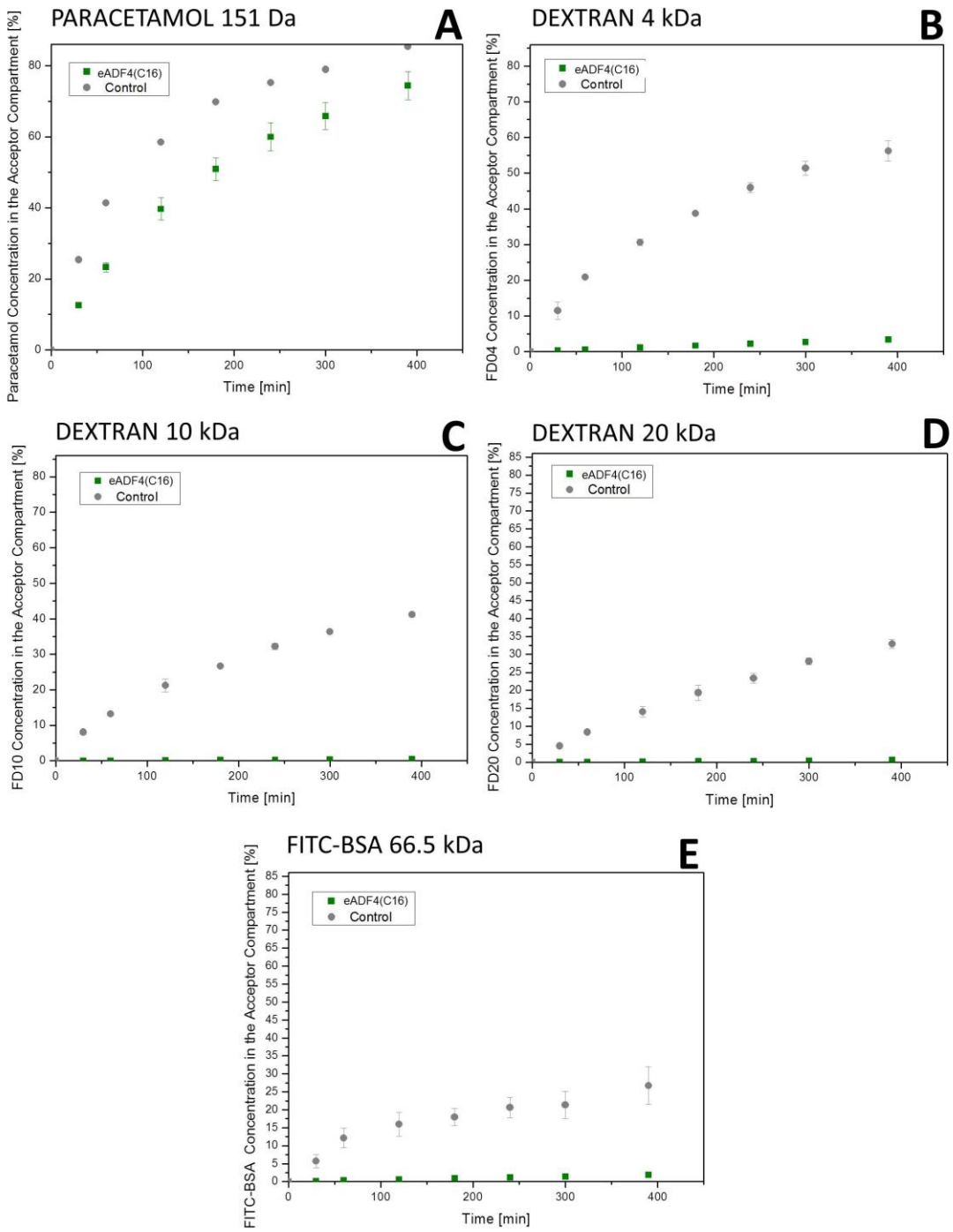

Figure 8: Concentration of different molecules (A: paracetamol, B: Dextran 4 kDa, C: 10 kDa, D: 20 kDa and E: BSA) measured in the acceptor compartment of the Franz Cells. Displayed by the square points in the graphs is the average concentration measured in the three Franz Cells having between the donor and acceptor compartment one spider silk film placed between two polypropylene membranes. Displayed by circle points is the average concentration measured in the Franz Cells used as controls, where no spider silk film was placed between the two membranes.

3.3.3. Protein Secondary Structure

Spider silk films after casting were analyzed by FT-IR spectroscopy. The analysis of the second derivate of the amide I band showed that water-based eADF4(C16) films were characterized by a very homogenous protein structure, with high β-sheet content (peaks at: 1625 cm^{-1} and 1690 cm^{-1}), as shown in Figure 9. This is true in both cases when the measurements were performed in different film areas, as well as in different films analyzed. The content of β-sheet structures determines the stability of silk films and their mechanical properties. eADF4(C16) is characterized by its hydrophobic nature and it is therefore insoluble in water. For this reason, in the past years, spider silk films have been generally cast from hexafluoro-2-propanol [127, 147]. Those films needed to be additionally processed by treating them with phosphate ions or alcohol [146, 152] in order to increase their β-sheet content. In agreement with the literature [48], water-based films usually do not contain a large amount of β-sheet protein, they mainly consist of random coil structures, and are therefore soluble in water. However, the preparation procedure described in this chapter results in a high content of β-sheet protein secondary structures. This is probably caused by the drying step of the casting solution. During overnight, the eADF4(C16) proteins have enough time to fold in ordinate ß-sheet structures. Moreover, the manufacturing process used in this study did not involve the use of any organic solvent and did not require any additional post-treatment. This opens the possibility to load therapeutic proteins on spider silk films, without damaging this sensitive class of drugs.

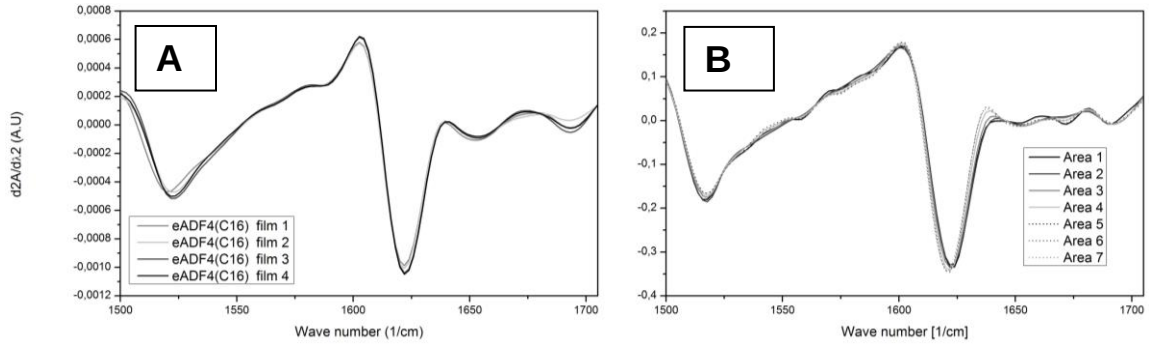

Figure 9: A: secondary derivative FT-IR spectra of water-based spider silk films (n=4, every spectra is the average of three different measurements of the same film). B: secondary derivative FT-IR spectra of one single water-based spider silk film, where seven different areas where analyzed.

3.3.4. Thermal Analysis

DSC scans showed the typical bimodal melting/thermal decomposition of the spider silk films [145] with a shoulder at 259 ± 3.5°C and an endothermic peak at 335.8 ± 1.4°C (Figure 10). The glass transition temperature (T_g) was measured at 214.2 ± 1.5°C, showing excellent thermal stability of the films up to 200°C, which could be relevant for several future technical applications as it allows steam sterilization of eADF4(C16) films. In a recent work, spider silk particles have been successfully sterilized by moist heat. Lucke et al. showed that the combination of high temperature, humidity and pressure did not affect the secondary structure of eADF4(C16) particles [158].

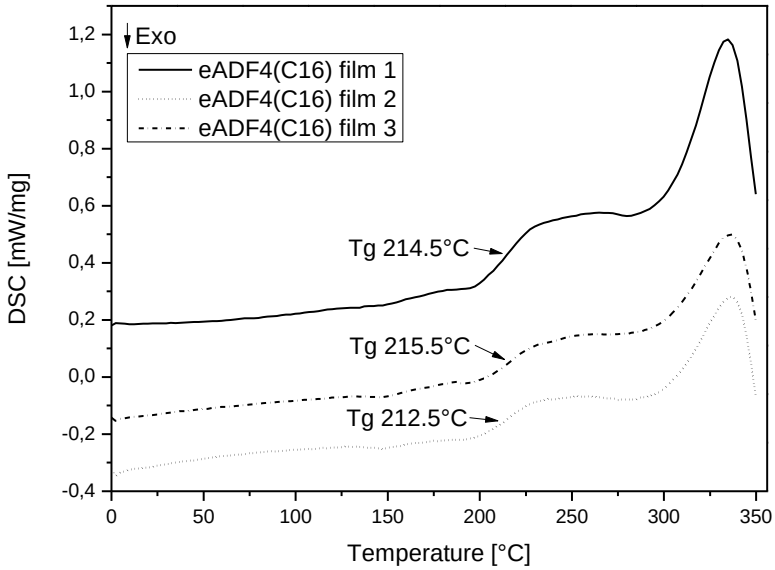

Figure 10: DSC thermograms of water-based spider silk films (n=3); T_g represents the glass transition temperature.

3.3.5. Water Solubility

After preparation, it was important to determine the amount of spider silk protein within the films that may have not been converted into its water-insoluble form. Films were incubated in highly purified water at room temperature and in PBS buffer 10 mM at 37°C. It was observed that approximately 5-6% w/w of spider silk protein could be detected in the supernatant (Table 9), and that the majority of

spider silk protein dissolved during the first hour.

Table 9: Cumulative amount of eADF4(C16) protein solubilised from water-based spider silk films (n=3).

SOLUBILITY % (w/w)	1 h	1 day	3 days	6 days
HPW (RT°C)	4.67 ± 0.01	5.45 ± 0.06	5.63 ± 0.06	5.81 ± 0.05
PBS (37°C)	4.99 ± 0.01	6.02 ± 0.14	6.23 ± 0.15	6.43 ± 0.17

After 1 h incubation in highly purified water, three spider silk films were analyzed by DSC (Method 3.2.8) and FT-IR (Method 3.2.6). The thermograms presented in Figure 11 were characterized by an increased T_g: from 214°C of untreated films to 237°C of the films incubated in water. This change can be explained by an increase of β-sheet content in the film matrix. This hypothesis was confirmed by the analysis of the protein secondary structure performed using the FT-IR microscope. In fact, the intensity of the main β-sheet peak at 1625 cm^{-1} increased notably after incubation in water (Figure 12).

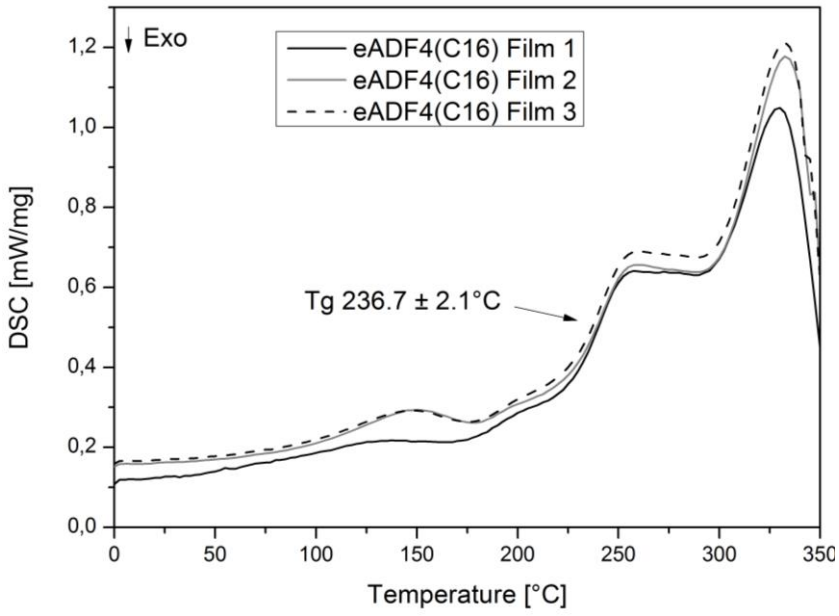

Figure 11: Thermograms of water-based spider silk films after incubated for 1 h in highly purified water, n = 3.

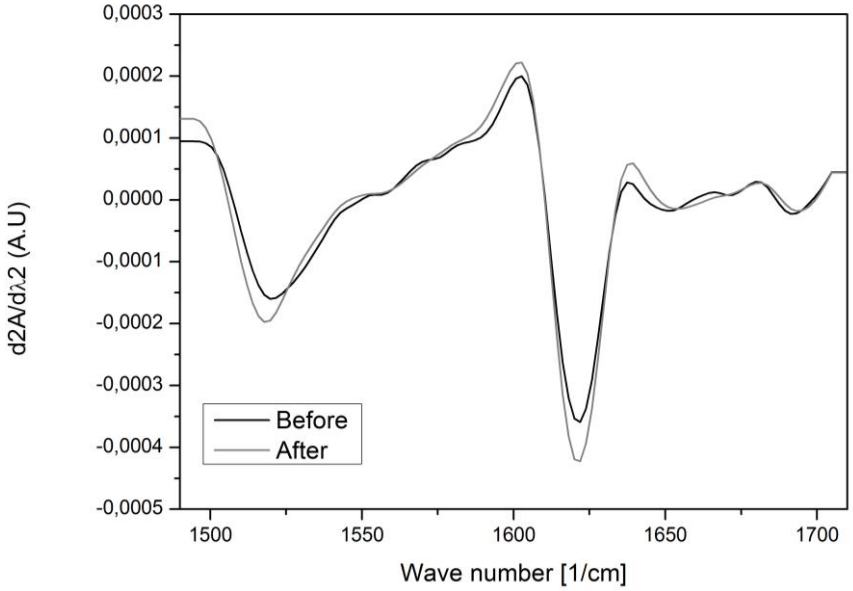

Figure 12: Second derivate of the FT-IR spectra of water-based spider silk films, before and after have incubation of the films in highly purified water for 1 h. Every spectra represents the average of nine different measurements of three different films (three measurements for each film).

3.3.6. Methanol Post-treatment

The treatment of silk films with methanol after casting is a common technique, as it is normally used to increase the content of crystal structures in the film matrix in order to achieve water insolubility [143, 146, 147, 152]. To investigate the impact of this particular post-treatment on water-based spider silk films, films were incubated in methanol for different time frames: 30 min, 1 h, 1 day and 3 days (Method 3.2.10). Afterwards, their thermal stability (Method 3.2.8) and protein secondary structure (Method 3.2.6) was analyzed. The glass transition temperature was found to be directly correlated with the time of treatment: the longer the incubation in methanol, the higher was the T_g measured (Table 10). This indicates that the content of β-sheet structures increased. In accordance with the DSC data, the FT-IR spectra showed that the β-sheet peak intensity (1625 and 1690 cm^{-1}) increased notably after 1 and 3 days treatment; while only smaller differences were measured for the films treated for 30 min and 1 h.

Table 10: Glass transition temperatures (T_g) measured from the thermograms of water-based spider silk films treated with methanol for different time frames, n = 3 for each condition.

Time MeOH Post-treatment	T_g (°C)
none	214.2 ± 1.5
30 min	230.6 ± 0.8
1 h	233.3 ± 2.3
24 h	239.8 ± 1.4
3 days	242.2 ± 2.6

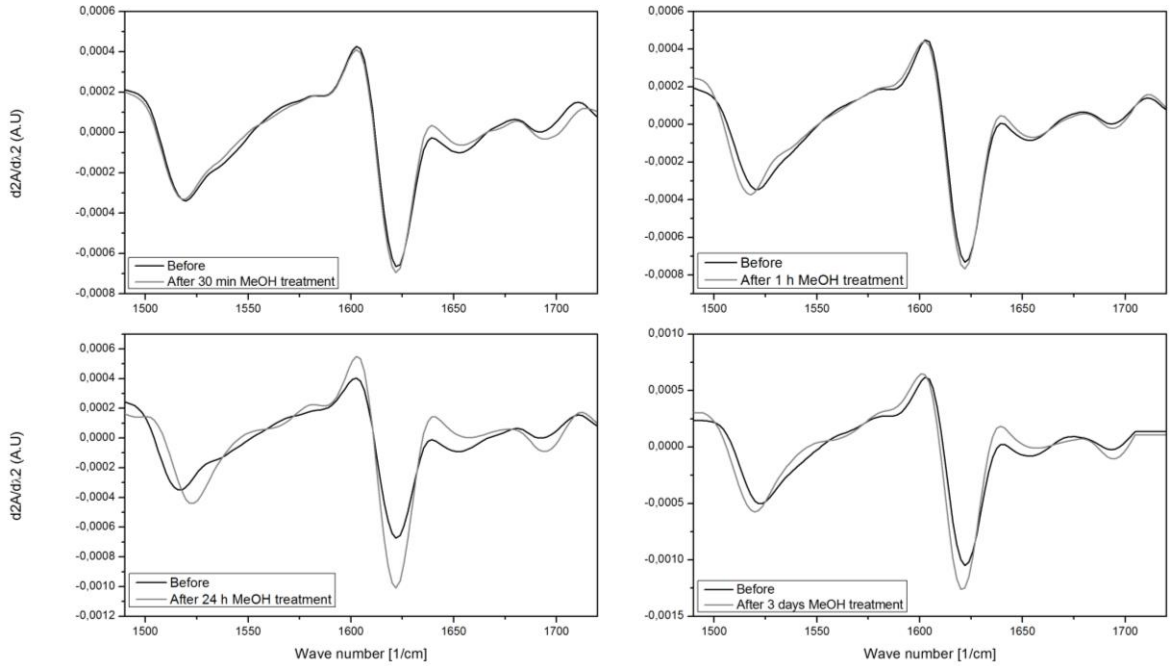

Figure 13: Second derivate FT-IR spectra of water-based spider silk films, before and after incubation in methanol water for: 30 min, 1 h, 24 h and 72 h. Every spectra is the average of nine different measurements of three different films (three measurements for each film).

Furthermore, the water solubility of the treated films was tested (Table 11). It was found that the methanol treatment did slightly decrease the water solubility of spider silk films. After 6 days of measurements, the untreated films lost around 5.8% of their initial mass, while films treated with methanol lost between 5.7 and 4.4%. Although, only after 1 day of post-treatment it was possible to notice a distinguished difference between untreated and treated films.

Table 11: Water solubility of water-based spider silk films post-treated with methanol for different time frames, n = 3 for each condition

	Loss in Mass % w/w measured after:			
Time of treatment with MeOH	1 h	1 day	3 days	6 days
none	4.67 ± 0.01	5.45 ± 0.06	5.63 ± 0.06	5.81 ± 0.05
30 min	4.55 ± 0.03	5.36 ± 0.04	5.56 ± 0.04	5.72 ± 0.06
1 h	4.32 ± 0.12	5.25 ± 0.06	5.48 ± 0.03	5.62 ± 0.04
1 day	3.36 ± 0.07	4.19 ± 0.07	4.47 ± 0.09	4.65 ± 0.07
3 days	3.12 ± 0.05	3.94 ± 0.04	4.23 ± 0.02	4.42 ± 0.01

In conclusion the methanol treatment was not employed for further studies in this thesis, as it did only slightly increase the water insolubility of films. Furthermore, the methanol treatment represents s an additional process, which requires rather long incubation times and involves the use of an organic and toxic solvent.

3.3.7. Water Absorption and Desorption

In order to analyze potential differences in hydration behavior of the films, water absorption and desorption isotherms were collected by IGASorp (Figure 14).

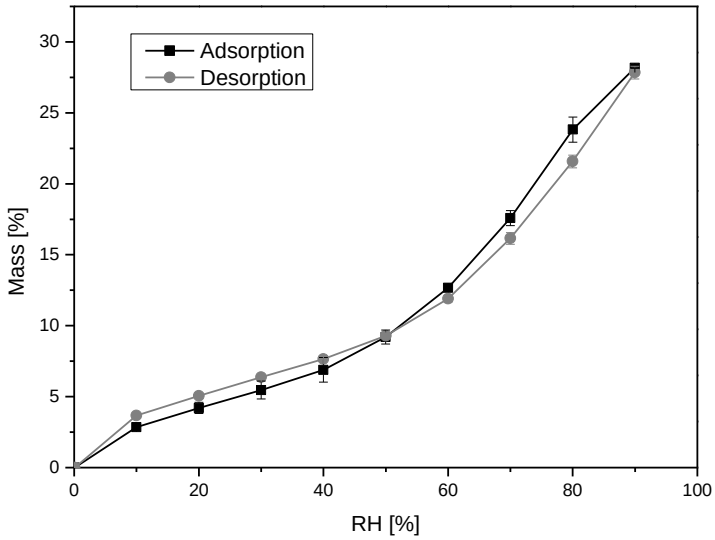

Figure 14: Water absorption and desorption profiles of water-based spider silk films. Each point represents three measurements of the same film.

As shown in Figure 14, after 3 cycles of water absorption and desorption, the hydration behavior of the film did not change. Spider silk films can adsorb water up to 28% of their weight. No substantial hysteresis was observed, suggesting a completely reversible hydration state of these protein films.

3.3.8. Zeta-potential

Electrostatic interactions have been shown to play a major role in drug loading onto spider silk particles [65] and spider silk films [143]. Therefore, water-based spider silk films were further characterized regarding their surface charge using the SurPass instrument (Figure 15). The experiment was carried out by Dr. Thomas Luxbacher from Anton Paar.

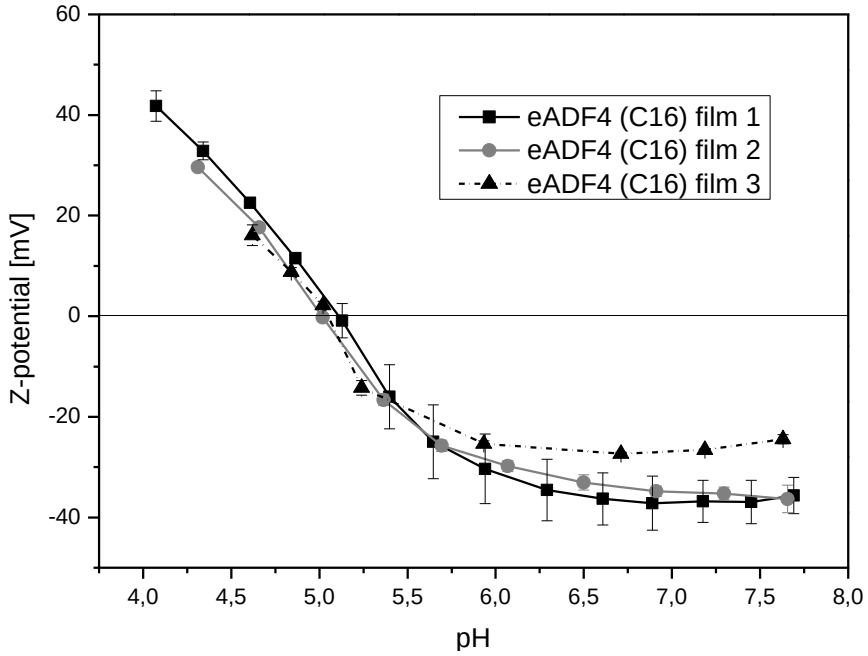

Figure 15: Zeta-potential measurements of water-based spider silk films (n=3).

The isoelectric point of eADF4(C16) proteins in films was measured at around 5, meaning that spider silk films were positively charged at a pH below 5 and negatively charged at a pH above 5. In conclusion, water-based spider silk films are negatively charged at physiological pH.

3.3.9. Mechanical Properties

With regard to the mechanical properties, spider silks are undoubtedly remarkable polymers [51, 77]. However, films prepared from aqueous solution showed a very high elastic modulus, although only a low elongation (Table 12). It appeared that spider silk films were not as elastic as natural spider silk [77]. This is due to the fact that the recombinant protein eADF4(C16) is based on the amino acid sequence of the natural spider silk protein ADF4, which along with the protein ADF3 composes the major ampullate silk produced by the spider *A. diadematus* [78]. This is a kind of silk characterized by high strength, while other silks, e.g. flagelliform silks, are known for their elastic properties [78]. According to that, water-based eADF4(C16) films exhibit impressive tensile strength, above 5000 MPa. This quality could be fundamental for different applications where stiffness plays an important role in designing products which have a maximum

deflection requirement. To assess the spider silk films´ tensile properties, those were compared with the mechanical properties of three standard materials in Table 12. Overall, spider silk films showed similar mechanical properties like poly(l-lactic acid) films. In general, eADF4(C16) films cast from water were stiffer than Nylon 66, poly-(l-lactic-acid) and ultra-high-molecular-weight polyethylene films. On the other hand, water-based spider silk films were very brittle compared to these standard films. In order to increase the film elasticity, plasticizers were included in the film casting solution. The addition of glycerol or 2-pyrrolidone as plasticizers in the film matrix resulted in a tremendous increase in elongation (60 times higher), and in a loss in stiffness (12 times lower) (Table 12). In conclusion, the incorporation of small hydrophilic plasticizers can affect the mechanical properties of water-based spider silk films increasing their elasticity but reducing their stiffness. These measurements were carried out by Michael Bergfield from AmSilk.

Table 12: Tensile test of different spider silk films and comparison with three standard films made from Nylon 66, poly(l-lactic acid) (PLLA) and ultra-high-molecular-weight polyethylene (UHMWPE) respectively. h: thickness Et: elastic modulus; σM: tensile strength maximal; εM: elongation at maximal strength (% over the initial length).

FILM	h (μm)	Et (MPa)	σM (MPa)	εM (%)
eADF4(C16)	29 ± 4	5500 ± 530	81.2 ± 34.8	1.8 ± 0.83
eADF4(C16) + glycerol	31 ± 5	458 ± 164	20.6 ± 1.97	110 ± 21
eADF4(C16) + 2-pyrrolidone	35 ± 6	274 ± 99.1	36.9 ± 4.35	130 ± 18
Nylon 66	25	1170 ± 62.7	68.6 ± 6.9	470 ± 86
PLLA	50	3210 ± 84	35.9 ± 0.2	1.3 ± 0.05
UHMWPE	75	752 ± 52	23.6 ± 0.01	350 ± 55

3.4. Conclusion

In this study, spider silk films cast from aqueous solution were prepared without the use of any organic solvent. The film surface was smooth, compact and homogeneous. Only small molecules were able to diffuse through the film matrix. Water-based spider silk films were characterized by a high content of β-sheet protein structures, which led to water insolubility and to a high elastic modulus. The elongation of the films can be increased by adding small hydrophilic plasticizers in the casting formulation. Methanol post-treatment slightly increased water insolubility, and therefore it was concluded that such treatment was not necessary. Thermal analysis showed that spider silk films showed excellent thermal stability up to 200°C. The films were negatively charged at physiological conditions. In conclusion, the protein secondary structure was responsible for the film properties, therefore its analysis is essential to predict and understand the film's behavior. An useful analytical tool to evidence the secondary structure of the protein eADF4(C16) in the film matrix were the combination of DSC and FT-IR.

4. SSP Films as Drug Delivery Matrices

4.1. Introduction

The aim of this Chapter is to investigate the potential of spider silk films as drug delivery matrices. Films were loaded with a variety of molecules (phenol red, paracetamol, ethacridine-lactate, nipagin, tetracaine hydrochloride, lysozyme, dextran, and albumin–fluorescein isothiocyanate conjugate) exploring two different loading techniques: remote loading and direct loading. Furthermore, different film designs were prepared, such as: monolayer, coated monolayer, multilayer (sandwich), and coated multilayer. This investigation focused also on possible improvements in the film's mechanical properties using glycerol and 2-pyrrolidone as plasticizers in the film matrix. Additionally, this Chapter reports on a new method to prepare spider silk multilayer films. Here the model protein BSA was embedded in a sandwich format. It was then studied how the presence of a plasticizer in the film matrix affects the release of the model protein BSA. Furthermore, various water-based eADF4(C16) films were coated with a concentrated spider silk solution and the release of the model protein BSA from these new systems was studied. Finally, the biodegradation *in vitro* of spider silk films containing 2-pyrrolidone was also considered. The main focus of this work was to obtain a drug delivery matrix characterized by biocompatibility, water insolubility and good mechanical properties. Moreover the preparation process should be compatible with protein encapsulation and the obtained matrix should be able to release a model protein for a prolonged time.

4.2. Methods

4.2.1. Remote loading of LMW Drugs and Lysozyme

Low molecular weight drugs phenol red, paracetamol, ethacridine-lactate, nipagin, and tetracaine hydrochloride were dissolved at a concentration of 0.5 mg/mL in highly purified water (HPW), Tris 5 mM pH 7, and formate buffer 5 mM, pH 3, respectively. After dissolving the drugs, all solutions were filtered through a

0.45 µm cellulose acetate filter to remove particles. Calibration curves for each drug solution were prepared using a NanoDrop 2000 (peqlab, Erlanger, Germany). For the remote loading process, the previously cast spider silk films were cut into 4 pieces, weighed and placed into 24-well plates. At least four film samples were incubated with 1 mL of each drug solution for 30 min at gentle agitation with 2 rpm at room temperature. After removing the films, the quantities of the loaded drugs were calculated indirectly by measuring the remaining loading solutions photometrically by NanoDrop. Finally, the loading efficiency (LE) for each experimental condition was calculated as follows:

$$\textbf{LE (w/w \%)} = \frac{mass\ of\ the\ drug\ loaded}{mass\ of\ the\ initial\ drug\ presented\ in\ the\ loading\ solution} \cdot 100 \quad [65]$$

For the remote loading of a model protein, the loading solution was prepared dissolving 1% w/v lysozyme in HPW. Three different films were weighed. Afterwards, films were incubated in a 6-well plate with 5 mL of the loading solution at room temperature at 2 rpm. After 30 min, films were removed and the loading solution was analysed UV-photometrically at 280 nm. Spectra were recorded using a spectrophotometer (Agilent Technologies 8453, Oberhaching, Germany). A calibration curve was prepared using a lysozyme solution. The loading and loading efficiency were calculated as described above.

4.2.2. Direct Loading and Release of Paracetamol, Dextran, and BSA

2.5% SSP1 protein solution was prepared as described in 3.2.1. Before casting the films, tetracaine hydrochloride and paracetamol as model drugs were added and dissolved directly in the spider silk protein solution, respectively. Films were casted as described above. The resulting films contained each 2.5 mg of drug (0.33 mg/cm^2). Three film samples containing paracetamol were incubated in 0.01 M PBS buffer pH 7.4 at 37°C, 5 rpm. 0.05% w/v sodium azide was added to the

phosphate buffer as preservative. At predetermined time points, the buffer was removed and replaced with fresh medium. The release buffer was analyzed by NanoDrop 2000 (peqlab, Erlangen, Germany) at 242 nm. The released paracetamol was quantified using a calibration curve.

A 20 mg/mL of FITC-BSA, or FITC-dextran (FD), solution in 0.01 M PBS buffer pH 7.4 was directly mixed with the spider silk solution. Films were cast as described above. Every film contained 25 mg of eADF4(C16) and 1.3 mg (173 μg/cm^2) of FITC-BSA or FD. Films containing the model drugs were incubated in 0.01 M PBS buffer pH 7.4 at 37°C, 5 rpm. Again, 0.05% w/v sodium azide was added to the phosphate buffer as preservative. At predetermined time points the buffer was removed and replaced with fresh medium. The release buffer was analyzed by a fluorescence spectrophotometer Cary Eclipse Varian (Agilent technology, Böblingen, Germany) applying an excitation wavelength of 490 nm and an emission of 520 nm. FD and FITC-BSA releases were quantified using a calibration curve. The drug, which was not released, was quantified by dissolving the film matrix in a 6 M GudmSCN solution. This solution was subsequently analyzed using the fluorescence spectrophotometer. The quantity of the non-released drug was determined again using a calibration curve. The sum of the non-released substance and the released amount of substance was calculated as 100%.

4.2.3. Preparation of Multilayer Films, Loading and Release of BSA

Films containing the model protein FITC-BSA were prepared by adding 1% w/v of glycerol directly in the casting solution (3.2.1.) and mixing it for 3 min. Afterwards, a 20 mg/mL FITC-BSA solution in 0.01 M PBS buffer pH 7.4 was directly mixed with the spider silk solution. Films were cast as described above. Every film contained 25 mg of eADF4(C16) and 1.3 mg of FITC-BSA. Typically, one film, containing the model protein and the plasticizer, was positioned between two spider silk films which did not contain any plasticizer (3.2.3) and using a hydraulic press 5T (Maassen GmbH, Reutlingen, Germany) films were pressed together applying 9.8 kN for 5 min, creating three-layers films where only the middle layer

contained the model protein. The release of FITC-BSA was investigated as described in 4.3.3.

4.2.4. Spider Silk Coating of Film Matrices

Monolayer films containing only the model protein FITC-BSA, monolayer films containing FITC-BSA and glycerol, and finally, the 3-layers films (containing 1% w/v glycerol and the model protein in the middle layer) were coated by dipping them in a 5% w/v eADF4(C16) solution. After the films were completely immersed in the silk solution they were placed on a plastic foil A5 22/5B from mtv-messtechnik (Koeln, Germany) using forceps. The contact with the forceps did not damage the coating formation process because once the films were positioned on the card, the liquid coating rearranged itself homogenously on the film surface. The coated films were left drying overnight at RT in the dark. The 5% w/v spider silk solution was prepared by a second dialysis of the previously protein solution obtained by the method described in 2.2.1 against 5 mM Tris/HCl buffer, pH 8 at 4°C, containing 10% w/v of PEG 20 kDa. The release of FITC-BSA, from all these different systems, was investigated as described in 2.2.9. At least three film samples for each condition were used for this study.

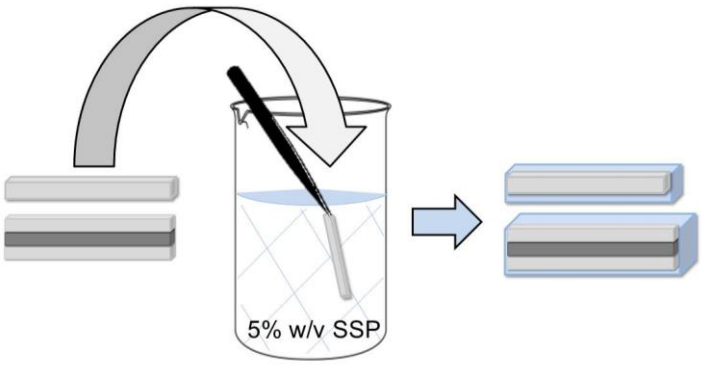

Figure 16: All-aqueous coating process using a highly concentrated spider silk solution of multi- or mono- layers made of the same spider silk protein eADF4(C16).

4.2.5. Biodegradation of Spider Silk Films

The biodegradability of water-based spider silk films containing 2-pyrrolidone (2.2.1.) was evaluated adapting the method described in [65] and in [143]. Briefly,

eight films were weighted using a microbalance. Four films were incubated at 37°C, 2 rpm, each in 2 mL PBS 10 mM pH 7.4 containing 0.8 μg of elastase and 12.5 μg of trypsin. Meanwhile, a control group, composed by four other identical films, was incubated at the same condition in PBS buffer without enzymes. After defined time points, the incubation media were removed and films were washed twice, each time with 5 mL of highly purified water. Films were left to dry overnight at room temperature. After that, films were weighed on a microbalance and a new incubation step was started using fresh enzymes or buffer solution respectively. After ten days of this set up, the experiment continued with three films for each group, and this time the enzymes' concentration was increased five times (4 μg elastase and 62.5 μg trypsin). The test was carried out in this new condition for another 6 days monitoring the film masses. After that, SEM film surface analysis was conducted. Scanning electron micrographs were collected after the films were immobilized on Leit-Tabs (Plano GmbH, Wetzlar, Germany) to a sample holder. Samples were carbon sputtered under vacuum and analyzed by Joel JSM-6500F field emission scanning electron microscope (Joel Inc., Peabody, USA).

4.3. Results and Discussion

4.3.1. Remote Loading

As described in paragraph 3.2.12 (page 40), the isoelectric point of spider silk films is around 5. Consequently, due to electrostatic interactions, molecules with positive charge are attracted to the negatively charged spider silk protein matrix at a higher pH value than 5, while molecules with a negative charge can diffuse into the positively charged spider silk protein matrix at pH values below 5. For the remote loading strategy, five low molecular weight drugs were chosen according to their predominant charge at different pH values (Table 13). The influence of pH was investigated by performing experiments using different solutions: formate buffer 5 mM pH 3, Tris buffer 5 mM pH 7, and in highly purified water (HPW).

Table 13: Predominant net-charge of the small molecules selected at different pH conditions.

	pH 7	pH 3	HPW
Paracetamol	neutral	neutral	neutral
Ethacridine-lactate	+	+	+
Nipagin	neutral	neutral	neutral
Phenol-red	-	-	-
Tetracain-HCl	+	+	+

Table 14: Remote loading of different small molecular weight drugs and the model protein lysozyme. The loading efficiency (LE) was determined at different pH and different ionic strength. HPW represents highly purified water.

	pH 7 LE (%)	pH 3 LE (%)	HPW LE (%)
LMW drugs			
Tetracaine HCl	24.3 ± 7.7	0.0 ± 0.0	35.1 ± 8.3
Ethacridine lact.	45.8 ±2.7	16.5 ± 5.4	54.2 ± 3.2
Paracetamol	0.0 ± 0.0	0.0 ± 0.0	0.0 ± 0.0
Nipagin	0.0 ± 0.0	5.3 ± 2.3	9.6 ± 4.3
Phenol red	7.2 ± 2.0	17.2 ± 5.0	2.8 ± 1.3
Model Protein			
Lysozyme	--	--	22.8 ± 0.7

For all the drugs investigated in this study, higher loading efficiencies were observed in HPW (Table 14). In this condition, the interactions between the film matrix and drugs may be maximized due the low ionic strength. Tetracaine hydrochloride and ethacridine monohydrate lactate were positively charged at all pH values tested. As expected, at pH 3 the loading was found to be considerably lower compared to the loading of the eADF4(C16) matrix at pH 7 and in HPW. That can be explained by the fact that at pH 3, eADF4(C16) films are positively charged and the remote loading of positively charged drugs is therefore severely limited. As expected, no loading of the spider silk films was measured for paracetamol. Since paracetamol is a neutral molecule, no loading was possible due

to the lack of electrostatic interactions. In contrast, some loading was observed for nipagin at pH 3 and in HPW. Nipagin is a neutral molecule such as paracetamol, but in these circumstances the remote loading probably occurred due lipophilic interactions. Nipagin is characterized by a logP of 1.86, while paracetamol has a logP of 0.38. Therefore it is conceivable to assume that the loading of nipagin took place due to its lipophilic affinity with the hydrophobic protein eADF4(C16). In fact, the mean hydrophaticity of this spider silk protein has been calculated -0.464, describing its poor water solubility [94]. A similar aspect was observed in case of remote loading of phenol red. Phenol red exhibits a negative charge at all conditions investigated in this study. Reasonably, the highest loading was measured at pH 3. Nevertheless, surprisingly some loading was also observed at pH 7 and in HPW. These measurements can be explained considering that phenol red is characterized by a logP about 3. This leads to the conclusion that not only electrostatic interactions, but also hydrophobic interactions seem to play an important role in the remote loading of spider silk films. In a similar experiment conducted on eADF4(C16) particles, the same drugs that we selected were dissolved in water and particles were incubated in these loading solutions [65]. Lammel et al. measured an encapsulation efficiency of about 98.2% for ethacridine, 53% for tetracaine, 0.2% for paracetamol, 17.3% for nipagin, and 0% for phenol red. These results are in accordance with the data presented here. The higher encapsulation efficiency of particles, in comparison with the film loading efficiency, can be explained by the larger surface area displayed by particles. In a further step, remote loading of the model protein lysozyme was considered. Lysozyme has an isoelectric point of 11.35, is positively charged at physiological pH and should be able to interact with the negative charged eADF4(C16) film matrix. In fact, the remote loading of eADF4(C16) films with lysozyme performed in HPW, demonstrated that it is possible to load high molecular weight molecules by remote loading by exploiting the electrostatic interactions between spider silk matrix and protein (Table 14).

4.3.2. Direct Loading

In the past, different molecules have been loaded on spider silk particles and spider silk films by remote loading [65, 67, 143]. In these studies, eADF4(C16) particles and films were incubated in a drug solution and the loading was mainly driven by electrostatic interactions. An alternative way for loading drugs is direct loading, which means that the water soluble drug is directly dissolved in the casting silk solution or, alternatively, the spider silk solution is mixed with a second solution containing the dissolved drug, and films are cast. The advantage of this method is the one-step process and the known amount of the drug directly incorporated, which leads to theoretical 100% of drug loading.

To investigate the potential of this manufacturing technique, both paracetamol and tetracaine HCl were chosen as small molecular weight drugs, FITC-dextran (20 kDa) as a middle molecular weight model and finally, lysozyme (14.3 kDa) and FITC-BSA (66.5 kDa) were chosen as model proteins. The direct loading of paracetamol was successfully performed by dissolving the drug directly in the 2.5% eADF4(C16) casting solution.

The resulting films showed a smooth, transparent, colorless surface that resembled the non-loaded films. On the contrary, when tetracaine hydrochloride was added to the spider silk protein solution, the protein solution turned into a milky non-transparent solution, which resulted in inhomogeneous drug distribution and an irregular film surface as shown in Figure 17. Paracetamol had a neutral charge at pH 8 (pH of the spider silk solution), while tetracaine hydrochloride was positively charged, which consequently resulted in a different spider silk protein-drug interaction.

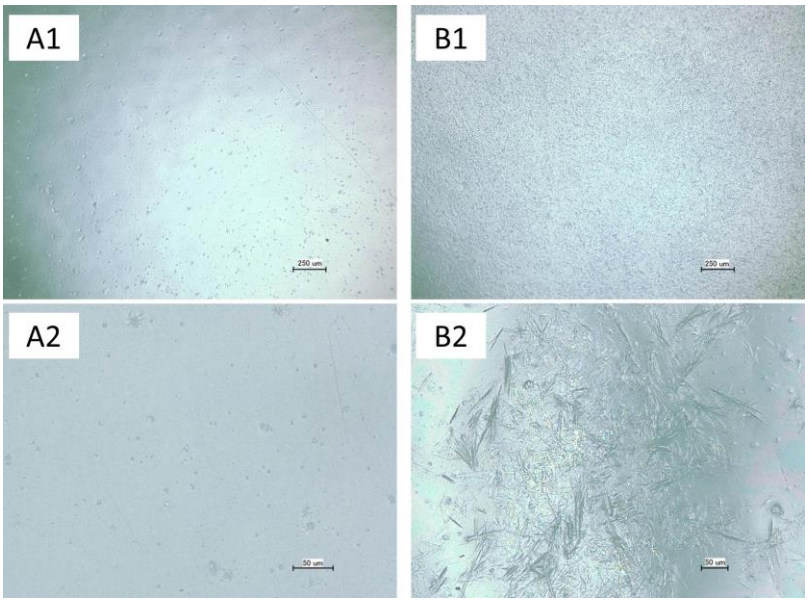

Figure 17: Image obtained with a digital microscope showing the surface of water-based spider silk films direct loaded with paracetamol (A1 and A2) and direct loaded with tetracaine hydrochloride (B1 and B2). A1 bar = 250 µm; A2 bar = 50 µm; B1 bar = 250 µm; B2 bar = 50 µm.

Similarly, no direct loading was possible in the case of lysozyme. When lysozyme was added to the casting solution of spider silk, protein aggregation was observed and no films could be cast using this mixture. Strong electrostatic interactions between eADF4(C16) and the direct loaded drug have a negative effect on the casting solution. On the other hand, direct loading of FITC-dextran, a non-charged polymer of 20 kDa, was achieved successfully. Similarly, direct loading was successfully performed by adding a solution of FITC-BSA to the casting solution. According with the product information of Sigma-Aldrich, BSA has a molecular weight of 66.43 kDa and an isoelectric point (PI) of 4.9, close to the one found for the spider silk protein in the film matrix (Figure 4). The two different proteins share the same charge at different pH values, and so, electrostatic attraction between them is highly unlikely. Interestingly, in a recent study it was shown that FITC-BSA is not able to permeate into eADF4(C16) spider silk particles [67]. So, while the remote loading of proteins, sharing the same charge as the spider silk protein (at the process pH), was impeded for a lack of electrostatic interactions, direct loading of these biomolecules was also difficult due to technical reasons for spider silk particles [65, 67]. On the contrary, direct loading of proteins was

possible for films. Neutral molecules (paracetamol, dextran) and molecules sharing the same charge (BSA) did not disturb the eADF4(C16) structure in buffer solution, therefore no aggregation was observed and direct loading was effectively accomplished. In summary, direct loading is a method applicable to those drugs that do not strongly interact with the spider silk protein in solution. On the contrary, remote loading is ideally recommended for loading of those drugs having a strong opposite charge and a high logP.

4.3.3. Release from Direct Loaded Spider Silk Films

Water-based spider silk films were direct loaded with various molecules: paracetamol, FITC-dextran, and FITC-BSA. Following, the *in vitro* release from these systems has been investigated. The results of the studies on monolayer films showed that the release depended on the molecular weight of the drugs. On the one hand, spider silk films completely released paracetamol and FITC-dextran in a short time period (Figure 18).

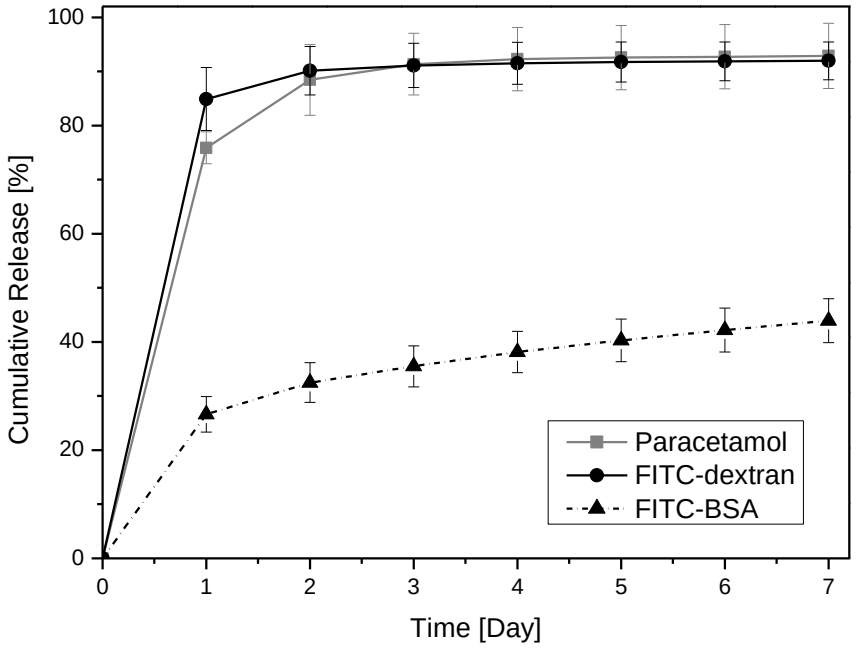

Figure 18: Release of paracetamol (n=3), FITC-dextran (n=3) and FITC-BSA (n=4) from water-based eADF4(C16) films (monolayers).

On the other hand, the release of FITC-BSA, which is six times larger than that of dextran, was observed to be slower. This is in agreement with a previous observation in the literature [159], where a molecular weight cut-off of 27 kDa was reported for spider silk microcapsules. Additionally, there are earlier reports in literature [160, 161] where it was shown that the release of dextran from silk fibroin films depends directly on the molecular weight of the polysaccharide.

It can be concluded, that monolayer eADF4(C16) films can be used to achieve a prolonged release for large molecules (>30 kDa). Interestingly, after a 27% burst release on day 1, spider silk films released the protein BSA in a constant amount per day with a quasi- zero order release kinetic.

4.3.4. SSP Monolayer Films Containing Plasticizers

To characterize eADF4(C16) films containing 1% w/v of plasticizer (glycerol or 2-pyrrolidone), thermograms of these films were collected as described in 3.2.8.

The thermograms (Figure 19), showed two endothermic peaks: the first one corresponded to the boiling point of the plasticizer and the second one correlated with the spider silk protein thermal degradation.

Interestingly, after 1 h incubation time in water, the plasticizers were completely washed out from the film matrix, the thermograms did not show the glycerol or 2-pyrrolidone boiling point peak anymore. Instead, the DSC profiles resembled one of spider silk films without plasticizers presented in Chapter 3.

Additionally, the protein secondary structure of spider silk films containing plasticizer was analyzed by FT-IR. Three different areas for every film were measured and three films each were considered, the average of these nine spectra is showed in Figure 20.

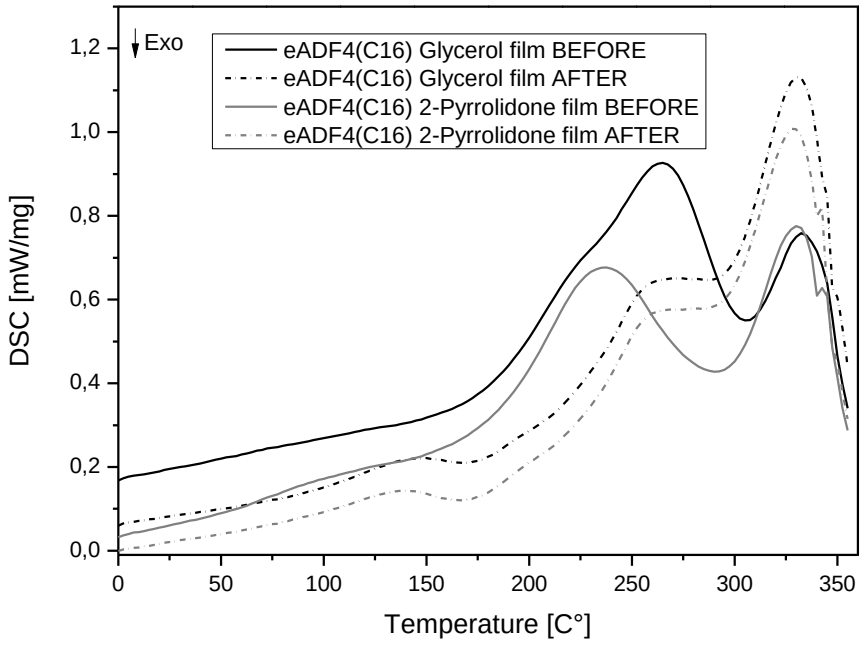

Figure 19: DSC thermograms of water-based spider silk films containing plasticizers before and after incubation for 1 h in highly purified water.

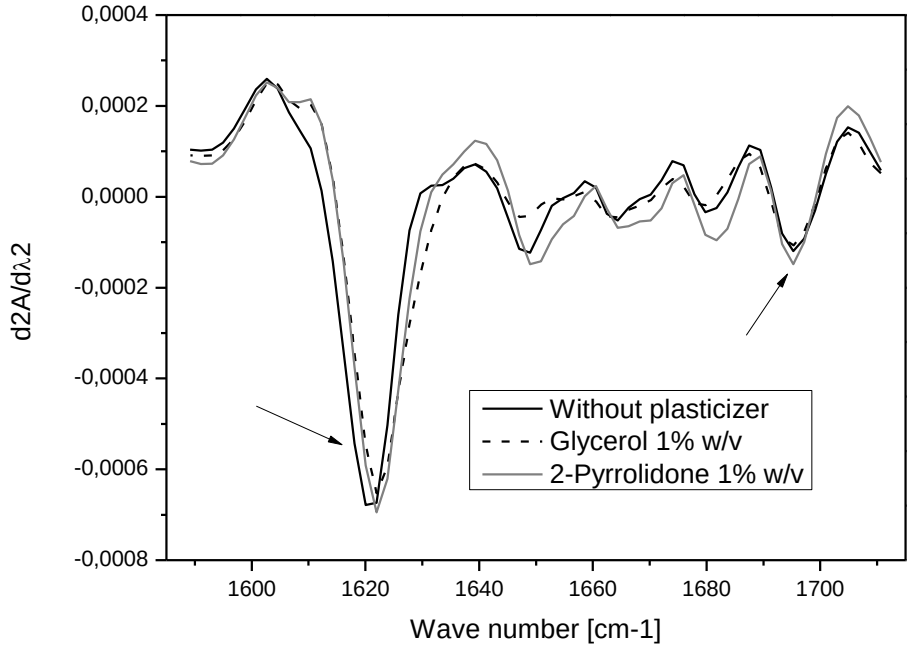

Figure 20: Second derivate of the FT-IR spectra of water-based spider silk films containing plasticizers. The two peaks indicating the presence of β–sheet structures are marked with an arrow.

The analysis of the second derivate of the FT-IR spectra of the amide I band, represented in Figure 20, did not detect major differences between spider silk film without glycerol or 2-pyrrolidone and films containing one of the two plasticizers. Additionally, the presence of plasticizers in the spider silk film matrix did not influence the content of the ß-sheet protein structures:

4.3.5. SSP Films Containing Glycerol: Monolayer

The group of Prof. Kaplan described in a preceding study [162], that the presence of glycerol affects the secondary structure of silk fibroin in silk films by increasing the content of stable silk II structures (crystalline, β-sheets). With regards to the data obtained in the study presented here, the content of β-sheet structures was already high and no alteration was observed in the secondary structure (Figure 20). Glycerol acted as a hydrophilic plasticizer and decreased the hydrophobicity of the spider silk film. This leads to the solubilization of the model protein in the film matrix. In this way BSA was free to diffuse out with glycerol and overall the film released the protein more rapidly as shown in Figure 21. So, if in one hand the addition of glycerol in the casting solution leads to spider silk films characterized by higher elongation in comparison to films without plasticizer (paragraph 3.3.9, page53); on the other hand, its hydrophilic nature is responsible for the releasing 80% of the encapsulated BSA after only one day, while the rest of the model protein was steadily released as before.

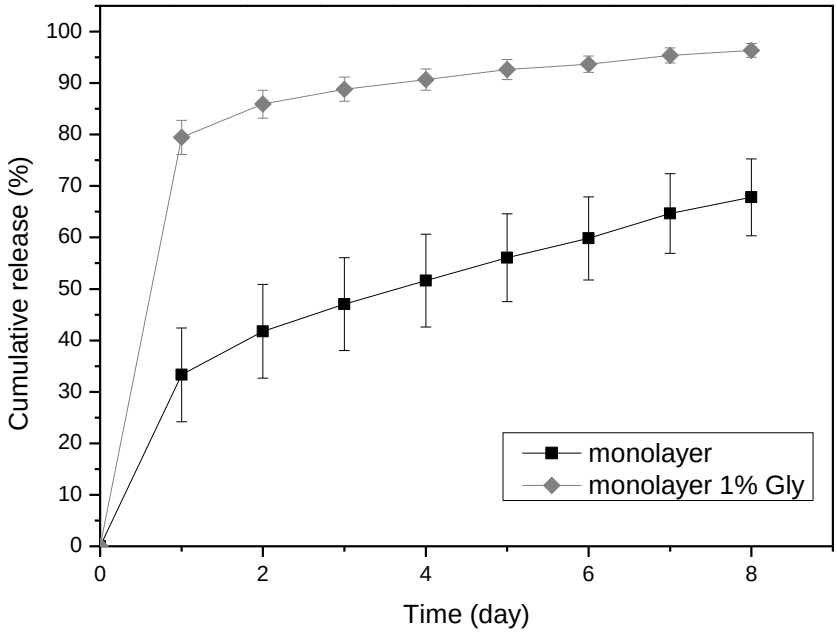

Figure 21: Cumulative release of FITC-BSA from water-based spider silk films (monolayer) and water-based spider silk films containing 1% w/v of glycerol in its casting formulation (monolayer 1% Gly).

4.3.6. SSP Films Containing Glycerol: Multilayer and Coating

Sandwich format films (multilayer) were prepared by compressing one spider silk layer which was directly loaded with FITC-BSA between two non-loaded spider silk films. This procedure (Method 4.2.3) permitted to obtain multilayer films by simply applying pressure, which resulted in an easy, quick and low priced manufacturing technique. One prerequisite for the successful formation of multilayer films was the addition of glycerol to the middle spider silk matrix, the one containing the model protein. The following picture is intended to show the concept of the sandwich format, while Figure 23 represents the cross section of a spider silk sandwich created using the Method 4.2.3.

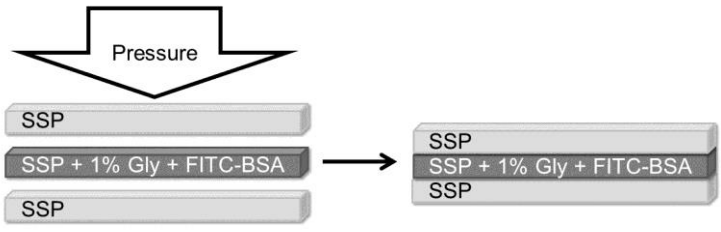

Figure 22: Graphical representation of a 3-layers spider silk film design, it consists of two layers of water-based spider silk protein film (SSP) and one layer of a film containing spider silk protein, glycerol and the model protein BSA (SSP + 1% Gly + FITC-BSA).

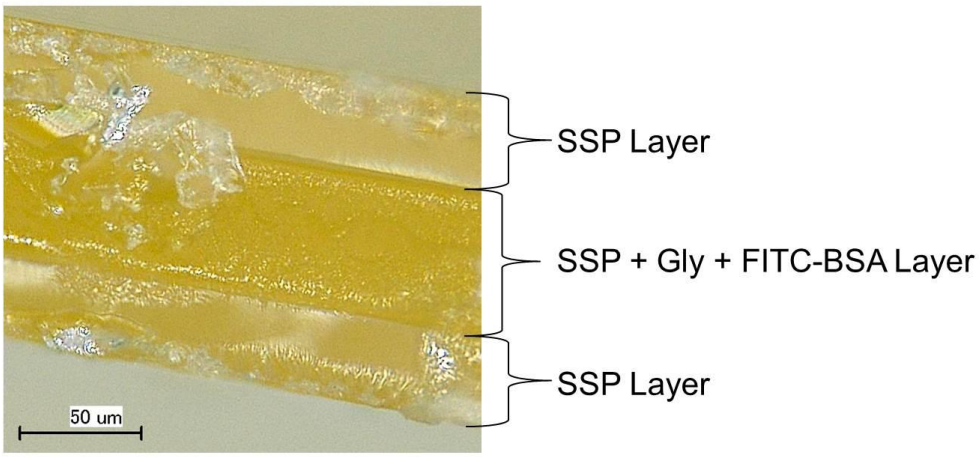

Figure 23: Image obtained with a digital microscope showing the cross section of a 3-layers (sandwich format) water-based spider silk film. The middle layer contains the model protein FTIC-BSA and 1% w/v of glycerol in its casting formulation. The other two layers are composed only by the spider silk protein eADF4(C16).

As described in the previous paragraph, the incorporation of glycerol in the film matrix had a negative impact of the in vitro release profile of the model protein BSA. In order to reduce the burst release and to prolong the release of BSA, the model protein was embedded in a sandwich format (Figure 23). Surprisingly, the release of BSA from a multi-layer system resulted to be much faster than from a monolayer film without plasticizer as shown in Figure 24 A. The reason related to the presence of glycerol in the middle layer of the sandwich, the one containing the model drug. The external layers of the multilayer are intended to slow down the diffusion of the protein through the film matrix, nevertheless BSA is free to diffuse out from the sides where these barriers are not present. In order to seal the multilayer completely, the sandwich was then coated by dipping in a concentrated spider silk protein solution. By coating eADF4(C16) 3-layer films, the desired release profile close to a zero order kinetic was achieved. The coating completely eliminated the burst release and the release of BSA was slowed down neutralizing the glycerol effect (Figure 24 A). A steady release of the model protein over 40 days was achieved (Figure 24 B). On the other hand, a high standard deviation for the release profiles from different samples was recorded.

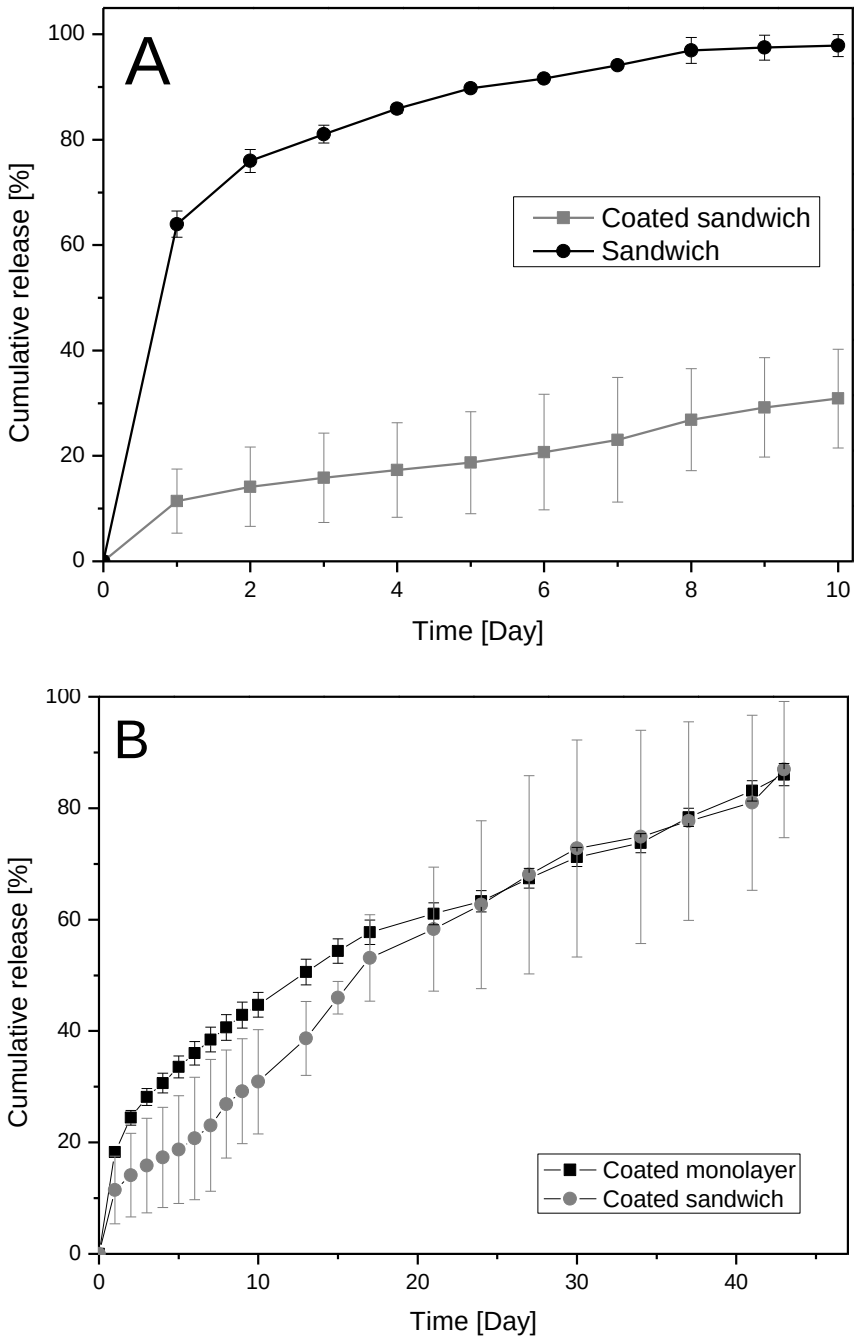

Figure 24: Cumulative release of FITC-BSA from coated 3-layers spider silk films (sandwich) and from coated spider silk film monolayer. A: 10 Days release study of FITC-BSA, released from water-based eADF4(C16) 3-layers films (Sandwich), n=3; and from coated 3-layers films (Coated sandwich), n=3. B: 43 Days release study of FITC-BSA, model protein released from coated 3-layers films (Coated sandwich; continuation of the experiment shown in A), n=3; and from coated water-based eADF4(C16) films (Coated monolayer), n=3.

At this point the possibility to employ a coated monolayer, avoiding the sandwich preparation was considered (Figure 24 B). The same coating process was carried out for the monolayer containing the model protein BSA (and no glycerol). In a subsequent FITC-BSA release study, a reduction of the burst release compared to the non-coated monolayer was observed, and all samples showed reproducible release profiles. This film design led to an improvement of the model protein release (Figure 24 B). However the absence of a plasticizer affected the mechanical properties. Coated monolayers were very brittle and difficult to handle.

Therefore, in a next step, it was investigated whether it was possible to coat the monolayer containing both the model protein BSA and the plasticizer glycerol (Figure 26). This resulted in an extreme decrease of the burst release of BSA (from 50% to 21%) and in a prolonged release of the model protein to over 90 days as shown in Figure 25.

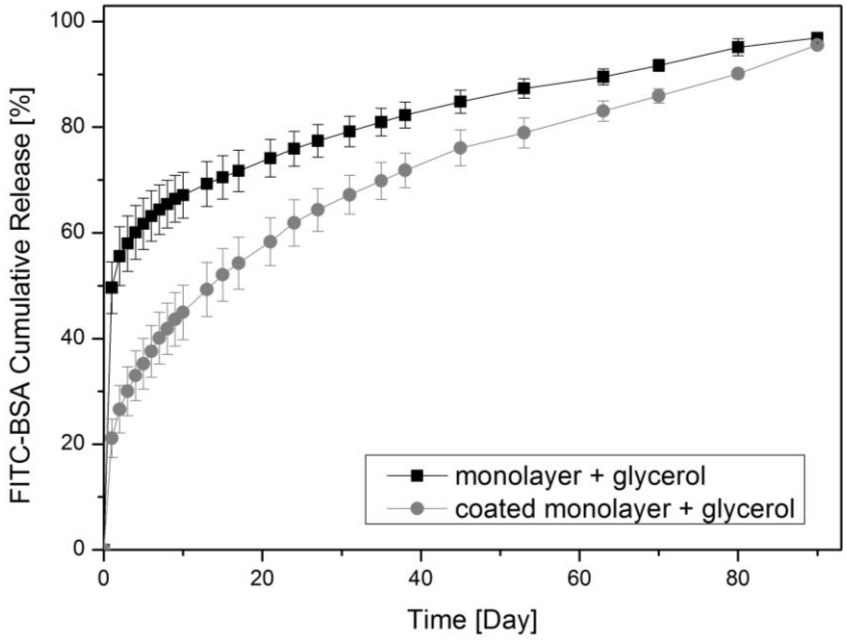

Figure 25: Cumulative release of FITC-BSA from water-based spider silk films containing 1% w/v of glycerol in its casting formulation (monolayer + glycerol) and from coated water-based spider silk films containing 1% w/v of glycerol in its casting formulation (coated monolayer + glycerol).

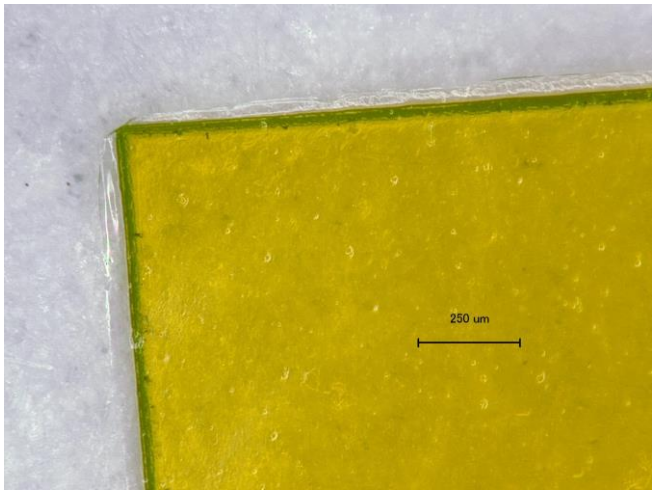

Figure 26: Image of a water-based spider silk film containing glycerol and the model protein FITC-BSA coated with eADF4(C16). Bar = 250 μm

4.3.7. Coating Characteristics

There are different methods in order to process silk materials into coatings, all of them have been presented in a recent review [125]. The techniques used so far include: casting, dip coating, spin coating, electrodeposition, electrospinning, spraying and other printing methods such as lithography. In the work presented in this chapter, dip coating was employed as method to seal spider silk film into a spider silk "capsule" (Method 4.2.4). The main aim of the coating is to act as mechanical barrier by retarding the diffusion of the drug out of the film matrix. Spider silk films loaded with the model protein FTIC-BSA were coated with different concentration of spider silk: 10, 25 and 50 mg/mL. The thicknesses of the resulting coatings are listed in Table 15.

Table 15: Thickness of different coatings

eADF4(16) Film containing:	eADF4(C16) coating solution	N° of films considered	Thickness (μm)
FITC-BSA	1% w/v	1	2
FITC-BSA	2.5% w/v	6	9.17 ± 6.6
FITC-BSA	5% w/v	4	15.75 ± 7.6

As discussed before, the secondary structure of the protein eADF4(C16) plays a major role in defining the film properties (Chapter 3). For this reason, the coatings were analyzed using the FT-IR microscope (Method 3.2.6). All the coatings were characterized by a high content in β-sheet structures, the higher concentrated coating (50 mg/mL) showed a higher intensity of the β-sheet peak at 1625 cm^{-1} (Figure 27). Since a higher content in β-sheets leads to a water insoluble and more stable silk protein matrix [146, 163], the spider silk solution of 50 mg/mL was chosen as preferred concentration for the coating solution.

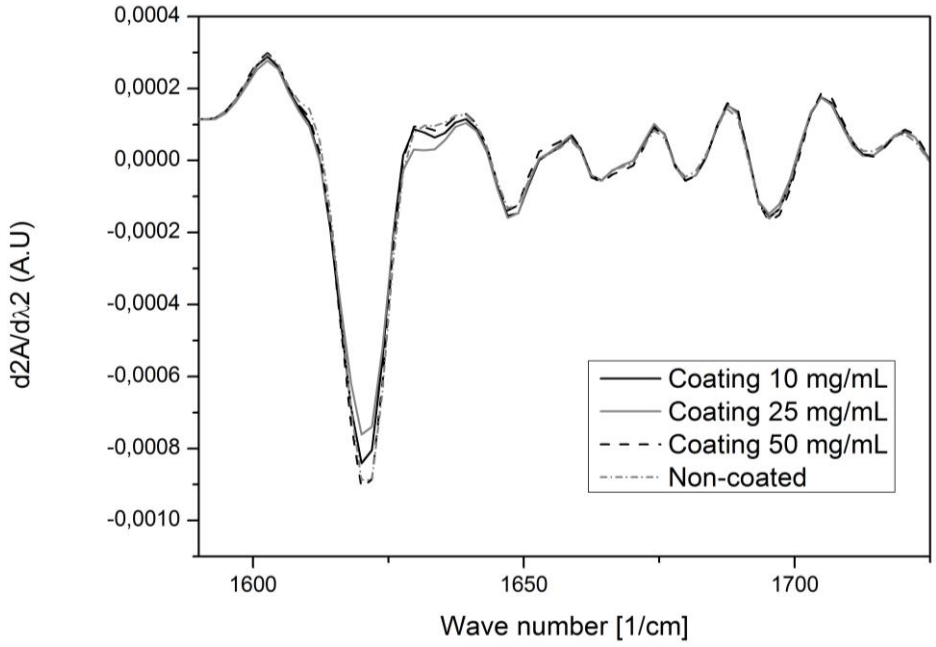

Figure 27: Second derivative FT-IR spectra of water-based spider silk films coated with different concentration of spider silk.

During the time needed for the coating to dry, the solid surface of the spider silk film was in direct contact with the coating solution phase creating a solid-liquid interface. In order to investigate if during this time frame the protein BSA presented in the film surface diffuses into the liquid coating, remains entrapped once the coating has dried, spider silk films containing the model protein were incubated in the liquid coating adapting the Method 4.2.2 for this simulation. The

presence of FITC-BSA in the coating solution was monitored by fluorescence spectroscopy and the quantity of the diffused BSA was calculated using a calibration curve (prepared using different FITC-BSA concentration dissolved in 50 mg/mL spider silk solution). Figure 28 shows the diffusion of BSA into the coating solution.

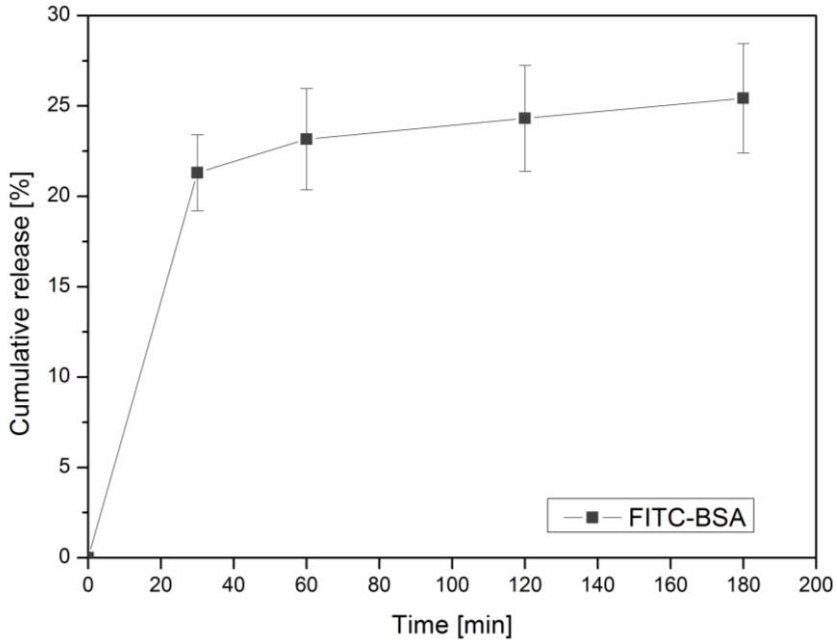

Figure 28: Simulation of FTIC-BSA diffusion from water-based spider silk films into the eADF4(C16) 50 mg/mL coating, n = 3.

After 3 h, about 25% of the BSA was released into the coating solution from the film matrix. The results of this experiment show that during the coating processing a small quantity of the model protein diffuses from the silk film into the coating. These data correlated well with the 20% burst release shown in Figure 24 and Figure 25. Most likely, the initial burst release was caused by the presence of BSA in the coating.

4.3.8. SSP Monolayer Films Containing 2-Pyrrolidone

In the last part of this study, the possibility to replace the plasticizer glycerol with 2-pyrrolidone was considered. eADF4(C16) monolayers containing the model protein FITC-BSA and 1% w/v 2-pyrrolidone were cast. The incorporation of this particular plasticizer led to an improvement of the film mechanical properties increasing 70 times the elasticity of the film (Table 12). Once the films were incubated in PBS buffer, films started to release the model protein with a similar kinetic recorded for the spider silk monolayers without plasticizers (Figure 30). This result is interesting in that the use of 2-pyrrolidone did not escalate the initial burst release as glycerol did (Figure 29). This effect may be explained by the difference between glycerol and 2-pyrrolidone. Glycerol has a logP value of -1.8 and is therefore more hydrophilic compared to 2-pyrrolidone, which has a logP of -0.9). Hence, glycerol may be able to coordinate more water molecules as it has three hydrogen bond acceptor groups, whereas 2-prrolidone only has one hydrogen bond acceptor group.

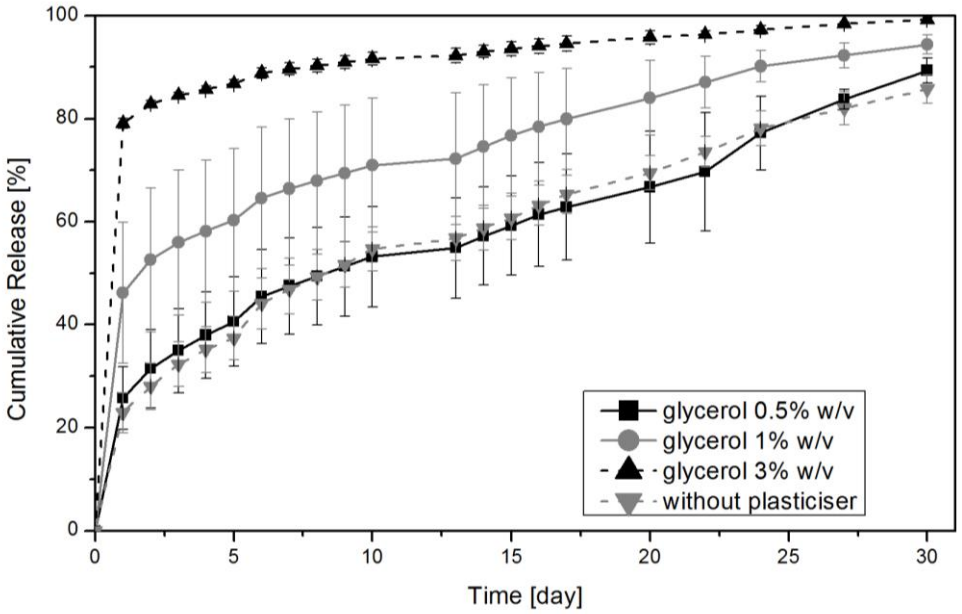

Figure 29: Cumulative release of FITC-BSA from water-based spider silk films containing different concentration of plasticizers. Release of FITC-BSA from eADF4(C16) films containing respectively 0.5, 1 and 3% w/v of glycerol, n = 3 for each condition.

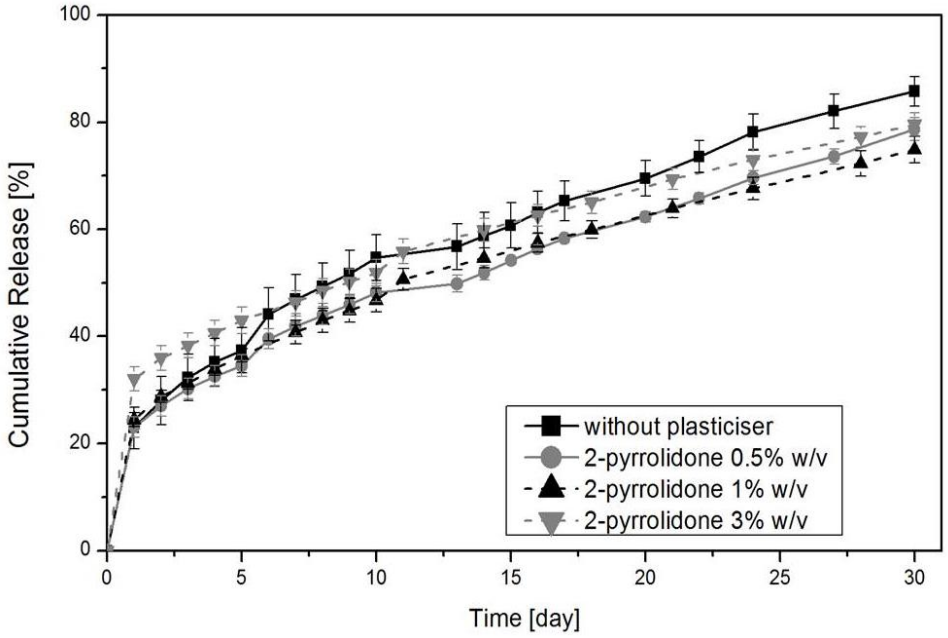

Figure 30: Cumulative release of FITC-BSA from water-based spider silk films containing different concentration of plasticizers. Release of FITC-BSA form eADF4(C16) films containing respectively 0.5, 1 and 3% w/v of 2-pyrrolidone, n = 3 for each condition.

In order to further decrease the 20% burst release occurring at day one, films containing 2-pyrrolidone were coated with eADF4(C16) (Figure 32). Interestingly, the coating did not affect the release of BSA (Figure 31). A large burst release of 20% implicated that a substantial portion of the encapsulated molecule was released rather fast. This phase was followed by a sustained release of the molecule. In some cases it was stated that a zero-order release kinetic is not necessary to create a DDS for sustained release of drugs [164]. The plasticizer 2-pyrrolidone has a higher logP (-0.9) in comparison to glycerol (-1.8). Therefore, the incorporation of 2-pyrrolodone did not influence the release of BSA as previously described for glycerol. The replacement of glycerol with 2-pyrrolidone allowed the formation of a spider silk monolayer which showed good mechanical properties and an interesting *in vitro* release profile, where the bust is limited to 20%. Additionally, this last film design did not require a coating to slow down the release of BSA. In conclusion, spider silk films can be designed as monolithic matrices where a drug is homogenous dispersed. Consequently, the release depends on the drug diffusion in the silk matrix. In accordance with the findings

presented here, it is conceivable to consider the release *in vitro* of a biomolecule from eADF4(C16) films following the Higuchi law [165]. In fact, if the fraction of the released BSA is plotted against the root square of the time, the linear regression has a coefficient of determination (R^2) of 0.9976 for the monolayer and a R^2 of 0.9971 for the monolayer containing 1% w/v 2-pyrrolidone. The films involved in this study were used for in vitro release studies directly after preparation. Therefore a study considering the possible effect of storage on the release profiles should be considered in the future.

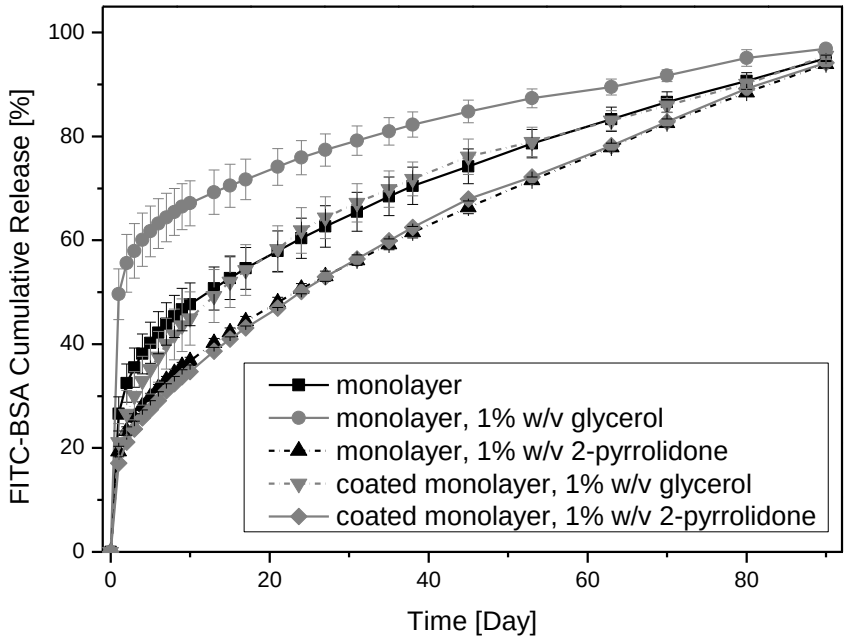

Figure 31: Release of FITC-BSA from different water-based spider silk film films: films containing the plasticizer glycerol (monolayer, 1% w/v glycerol), n=3; coated spider silk films containing glycerol (coated monolayer, 1% w/v glycerol), n=4; films containing the plasticizer 2-pyrrolidone (monolayer, 1% w/v 2-pyrrolidone), n=4; coated spider silk films containing 2-pyrrolidone (coated monolayer, 1% w/v 2-pyrrolidone), n=4; and finally spider silk films without excipients (monolayer), n=4.

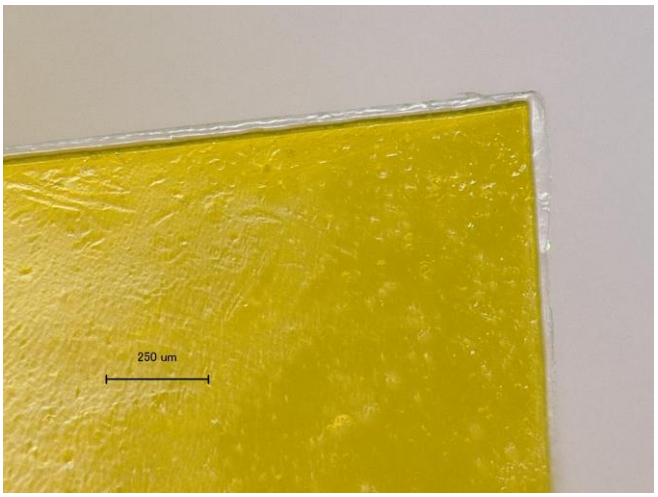

Figure 32: Image of a water-based spider silk film containing 2-pyrrolidone and the model protein FITC-BSA, coated with eADF4(C16). Bar = 250 µm

4.3.9. Biodegradation of SSP Films

One of the great advantages of using eADF4(C16) proteins in developing depot systems is the biodegradability of this protein material. Once the film will be implanted, the spider silk matrix will be slowly cleaved by proteases. The degradation of the spider silk depot system will avoid any additional surgery necessary to remove the DDS. Furthermore, the biodegradation of a DDS is an important characteristic because it can affect drug release kinetics [166].

A multiphase release mechanism for silk matrix was described by Hines and Kaplan [161]. The silk multiphase release is first defined by a phase of diffusion and then followed by a phase of degradation of the silk protein matrix, which is very similar to the mechanism reported for poly(lactic-co-glycolic acid) (PLGA) materials [161]. Silk is an important alternative to PLGA and the advantage of using silk materials lies in the fact that silk will degrade slower than PLGA [161]. Moreover, degradation of PLGA-based DDS can affect the local area where it is implanted, such as changing the local pH [167] or even stimulate an undesired immune response [168-170].

As a preliminary proof of the enzymatic degradation, spider silk films containing 2-pyrrolidone as plasticizer were incubated at 37°C with a buffer solution containing elastase and trypsin, while other films were incubated only in PBS. Elastase is a protease that cleaves specific peptide bonds on the carboxyl side of small, hydrophobic amino acids such as glycine, alanine, and valine. The presence of trypsin was necessary to produce the active form of elastase [65].

Figure 33 presents the loss in mass of spider silk films during the experiment.

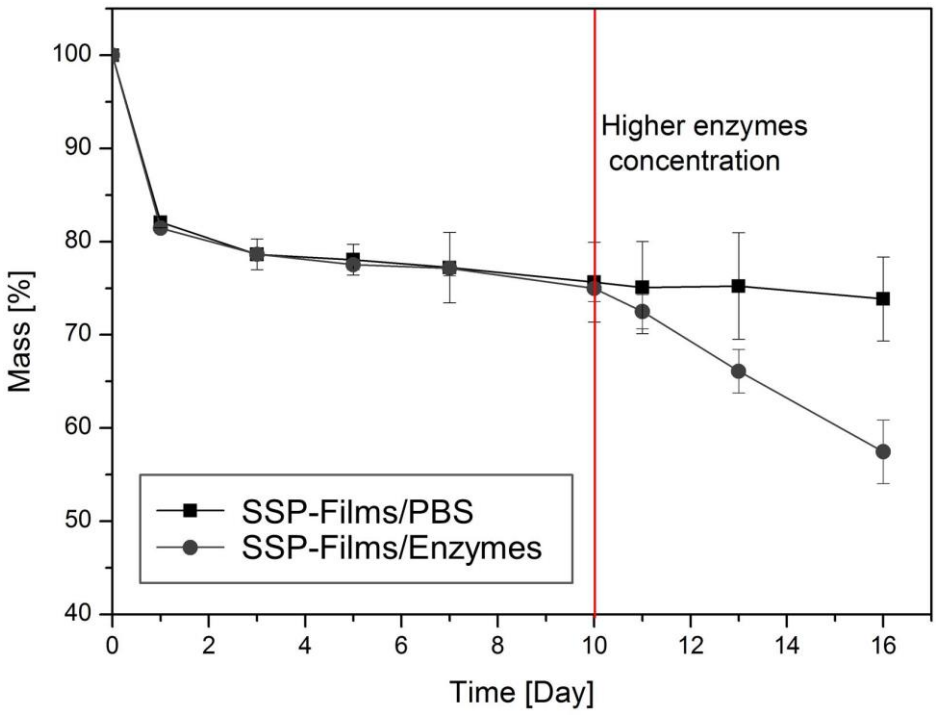

Figure 33: Mass of spider silk protein films containing 1% v/w 2-pyrrolidone during the biodegradation experiment. The "SSP-Films/PBS" group refers to the films incubated in PBS buffer as control group; while the "SSP-Films/Enzymes" group refers to the films incubated with a PBS buffer containing the two enzymes elastase and trypsin. After 10 days the enzymes' concentration was increased five times (red line) in order to highlight the difference in mass loss between the two groups.

After the first day of incubation, both films incubated with enzymes and films incubated only in PBS buffer, showed a drop in weight, caused by the washing out of the plasticizer 2-pyrrolidone. After that, during the 10 days of the study no differences were noted between the two groups and films degraded very slowly. The films incubated with the enzymes lost about 6% of their mass from day 1 to day 10. At that rate, four months would be needed to completely degrade the spider silk film matrix.

Increasing five times the enzymes concentration after day 10, led to a substantial drop in the mass of the films incubated with elastase, and a remarkable difference between the two groups was observed. With this set up, only about one month would be needed to completely degrade the eADF4(C16) films.

Scanning electron micrographs (Figure 34) were additionally acquired to document the degradation observed in this experiment. At the beginning (Figure 34 A; B) the eADF4(C16) film was characterized with a very smooth and homogeneous surface. At the end of the experiment, after 16 days, pores were visible on the film surface (C; D; E; F). SEM micrographs of the film incubated with elastase (E; F) showed more and larger pores compared to films incubated only in PBS buffer (C; D), suggesting the degradation action of the protease. In conclusion, the enzymatic degradation of spider silk films, takes place in presence of elastase and it highly depends on the protease concentration. Appropriate in *vivo* studies are necessary to better elucidate the biodegradation mechanism and its kinetic, as they were carried out in the past for PLGA materials [24, 171, 172].

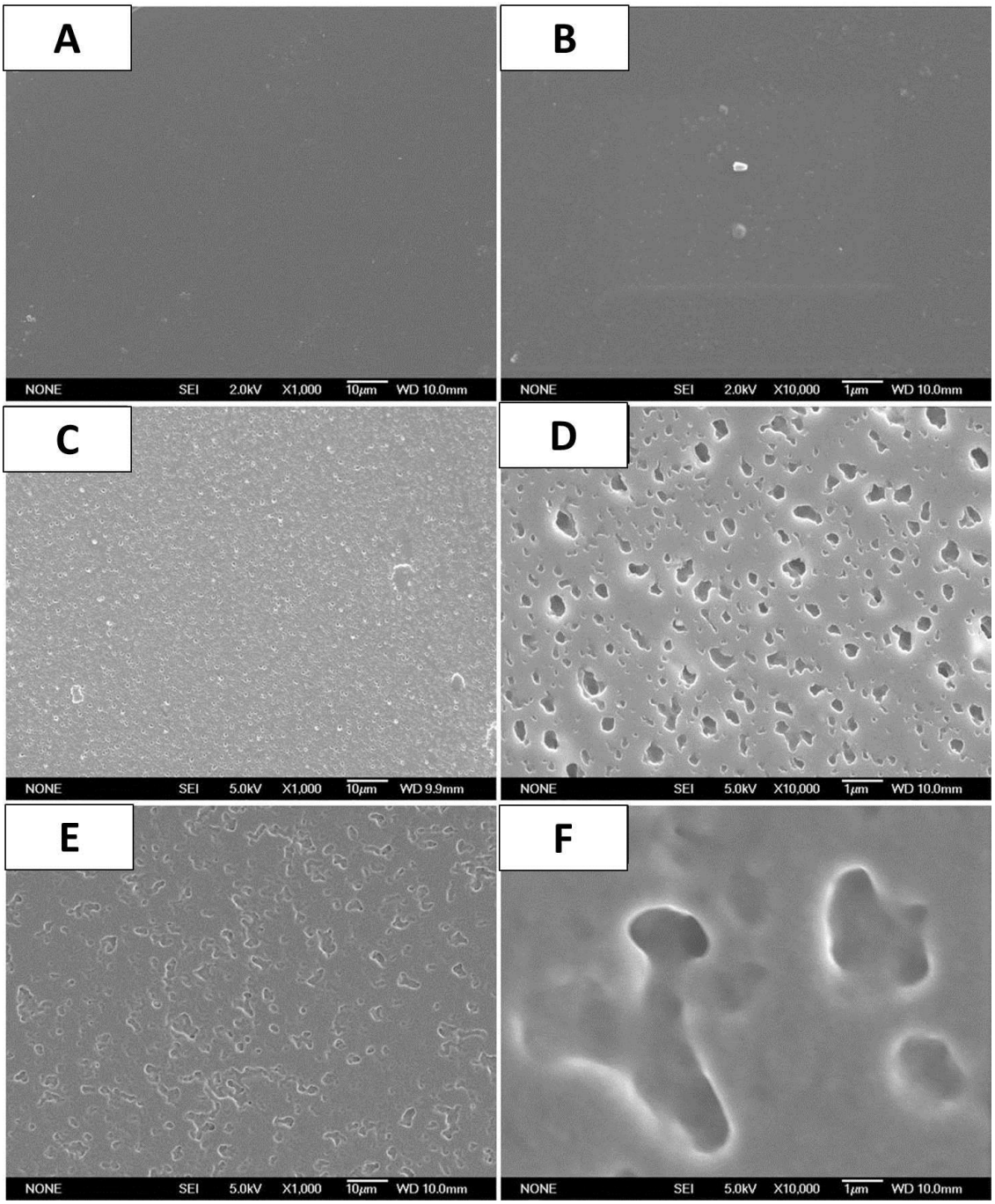

Figure 34: Scanning electron micrographs of spider silk films containing 1% v/w 2-pyrrolidone before and after biodegradation. A: spider silk film´s surface before biodegradation, bar = 10 µm; B: spider silk film´s surface before biodegradation, bar = 1 µm; C: spider silk film´s surface after biodegradation, control group, incubated in phosphate buffer, bar = 10 µm; D: spider silk film´s surface after biodegradation, control group, incubated in phosphate buffer, bar = 1 µm; E: spider silk film´s surface after biodegradation, enzymes group, incubated in phosphate buffer containing elastase and trypsin, bar = 10 µm; F: spider silk film´s surface after biodegradation, enzymes group, incubated in phosphate buffer containing elastase and trypsin, bar = 1 µm.

4.4. Conclusion

This Chapter investigated the potential of spider silk films as drug delivery matrices. The evaluation started with the loading of a variety of drugs exploring two different loading techniques: the remote and direct loading. The remote loading occurred due to electrostatic and hydrophobic interactions. Therefore, this type of loading is ideally recommended for those drugs having a high logP and a strong opposite charge from the spider silk protein. On the contrary, the direct loading is only applicable to those drugs that do not interact with the spider silk protein in solution.

Drug release from direct-loaded eADF4(C16) films was found to be directly related to the molecular weight of the drugs. This release behavior could be advantageous in cases where a small molecule needs to be released immediately from a DDS, e.g. for local, topic, or targeted delivery. On the contrary, larger molecules, as therapeutic proteins, may show a prolonged release from the spider silk films. The incorporation of a plasticizer in the film matrix was necessary to improve its mechanical properties. The presence of glycerol in eADF4(C16) layers affected the films properties tremendously. Although the incorporation of this plasticizer improved the film elongation, it also accelerated the release of the model protein BSA. On the contrary, the use of 2-pyrrolidone did not increase the burst release, nor did it lead to a fast continuous release.

Coating the films with concentrated eADF4(C16) protein solution counterbalanced in part the negative effect of glycerol on the release of BSA. It was possible to produce sandwich format films by compressing different eADF4(C16) layers, when the middle layer contained glycerol. This process was an easy, quick, and low priced manufacturing technique. The production of multilayer films could be advantageous in cases where the quantity of the drug loaded in one monolayer is not sufficient to obtain a therapeutic effect; or when it is necessary to load different drugs which are incompatible together. Incompatible drugs could be loaded in separate layers and then it would be possible to combine the different layers together. Another opportunity could be to create a multilayer composed by layers having different properties and scopes. A monolayer containing 2-

pyrrolidone as plasticizer on the other hand, is easy to prepare, has good mechanical properties and can release a protein in a sustained manner over three months. It was a slow biodegradable film and this particular spider silk film composition is a promising protein drug delivery matrix. Such film could be used for several pharmaceutical and medical purposes, especially in situations in which the mechanical strength of a drug eluting matrix is of high relevance.

5. Scale-up process

5.1. Introduction

As it has been discussed in the general introduction, spider silk proteins for applications in drug delivery have attracted an increased interest during the past years. Some possible future medical applications for this biocompatible and biodegradable material include scaffolds for tissue engineering, implantable drug delivery systems and coatings for implants. The most adopted method to cast spider silk films remains the solvent evaporation technique (Paragraph 1.5, page 23). Since this technology is already integrated in cast film lines in industry, it is in principle easy to adapt from lab-scale to industrial production. But so far, the solvent evaporation technique for spider silk films has only been used in lab scale by direct casting into PTFE forms. Challenges of this manual process are the variation in films thickness and the control of film geometry. Additionally, the number of films produced per time is very limited. In the previous chapter, the preparation of water-based spider silk films for drug delivery applications was shown. The work reported in this chapter describes the development of a manufacturing technique for casting larger spider silk films from aqueous solution employing a film applicator. Films were characterized in terms of morphology, water solubility, protein secondary structure, thermal stability, and mechanical properties. Since the water-based films were first soluble in water, different post-treatments were evaluated (phosphate ions, ethanol, steam sterilization and water vapor) to increase the content of β-sheets to achieve water insolubility. Finally, the mechanical properties of the spider silk films were notably improved by incorporating 2-pyrrolidone as plasticizer.

5.2. Methods

5.2.1. Film Production

Spider silk proteins were dissolved in 6 M guanidinium thiocyanate and subsequently dialyzed against 5 mM Tris/HCl buffer, pH 8 at 4°C. The pH of the protein solution was determined using a pH meter MP 220 (Mettler Toledo, Giessen, Germany). The protein solution was centrifuged at 4°C for 15 min at

10,000 rpm and subsequently filtered through a 0.45 µm cellulose acetate filter. Afterwards, the spider silk solution was dialyzed against 5 mM Tris/HCl buffer, pH 8 at 4°C, containing 10% w/v of PEG 20,000 Da. Protein concentration was determined photometrically using a NanoDrop 2000 system from peqlab (Erlangen, Germany). The protein concentration of the casting solution was finally adjusted to 5% w/v adding 5 mM Tris/HCl buffer. Spider silk films were cast on a plastic foil A5 22/5B from mtv-messtechnik (Koeln, Germany) at room temperature using a film applicator Coatmaster 510 (Erichsen, Hemer, Germany) equipped with a casting knife of 2000 µm. Casting was performed at a velocity of 1 mm/sec. 2 mL of the casting solution were used to cast each film. The surface coverage was about 100 cm^2. The film applicator was placed in a laminar flow cabinet (Thermo scientific, Munich, Germany). After preparation, films were dried overnight at room temperature in the laminar flow cabinet which was closed and switched off. Finally, films were cut into samples of 2.5 x 3 cm using a scalpel. Films containing 2-pyrrolidone were prepared dissolving 2% w/v of the plasticizer directly in the casting solution.

5.2.2. Spider Silk Film Morphology

Photographs of eADF4(C16) films were obtained using a digital camera DSC-S75 (Sony Corporation, Tokyo, Japan). Scanning electron micrographs of the film surface were collected after the films were immobilized on Leit-Tabs (Plano GmbH, Wetzlar, Germany) to a sample holder. Samples were carbon sputtered under vacuum and analyzed using a Joel JSM-6500F field emission scanning electron microscope (Joel Inc., Peabody, USA). SEM pictures were collected with the support of Christian Minke.

5.2.3. Thermal Analysis

Thermograms of spider silk films were obtained by differential scanning calorimetry (DCS 204 Netzsch, Selb, Germany). Spider silk films were loaded in aluminum pans and a small hole was punched in the pan covers. Samples were heated under nitrogen flow at 10 K/min up to 110°C, then cooled to -40°C, followed by heating to 400°C as described previously [145].

5.2.4. Protein Secondary Structure

Fourier transform infrared (FT-IR) spectra were collected using the Hyperon microscope from Bruker Optik (Bruker, Germany) using a 20x attenuated total reflectance objective (ATR). The spectra were an average of 120 scans at the resolution of 4 cm^{-1}. All measurements were performed in the range of 600 and 4000 cm^{-1}. Films were measured in three different areas: in the middle, next to the edge and between the middle and the edge.

5.2.5. Dissolution of spider silk protein from cast films in water

Films were weighed using a balance AT261 Delta Range from Mettler Toledo (Giessen, Germany) and placed in a 6-well plate. Each film was covered with 2 mL of highly purified water (HPW). The well plate was positioned on a shaking plate at 2 rpm at room temperature. After 1 h, the water was removed and analyzed using a spectrophotometer (Agilent 8453, Boeblingen, Germany). Protein concentration in solution was determined photometrically. The amount of the dissolved spider silk was compared with the initial mass of the film obtaining the percentage of the loss in mass of the film in water.

5.2.6. Post-treatments

5.2.6.1. PO_4^{3-} Post treatment

Films were post-treated by spraying a 2 M phosphate solution on the film surface using an ultrasonic nozzle Sonotek 120-00456 (Sonotek, Milton, USA) at a flow rate of 1 mL/min at 120 kHz for10 seconds. Post-treated films were left to dry at room temperature under laminar flow.

5.2.6.2. Ethanol Post-treatment

Films were post-treated by spraying a 70% ethanol-water solution on the film surface using an ultrasonic nozzle Sonotek 120-00456 (Sonotek, Milton, USA) as described above. Post-treated films were left to dry at room temperature under laminar flow.

5.2.6.3. Steam Sterilization

Spider silk films were steam sterilized using an autoclave GTASO (Fritz Goessner GmbH&Co, Hamburg, Germany). Briefly, air was saturated with water vapor, then the temperature was raised to 121°C, 1 bar, held for 15 min, and finally the system was cooled down to room temperature.

5.2.6.4. Water Vapor Treatment

Spider silk films were sealed in autoclave bags and stored for 60 min in a desiccator (Figure 35). The desiccator's reservoir was filled with highly purified water preheated at 60°C. The temperature was monitored using a digital temperature and humidity sensor (TFA Dostmann, Wertheim-Reicholzheim, Germany).

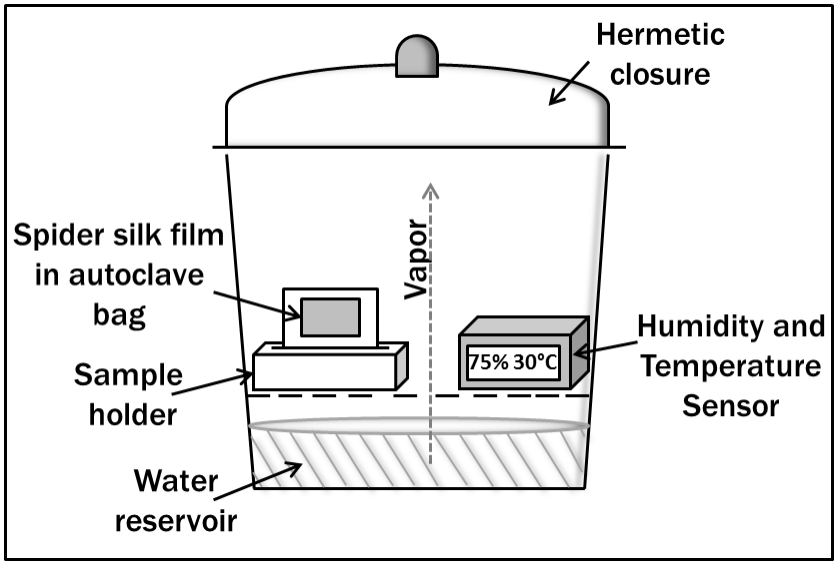

Figure 35: Water vapor treatment.

5.2.7. Mechanical Properties

Films were cut into samples of 2x120 mm. The thickness was determined using a Mitutoyo pen (Mitutoyo Deutschland GmbH, Neuss, Germany). Tensile test of spider silk films (n=5) were carried out at 24°C and 32% RH; spider silk films containing 2% w/v 2-pyrrolidone (n=5) were analyzed at the same conditions. All

spider silk films were tested in a dry state. Measurements were performed using a Zwick tensile tester Z0.5 (Zwick GmbH & Co. KG, Ulm, Germany), equipped with a 5 N capacity load cell. The mechanical properties measuraments were carried out with Michael Bergfield from AmSilk.

5.3. Results and Discussion

5.3.1. The Scale up Process

The film applicator used in this work is represented in Figure 36. The device is controlled by a microprocessor and has an adjustable drawing speed in the range of 0.1 - 19.9 mm/s. Additionally it has an integrated vacuum function to adhere substrates on its working surface. The casting solution was loaded in the casting knife and the automatic arm moved the casting knife forward on the substrate. The thickness of the resulted film was mainly determined by the casting solution properties (e.g. protein concentration, viscosity and surface tension), by the velocity of the automatic arm, and the size of the casting knife. In principle the process is representative of large scale film casting systems that are able to produce hundreds/thousands of square meters of film pro day.

In this study, spider silk films were cast from aqueous solvent and transparent, homogenous films with a visible smooth surface in the dimensions of 90 cm^2 were obtained. The geometry and the number of the films produced in one casting step were adjusted by cutting the larger film with a scalpel. The process allowed a reproducible production of spider silk protein films. In Figure 37, a photograph of eADF4(C16) film samples and in Figure 38 the respective SEM micrograph are presented. Compared to manually casted films described previously in Chapter 3, a notable difference is the film thickness. The main difference between the manually cast films and films cast with the film applicator regards the water solubility of the films. Films cast from aqueous solution using the film applicator dissolve almost immediately, indicating that the protein structure within the film

is different compared to manually cast films which are not water soluble, although having the same composition [144].

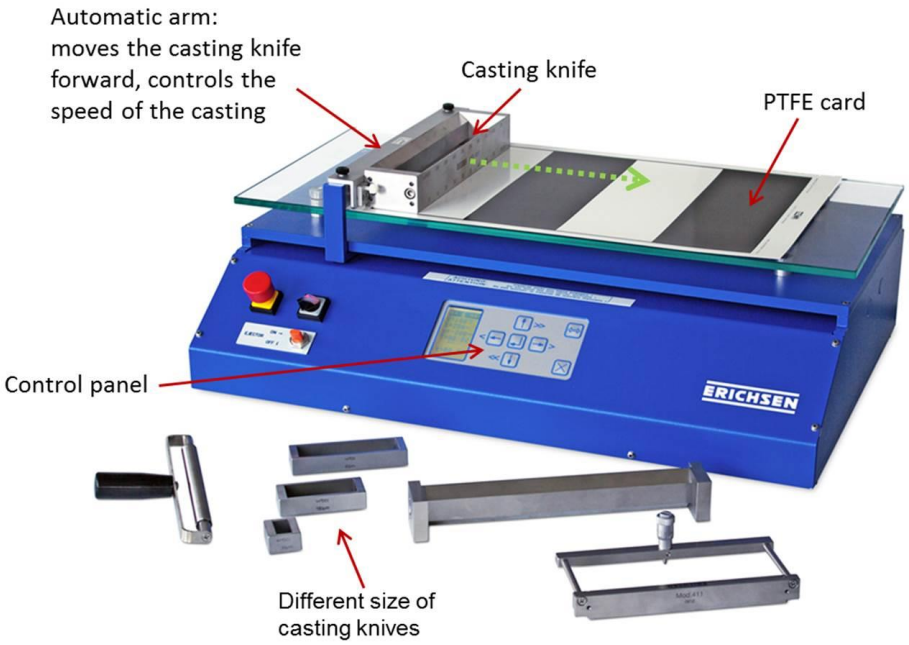

Figure 36: Film applicator Coatmaster 510, modified and reproduced with permission of erichsen

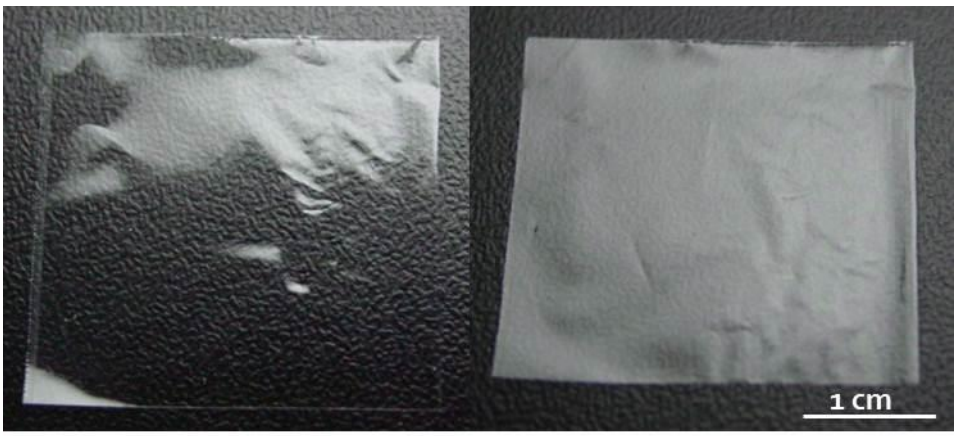

Figure 37: Photograph of eADF4(C16) spider silk film cast using the film applicator. Same film photographed from different angles leading to a different light reflection.
Bar = 1 cm

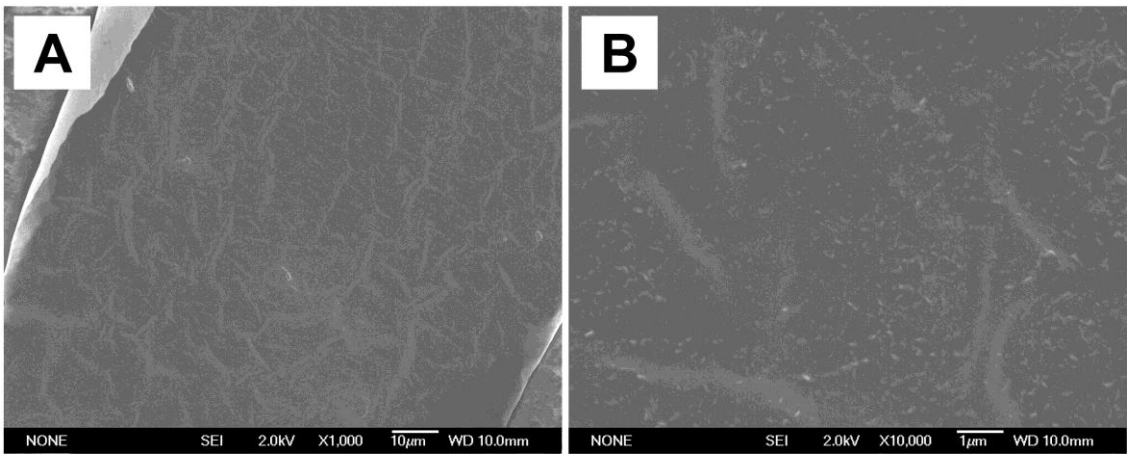

Figure 38: Scanning electron micrographs of spider silk films cast using the film applicator. A: bar = 10 μm; B: bar = 1 μm.

Besides the difference in thickness and protein concentration, the main difference between the manually cast films and films cast using the film applicator occurred regarding water solubility of the films. Films cast from aqueous solution using the film applicator dissolved almost immediately, indicating that the protein structure within the film may differ compared to manually cast films. In order to understand this new behaviour, the protein secondary structure has been investigated.

5.3.2. Protein Secondary Structure

As discussed earlier (Paragraph 3.2.6), the properties of spider silk protein films, including water solubility, are mainly influenced by the secondary structure of the spider silk protein. Two analytical tools selected at the beginning of this work to characterize the protein secondary structure within the film matrix were: DSC (Method 3.2.8) and FT-IR (Method 3.2.6).

Thermograms of eADF4(C16) films cast with the film applicator represented in Figure 40 are different from the ones obtained for films cast manually in Chapter 3, page 46. In fact, in this work the thermograms showed an exothermic peak around 220°C, which was not previously noted in the films cast manually [144]. This particular peak is correlated with the formation of β-sheet structures induced by temperature [145].

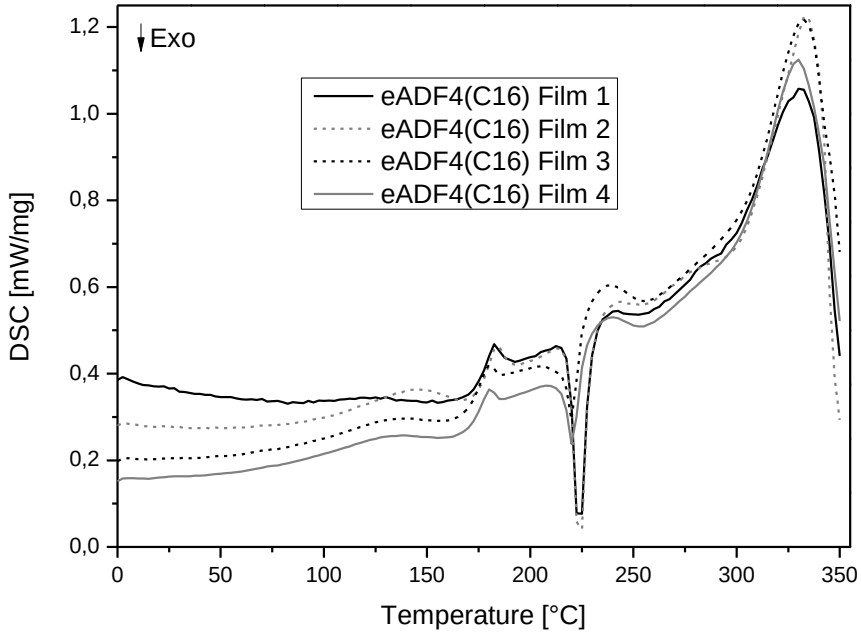

Figure 39: Thermogramms of spider silk films cast using the film applicator (n=4).

This is a first indication that the secondary structure of the eADF4(C16) proteins composing the film matrix had changed upon manufacturing. The endothermic peak around 330°C represents the decomposition of the protein.

Moreover, spider silk films cast using the film applicator showed two different secondary structure trends as highlighted in Figure 40.

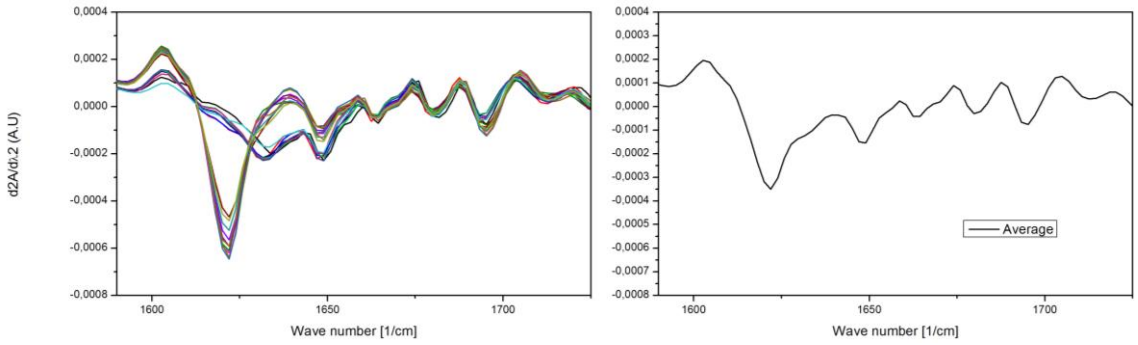

Figure 40: Second derivate of the FT-IR spectra obtained from spider silk films produced using the film applicator. Left: spectra obtained analysing three different areas of 6 different spider silk films cast using the film applicator. Right: average of the 18 spectra.

The first trend resembles the spectra recorded for the films cast manually [144], which is characterized by the two typical peaks of β-sheets structures (1690 cm^{-1} and 1625-1640 cm^{-1}). The second profile clearly showed these peaks shifted closer to the β-turn (1660-1685 cm^{-1}) and random coil regions (1652-1660 cm^{-1}). This indicates that within the same film, it is now possible to detect areas characterized by a high content of β-sheets and areas having low content of β-sheets structures. In conclusion, both DSC thermograms and FT-IR analysis show a change in the type of secondary structures in the spider silk film cast using the film applicator. One possible explanation may be the difference in drying time of the casting solution. The casting solution spread on the surface by the film applicator results in a thinner layer in comparison with the layer deposited manually. The spider silk proteins do not have sufficient time to fold in organized structures. Another reason may be the difference alignment of the protein chains due to the film applicator fluid dynamics, where more time is needed in order to rearrange the random entanglement of the protein chains from a more laminar orientation immediately after casting. Consequently, in order to increase the content of water insoluble regions within the film matrix, a post-treatment needed to be introduced following the casting process.

5.3.3. Post-treatments

In the past, different methods have been tested and investigated in order to increase the content of β-sheet structures in silk films. The most commonly used post-treatments are: kosmotropic ions, alcohol, high temperature, and water vapor [48]. An alternative treatment consists of immersing silk films in water, the so called water-annealing [173, 174]. However, this method cannot be applied to the spider silk films because the films will dissolve instantaneously before any changes in the protein secondary structure can occur. Another treatment option implicates the treatment of films with high temperature. As shown in Figure 39, heating of cast films to 220°C can trigger the formation of β-sheet structures. However, this may result in possible damage to drugs (such as proteins and peptides) incorporated in the film matrix.

In this study, the following post-treatments have been investigated: phosphate ion and ethanol treatment using an ultrasonic nozzle, steam sterilization, and water vapor treatment..

5.3.3.1. Phosphate Ions Treatment

Water-based spider silk particles characterized by high β-sheets content have been already prepared using a salting-out process, where potassium phosphate was used as lyotropic salt [65, 67, 158, 175, 176]. Furthermore, spider silk films cast from organic casting solution such as hexafluoroisopropanol (HFIP) have been incubated in solutions containing phosphate ions to obtain water insolubility [147, 152]. In this work water-based eADF4(C16) films cast with the film applicator where post-treated by spraying a phosphate solution on the film surface using an ultrasonic nozzle. However, the method had a negative impact on the films. The formation of salt crystals on the film surface after drying combined with the low thickness, resulted in breaking most of the films treated. Figure 41 shows how the spider silk film looks like before and after the treatment.

Figure 41: Pictures of spider silk films produced using the film applicator before (left) and after (right) the phosphate ions post-treatment.

5.3.3.2. Ethanol Treatment

The most commonly used post-treatment to convert the water soluble silk fibroin type I structure to the water insoluble silk fibroin II structure is the immersion of

silk materials in methanol mixtures [160, 173, 174, 177-179]. This practice has been also applied on acid-based spider silk films in the past [143, 146, 147, 152]. To avoid using methanol as a solvent, this work considered the replacement of this particular alcohol with ethanol. A mixture of 70% v/v ethanol has been previously employed to sterilize silk fibroin films [173] and to treat silk fibroin membranes [180]. Moreover, Xin Chen at al. tested different ethanol concentrations and found out that using 70% ethanol resulted in an immediate increase of β-sheet structures in silk fibroin films [181]. In this study, the ethanol solution was sprayed on the film surface employing an ultrasonic nozzle. This method allows covering the film surface with a thin layer of ethanol which quickly evaporates. An example of treated film is shown in Figure 42.

Figure 42: Pictures of spider silk films produced using the film applicator before (left) and after (right) the ethanol post-treatment.

The processed films were analyzed by DSC and FT-IR to evaluate changes in the protein secondary structures (Figure 43). The DSC-thermograms did not show any exothermic peak at 220°C, meaning that a phase transition from unordered structures (such as helices, β-turns, random coils) to ordinate structures (β-sheets) did not take place because the content in β-sheets was already high. This assumption was then confirmed by FT-IR measurements (Figure 43).

It has been shown that most of the spider silk film dissolution in water occurs during the first hour, after that, the protein film matrix results to be water stable [144]. For this reason, three films were incubated in water for 1 h.

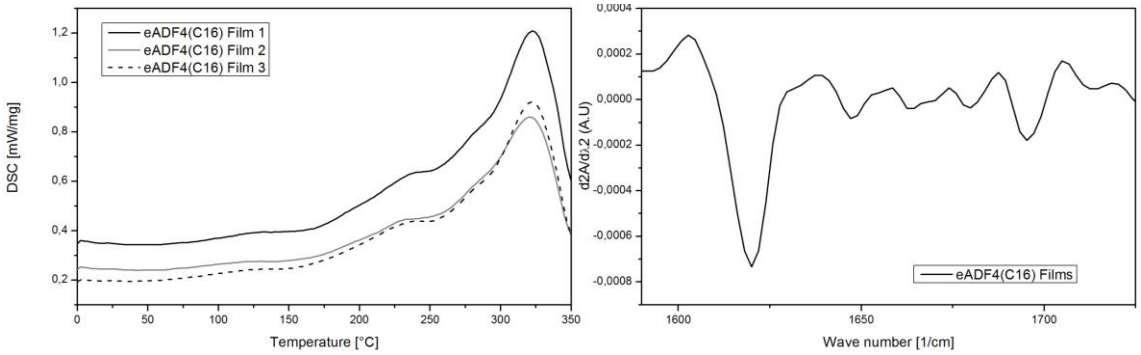

Figure 43: Left: DSC-thermograms of spider silk films produced using the film applicator after the ethanol post-treatment, Exo ↓, n=3. Right: Second derivate of the FT-IR spectrum obtained from spider silk films produced using the film applicator after ethanol post-treatment. The presented spectrum is the average of 18 spectra recorded from 6 different films. Every film was analysed in three different areas.

Only 0.72 ± 0.06% w/w of the film matrix dissolved. In conclusion, the method presented here was successfully able to increase the content in β-sheets resulting in water-based spider silk films cast using the film applicator stable in water. On the other hand, working further with ethanol will jeopardize the aim of producing organic solvent free spider silk films.

5.3.3.3. Steam Sterilization

Consulting the decision trees document prepared from the European Agency for the Evaluation of Medicinal Products (EMA) for the selection of sterilization methods, it is clear that the autoclave treatment is the preferred method for final sterilization [182]. The autoclave combines both heat and vapor, which both could be beneficial to increasing the content of β-sheets within the spider silk film matrix. Moreover, this method has been already successfully tested on eADF4(C16) submicron and micron particles [158]. In Figure 44, an optical image is provided showing the appearance of spider silk films after autoclave treatment. As performed before in the case of the ethanol post-treatment, the presence of β-sheets in the autoclaved spider silk matrix was investigated by DSC and FT-IR (Figure 45).

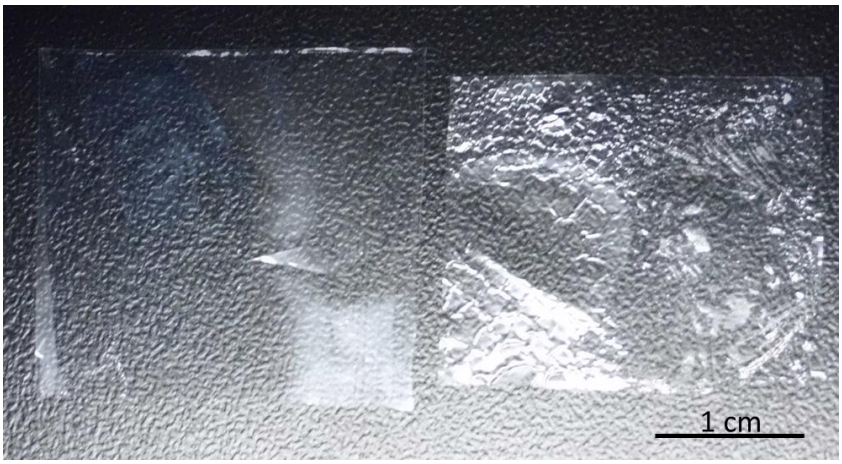

Figure 44: Pictures of spider silk films produced using the film applicator before (left) and after (right) the autoclave post-treatment.

Additionally the water solubility was also assessed. The autoclave treatment was able to increase the presence of water insoluble β-sheet structures. DSC thermograms showed the absence of any exothermic peaks, while FT-IR analysis highlighted the two major peaks for β-sheet structures (1690 cm^{-1} and 1625-1640 cm^{-1}). Finally, the autoclaved films were stable upon incubation in water, since after 1 hour incubation in water, only 1.10 ± 0.64% w/w of three film matrices dissolved. Steam sterilization can achieve two purposes in one step, is able to convert water soluble spider silk films in water stable matrices and provides final sterilization of films.

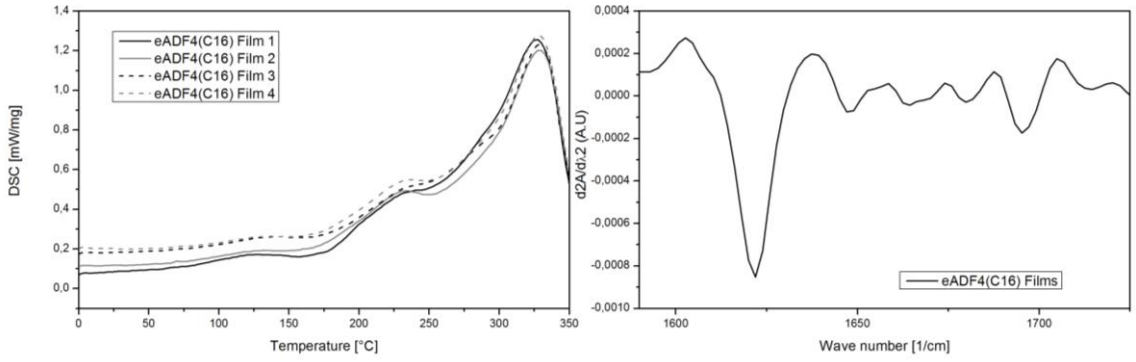

Figure 45: Left: Thermograms of spider silk films produced using the film applicator after autoclave post-treatment, Exo ↓, n=3. Right: Second derivate of the FT-IR spectrum obtained from spider silk films produced using the film applicator after autoclave post-treatment. The presented spectrum is the average of 18 spectra recorded from 6 different films. Every film was analyzed in three different areas.

5.3.3.4. Water Vapor Treatment

In the previous paragraph, it has been shown that the combination of heat and vapor can increase the content of β-sheets within eADF4(C16) film matrices cast using the film applicator. Nevertheless, the autoclave treatment is not applicable if sensitive drugs are encapsulated in the film. Recently, it has been shown that eADF4(C16) films are promising therapeutic proteins delivery systems [144]. Since the temperature would damage this sensitive class of actives [183-185], the autoclave treatment can be considered neither for final sterilization nor for increasing the content of water insoluble silk protein structures. Hence, the last post-treatment investigated in this work concerns the exposure of spider silk films to a high relative humidity environment, without the application of high temperature. In the past, silk fibroin particles have been treated with 89% or 96% RH for 24 h [178, 186], while fibroin films have been processed with >90% RH for 12 h [187]. Moreover, silk fibroin films have been also placed in dedicated containers partially filled with water, where vacuum has been applied for 6 [177] and 5 h [174]. The method employed in this project was designed in order to decrease the time of treatment to 1 h, to avoid the use of vacuum, and therefore allowing later scale-up of the method forwards a semi-continues production process. A schematic representation of the method setup is provided in Figure 35, page 90. Temperature and relative humidity obtained during the post-treatment are listed in Table 16. An optical image of the spider silk films is provided in Figure 46. Film analysis by DSC and FT-IR revealed the presence of a high β-sheets content as represented in Figure 47. The extraction of spider silk protein of treated films after 1 h incubation in water was measured as 0.94 ± 0.36% w/w. The water vapor treatment resulted to be an efficient, quick and simple method to increase the β-sheets content in eADF4(C16) films. Furthermore, during the treatment the temperature never raised above 33°C (Table 16), suggesting the use of this method in cases where spider silk films are loaded with temperature sensitive drugs.

Table 16: Temperature and relative humidity (RH) measured during the water vapor treatment.

Films treated (n°)	Time of treatment (min)	Temperature (°C)	RH (%)
10	60	33	78
12	60	33	74
12	60	32	75
14	60	33	77

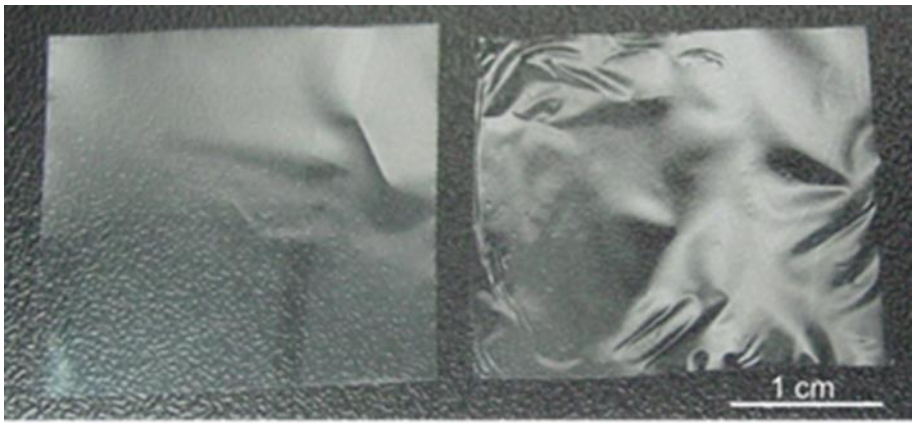

Figure 46: Pictures of spider silk films produced using the film applicator before (left) and after (right) the water vapor post-treatment.

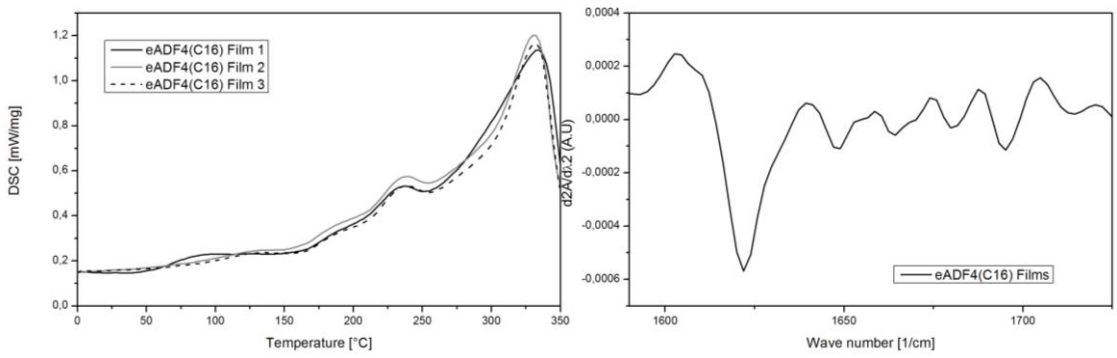

Figure 47: Left: Thermograms of spider silk films produced using the film applicator after the water vapour post-treatment, Exo ↓, n=3. Right: Second derivate of the FT-IR spectra obtained from spider silk films produced using the film applicator after the water vapor post-treatment. The presented spectrum is the average of 9 spectra recorded from three different films. Every film was analyzed in three different areas.

5.3.4. Increasing the Mechanical Properties of Spider Silk Films cast using the Film Applicator

Dry non-treated films cast with the film applicator were characterized by a rather low elongation (Table 17).

Table 17: Tensile test of different spider silk films, cast using the film applicator. h: thickness Et: elastic modulus; σB: tensile strength at break; εB: elongation at break (% over the initial length).

FILM	h (µm)	Et (MPa)	σB (MPa)	εB (%)
eADF4(C16)	13 ± 2	885 ± 140	18.3 ± 2.06	2.1 ± 0.17
eADF4(C16) + 2-pyrrolidone	14 ± 2	497 ± 103	13.2 ± 1.48	77 ± 14

Spider silk films containing 2-pyrrolidone as plasticizer had a 35 times higher elongation in comparison with films without 2-pyrrolidone, as shown in Table 17. The water vapor treatment method was now also evaluated for eADF4(C16) films containing the plasticizer 2-pyrrolidone. Figure 48 reports the thermograms and the FT-IR spectra obtained from the films before and after post-treatment.

DSC scans, before the water vapor treatment (Figure 48 left up), reveled two endothermic peaks: the first one is correlated with the presence of the plasticizer and the second one is related to the degradation of the film matrix.

In this particular case it is not possible to observe the exothermic peak of the β-sheets formation, since the endothermic peak of 2-pyrrolidone is covering it. After the vapor treatment (Figure 48 bottom left) it is possible to discriminate the same two peaks again. FT-IR analysis highlighted the increment of β-sheets after the treatment, represented by the disappearance of the peak at 1650 cm^{-1} and the increment of the peak at 1624 cm^{-1} (Figure 48 top to bottom right).

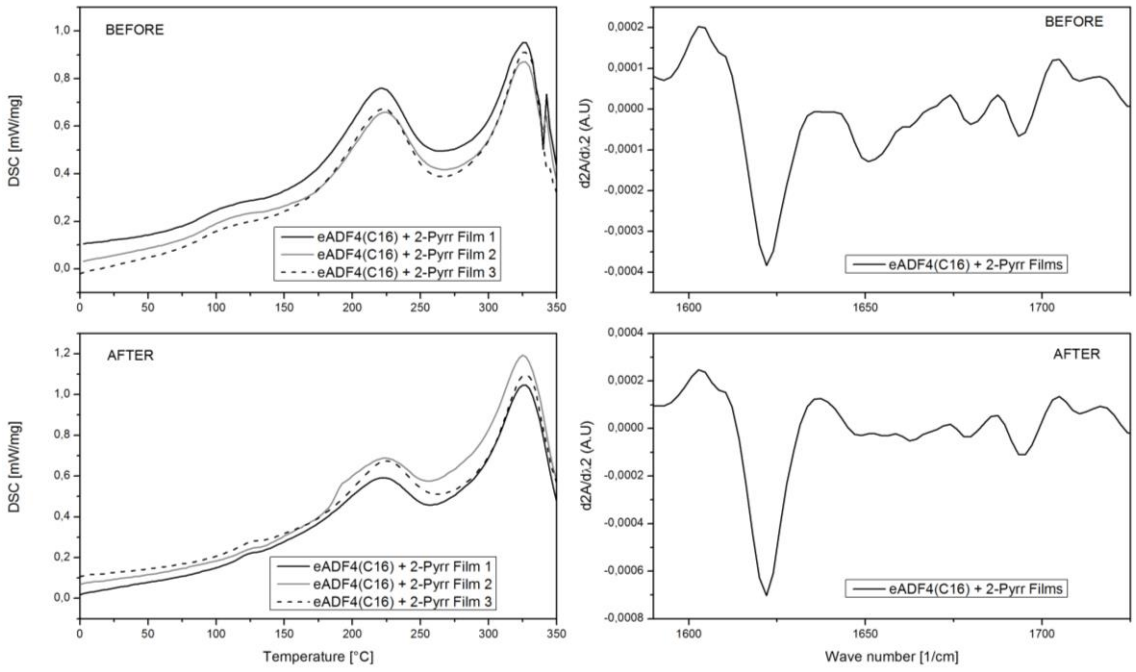

Figure 48: Top left: Thermograms of spider silk films containing 2-pyrrolidone produced using the film applicator before the water vapour post-treatment, Exo ↓, n=3. Bottom left: Thermograms of spider silk films containing 2-pyrrolidone produced using the film applicator after the water vapor post-treatment, Exo ↓, n=3. Top right: Second derivate of the FT-IR spectra (amide I) obtained from spider silk films containing 2-pyrrolidone produced using the film applicator before the water vapour post-treatment. The presented spectrum is the average of 9 spectra recorded from three different films. Every film was analyzed in three different areas. Top right: Second derivate of the FT-IR spectra (amide I) obtained from spider silk films containing 2-pyrrolidone produced using the film applicator after the water vapor post-treatment. The presented spectrum is the average of 9 spectra recorded from three different films. Every film was analyzed in three different areas.

In conclusion, it is possible to improve the mechanical properties of water-based spider silk films cast using the film applicator by incorporating 2-pyrrolidone, and water stability of the films can be achieved by water vapor treatment.

5.4. Conclusion

In this work, water-based spider silk films have been produced using an automatic film applicator. These films have a visible better appearance, a smoother and more uniform surface, compared to films cast manually. The analysis of the secondary structure of eADF4(C16) proteins within the film matrix revealed the poor presence of β-sheet structures. This resulted in films which are no longer water stable. In order to increase the content in β-sheets and produce water insoluble films, different post-treatments have been investigated. Among all the tested treatments (phosphate ions, ethanol, steam sterilization and water vapor), water vapor was the one that showed the most promising results. Further, it has been assessed that the incorporation of 2-pyrrolidone in the film matrix can improve the mechanical properties of the spider silk films. These films can also be treated with water vapor in order to achieve water insolubility. In conclusion, the solvent evaporation method presented in this paper allows the production of larger spider silk films, which are visibly transparent and flat. The scale-up production of these films is easy and possible as both casting and water vapor treatment can be carried out in available industrial equipment. Industrialization could lead to the development of spider silk-based products such as scaffolds for tissue engineering, implantable drug delivery systems, and coatings for implants with improved biocompatibility.

6. Proof of Concept: SSP Films for Delivery of Therapeutic Proteins

6.1. Introduction

The previous chapters described how to manufacture water-based spider silk films. The process presented in this thesis enables the encapsulation of large biomolecules, such as proteins, directly in the spider silk film matrix (Chapter 4). These biocompatible and biodegradable films can be produced in large scale using a film applicator, as seen in Chapter 5. Furthermore, these films have been investigated as drug delivery systems, and different film designs have been prepared in order to control the *in vitro* release of one model protein [144]. Overall, in this thesis it has been argued that SSP films are promising implantable DDS for proteins. It is now essential to investigate the described DDS as a release system for therapeutic biomolecules to finally assess its potential. Therefore the last part of this work focuses on the loading of two different therapeutic proteins: nerve growth factor and erythropoietin. The majority of this study consisted in the chromatographic analysis of the two molecules upon release from the DDS in order to collect first evidence of any changes occurring after the loading process.

6.2. Methods

6.2.1. Remote Loading of Nerve Growth Factor (NGF) on Spider Silk Films

SSP films cast with the film applicator Coatmaster 510 (Erichsen, Hemer, Germany) (Method 5.2.1, page 87) and treated with water vapor (Method 5.2.6.4, page 90), were weighted using the balance AT216 DeltaRange® (Mettler Instruments, Giessen, Swizerland). Films were transferred in 6-well plates and 1 mL of the NGF loading solution was added to each film. The NGF loading solution was prepared dialyzing the original nerve growth factor solution against a 10 mM PBS buffer pH 7. Afterwards, the solution was filtered through 0.2 µm polyethersulfone (PES) filter. Protein concentration was determined photometrically at 280 nm using the NanoDrop 2000 (Peqlab, Erlangen,

Germany). The extinction coefficient used in this part of the study was: $E^{1\ mg/mL}$ (280 nm) = 1.5 [188]. The concentration of NGF was finally adjusted to 0.25 mg/mL using the same dialysis buffer. Spider silk films were incubated with the NGF solution for 30 minutes at room temperature at 30 rpm. Later, films were removed from the 6-well plates and the un-loaded growth factor content in solution was analyzed by SEC-HPLC. The Dionex HPLC system (ASI 100, P 680, RF 2000, Dionex Softron GmbH, Germering, Germany) was equipped with the size exclusion column YMC-Pack Diol-120 (YMC Europe GmbH, Dinslaken, Germany). The mobile phase consisted of 200 mM potassium phosphate and 450 mM potassium chloride, pH 7. 50 µL of each sample were injected by the auto sampler ASI-100 (Dionex Softron GmbH, Germering, Germany). The chromatography was performed with a flow rate of 0.5 mL/min. The concentration of NGF was calculated using a calibration curve. Data analysis was performed with Chromeleon® software (Dionex GmbH, Germering, Germany). The loading efficiency was calculated as shown in Paragraph 4.2.1, page 57.

6.2.2. Direct Loading of Erythropoietin (EPO) in Spider Silk Films

An erythropoietin (EPO) solution (1.9 mg/mL in 5 mM phosphate buffer pH 7.2) was first filtrated through a 0.2 µm PES filter. After that, the solution was concentrated using a Vivaspin 20 tube (MWCO 30 kDa, Sartorius, Göttingen, Germany) at 8000 rpm. A final EPO concentration of 5 mg/mL was obtained. Spider silk solution prepared according with the Method 5.2.1 (page 87) was mixed with the EPO solution in order to obtain 100 mg of eADF4(C16) and 2.5 mg EPO in 2.5 mL of casting solution containg 2% w/v of 2-pyrrolidone. This volume was used to cast one film following the Method 5.2.1. Films were treated with water vapor as described in Method 5.2.6.4, page 90.

The therapeutic protein was analyzed by SEC-HPLC (Method 3.2.2.3, mobile phase listed in Table 5) and RP-HPLC (Method 3.2.2.3; mobile phase Table 5; injection volume 50 µL; flow 0.5 mL/min; column: YMC-Triart C18, 3 µm, 120 Å, 150 x 4.6

mm from YMC, Kyoto, Japan). Samples were analyzed during the manufacturing process, meaning: after filtration, after up-concentration with Vivaspin, and after the films have been incubated in 2 mL PBS at room temperature for 3 h applying 2 rpm, in order to partially extract the therapeutic protein out of the spider silk matrix for the analysis.

6.2.3. *In vitro* Release of Erythropoietin (EPO) encapsulated in Spider Silk Films

The release of EPO was investigated from spider silk films cast manually. Films were prepared as described in 4.2.2. Each film contained 1.5 mg of EPO and 25 mg of spider silk protein. The release study was performed according to 4.2.2. RP-HPLC for measuring protein released from the film matrix was performed using a Dionex Ultimate 3000 HPLC system (Dionex, Softron GmbH, Germering, Germany) equipped with a Jupiter 5u C4 column (300 Å, 250 mm x 4.6 mm, Phenomenex, Achaffenburg, Germany).

6.3. Results and Discussion

6.3.1. Loading and Release of Therapeutic Proteins

According to the findings from paragraph 4.3.1 and 4.3.2 (pages 61-64), therapeutic proteins can be loaded by remote loading or direct loading giving their isoelectric point as shown in Figure 49. Positively charged biomolecules need to be remote loaded on the film surface, while negatively charged proteins can be directly included in the casting solution prior to casting the film.

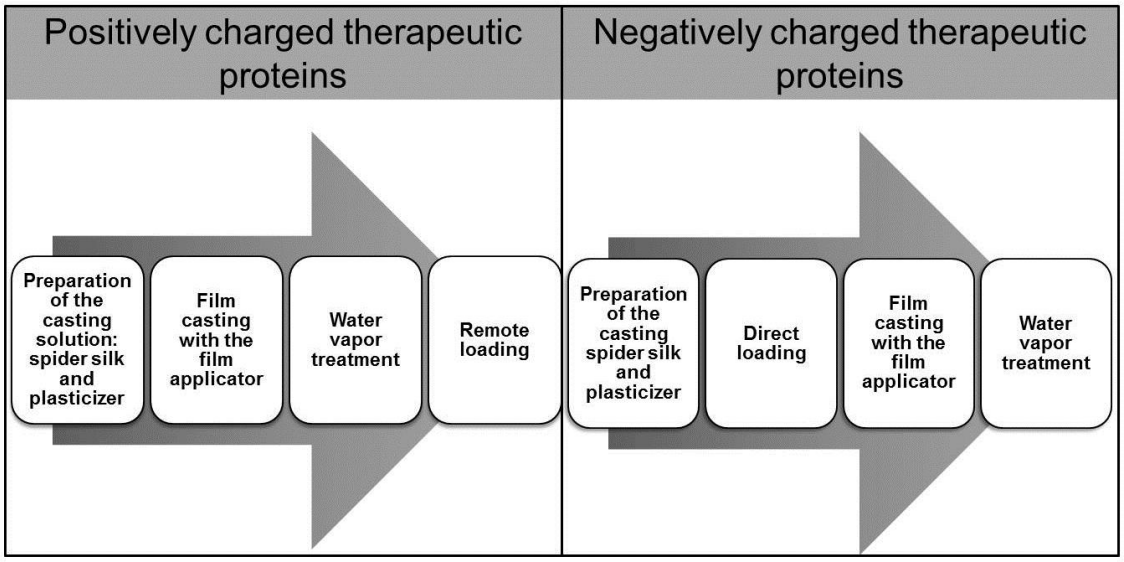

Figure 49: Manufacturing steps for preparing water-based spider silk films loaded with therapeutic proteins using the film applicator.

As a first attempt in this direction, two therapeutic proteins having different isoelectric points have been selected: nerve growth factor (NGF) characterized by an isoelectric point of 9.5 and molecular weight of 13.5 kDa [66], and erythropoietin (EPO), isoelectric point of 4.4 and MW of 34 kDa [189]. In agreement with Figure 49, NGF should be loaded by remote loading and EPO by direct loading.

6.3.1.1. Remote Loading of NGF

The primary physiological role of NGF consists in promoting and developing neurons in vertebrates, both sympathetic and sensory [190]. Moreover, NGF supports nerve regeneration and additionally it plays a role in tissue repair [191, 192]. NGF exists mostly in its homodimer form, characterized by a dissociation equilibrium constant of less than 10^{-13} M, and is biologically active [190]. Since NGF has a zeta-potential of +15 mV at pH 7 [66], this protein is positively charged at physiological condition and should interact with the negatively charged surface area of e(ADF4)C16 films (paragraph 3.3.8, page 52).

After preparing a remote loading solution containing NGF, water-based spider silk films produced with the film applicator and treated with water vapor to assure water insolubility, were incubated in the loading solution. After removing the films the content of the non-loaded NGF was measured by HPLC.

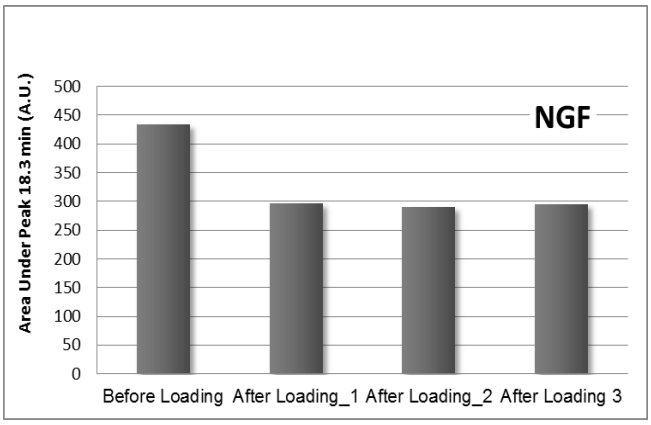

Figure 50: Remote loading of NGF, the bars show the area under the NGF peak measured by SEC-HPLC in the loading solution after the incubation with spider silk films. 'After Loading 1, 2, and 3' refer to three different spider silk films tested with the same condition described in Method 6.2.1. N=1

The loading efficiency has been calculated to be 41.45 ± 0.7% (n= 3).

Figure 51 shows an example of a chromatogram obtained by analyzing the protein NGF in the remote loading solution before and after the process. In general, protein physical stability in solutions can be jeopardized by interfacial interaction with solid surfaces [193-195], such as the one occurring during the remote loading. In this case, the collected chromatograms highlighted the fact that the protein colloidal stability has not been altered during the process since it is possible to recognize one single peak corresponding to the protein dimer [66] in both chromatograms.

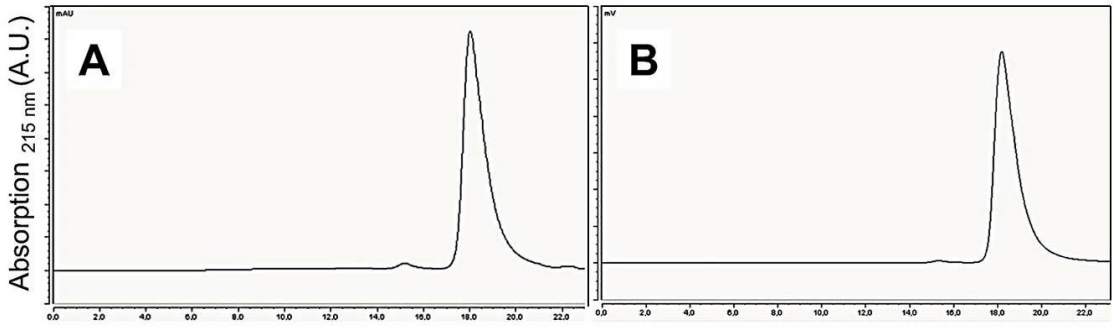

Figure 51: SEC-HPLC chromatograms of NGF in the loading solution before (A) and after loading (B).

In conclusion, what has been previously shown for small molecules and for one model protein (Lysozyme) in paragraph 4.3.1 (page 61) is in principle possible for therapeutic proteins as well. In general if a biomolecule is positively charged at the pH of the loading solution, it can be successfully loaded on the spider silk film surface due to electrostatic interactions. Additional work is needed in order to optimize the remote loading process to increase the loading efficiency. The *in vitro* release of NGF will not be presented in this work since its release kinetic depends on the ionic strength of the release medium (the higher the ionic strength, the faster the release) and on the sampling time [66].

6.3.1.2. Direct Loading of Erythropoietin in Water-based Spider Silk Films and *in vitro* Release

Erythropoietin (EPO) is a glycoprotein mainly produced in the kidneys. The most important function of EPO is stimulating the proliferation and differentiation of red cells in the bone marrow [196]. It is clinically used in the chronical therapy of renal anemia [197, 198].

This therapeutic protein was incorporated directly in the spider silk casting solution, and films have been cast using this solution (Method 6.2.2). After casting, films were post-treated with water vapor in order to assure their water

insolubility (Method 5.2.6.4, page 90). A picture of SSP films cast using the film applicator directly loaded with EPO is represented in Figure 52.

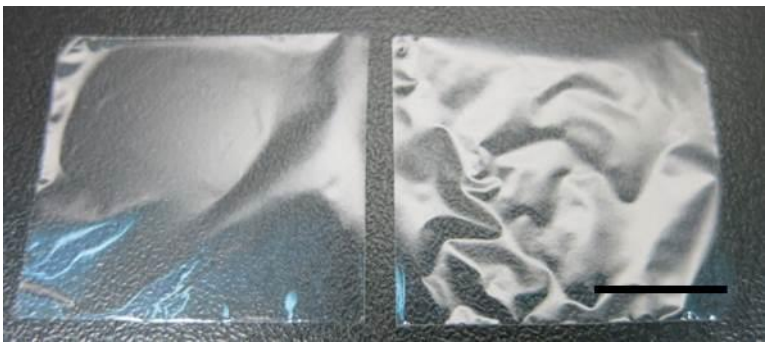

Figure 52: Spider silk films cast using the film applicator directly loaded with erythropoietin, treated with water vapor. Bar = 1 cm

Figure 53 represents the qualitative analysis performed by HPLC-RP chromatograms of the spider silk protein e(ADF4)C16 and EPO before and after casting the films with the film applicator. While, Figure 54 shows examples of the chromatograms obtained by SEC-HPLC analysis of the same samples.

Erythropoietin was characterized by a single peak by both chromatography methods, and eADF4(C16) showed two peaks by RP and two peaks with a large tailing by SEC analysis. The difference in the areas under the peak reported in Figure 53 and in Figure 54 is related to the use of two different HPLC columns. Overall, the chromatographic analysis suggested that the therapeutic protein was not negatively affected by the encapsulation and casting process.

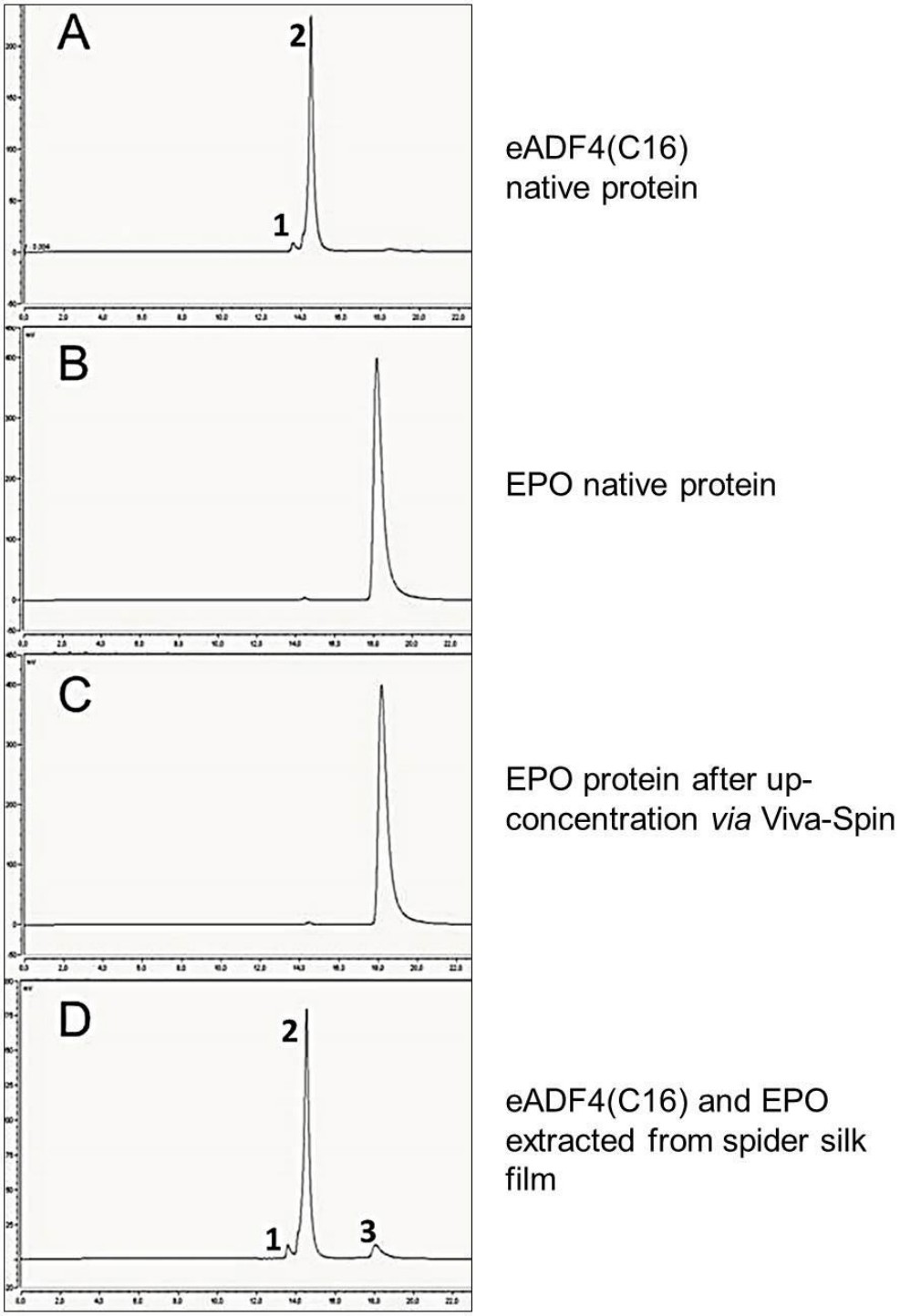

Figure 53: RP-HPLC chromatograms of A: eADF4(C16) in solution after dialysis; B: erythropoietin in its original solution after thawing; C: erythropoietin after up-concentration; D: eADF4(C16) (peaks 1 and 2), and erythropoietin extracted (peak 3) from spider silk film cast using the film applicator.

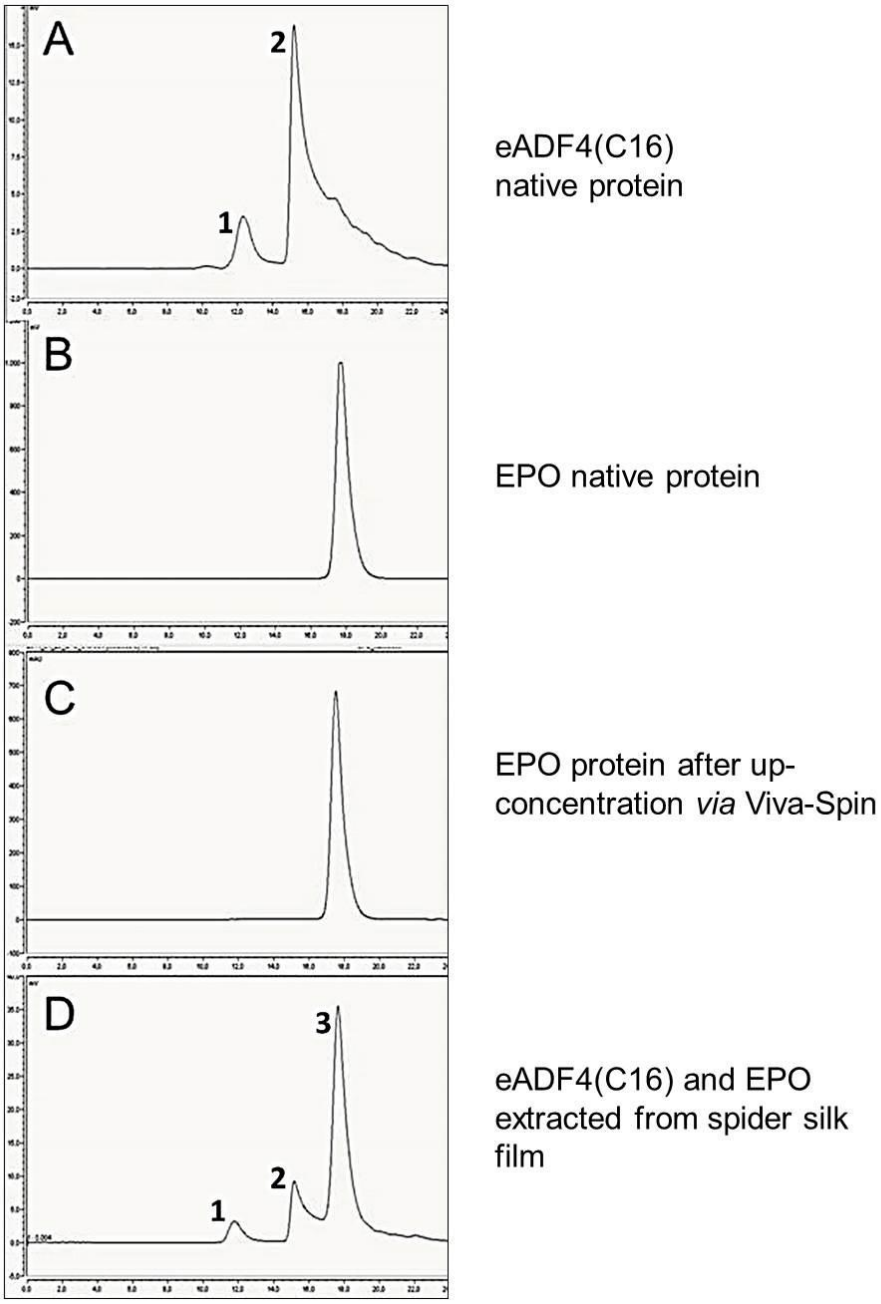

Figure 54: SEC-HPLC chromatograms of A: eADF4(C16) in solution after dialysis; B: erythropoietin in its original solution after thawing; C: erythropoietin after up-concentration; D: eADF4(C16) (peaks 1 and 2) and erythropoietin (peak 3) extracted from spider silk film cast using the film applicator.

The release of EPO from eADF4(C16) matrix has been studied but from films cast manually in order to compare the release profile with the one obtained encapsulating the model protein BSA in Chapter 4. Figure 56 shows that the

therapeutic protein is released more slowly than BSA. Overall the release profile of EPO (Figure 56) resembled the one of the model protein BSA but interestingly, the quantity of EPO released in the time considered was 10 times lower.

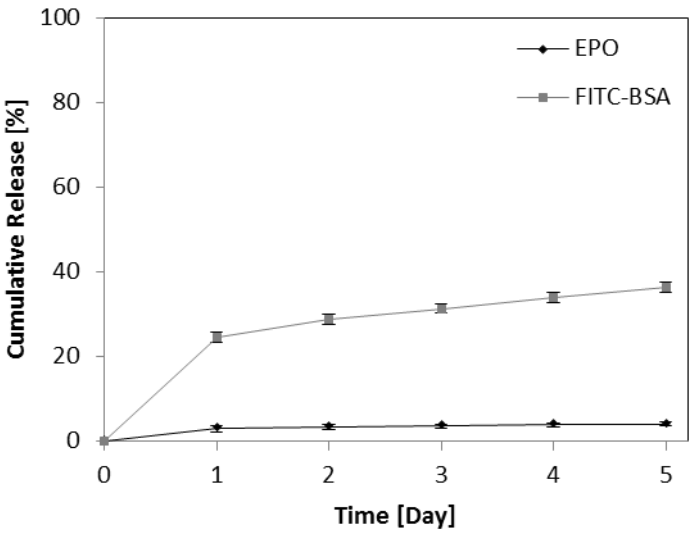

Figure 55: Cumulative release of erythropoietin and the model protein BSA from spider silk films cast manually containing 1% of 2-pyrrolidone.

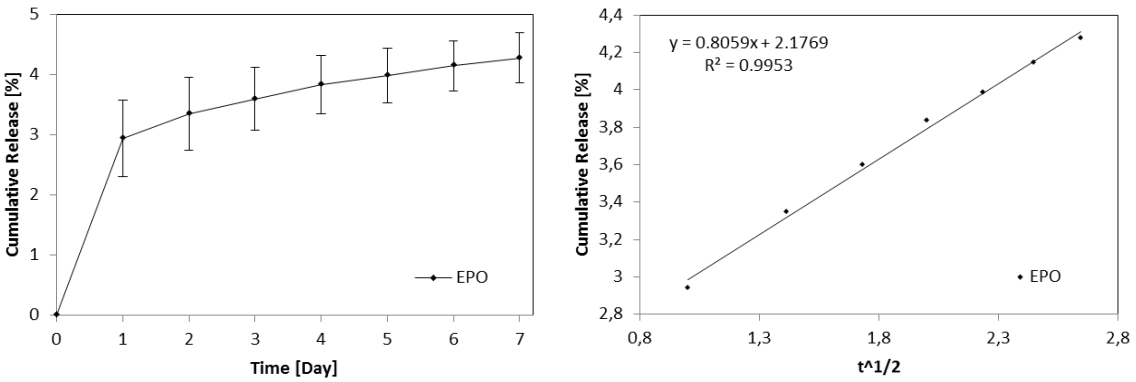

Figure 56: Left: cumulative release of erythropoietin from spider silk films cast manually containing 1% of 2-pyrrolidone. Right: Cumulative release plotted against the square root of time.

This data suggests the need to further study the interaction of biomolecules with the spider silk matrix. If the fraction of the released protein is plotted against the square root of the time, a straight line with R^2= 0.995 is obtained as showed in Figure 56. Proposing that the release profile can be described by the Higuchi model [165, 199] as it was observed previously for BSA [144].

This first study showed encouraging results, additional work should consider the encapsulation of different biomolecules and the study of their interaction with the spider silk protein matrix to better elucidate the *in vitro* release mechanism. Furthermore the activity of the therapeutic protein should be assessed after its release in order to guarantee the compatibility with the manufacturing process.

Table 18 lists therapeutic peptides and proteins characterized by an isoelectric point in the range of 4-6, and therefore compatible with the direct loading process described in this thesis.

Table 18: Proteins and peptides candidates compatible with the direct loading process

Biopharmaceutical	**pI**
Lepirudin	4.0
Epoetin alfa	4.4
Epoetin beta	
Methoxy polyethylene glycol-epoetin beta	
Epoetin zeta	
Darbepoetin alfa	
Dornase alfa	4.6
Exenatide	4.7
Factor IX	5.0
rhu-GM-CSF	
Insulin detemir	5.1
Galactosidase alfa	5.2
Galactosidase beta	
Growth hormone (GH)	5.3
Pegvisomant	
Recombinant human insulin	5.4
Insulin lispro	
Anakinra	5.5
Filgrastim	5.6
PEG-Filgrastim	
Interferon alfacon-1	6.0
Interferon-alfa-2a	
PEG-Interferon-alfa-2a	
Interferon-alfa-2b	
PEG-Interferon-alfa-2b	
Factor VIIa	6.1

6.4. Conclusion

In this chapter water-based spider silk films prepared using the film applicator were loaded with two different therapeutic proteins: nerve growth factor and erythropoietin. The first protein was loaded by remote loading, while the second one by direct loading.

The analysis of the two molecules before and after the different loading process did not highlight any changes occurring in the chromatograms, suggesting that both film casting and loading procedures were compatible with the two therapeutic proteins. Interestingly, the *in vitro* release profile of erythropoietin from manual cast films was found to be comparable with the one previously described for the model protein BSA but ten times slower.

Additional work should consider the loading of different biomolecules and the investigation of their interaction with the spider silk protein matrix. Another aspect that should be addressed in the future consists in the study of the long term stability of water-based spider silk films and of the encapsulated drugs. Ultimately, these novel DDS must show the ability to preserve their characteristics as well as the ones of the incorporated drug.

7. Summary and Conclusion

Spider silk proteins represent exceptional natural polymers due to their mechanical properties in combination with biocompatibility. As both hydrophobic and slowly biodegrading biopolymers, recombinant spider silk proteins fulfill the required properties for a drug delivery system. The recombinant production of spider silk proteins allows the cost-effective fabrication of these biopolymers.

The main focus of this thesis was to obtain a reproducible all-aqueous protein film production process in order to cast spider silk films characterized by biocompatibility, water insolubility and good mechanical properties. The evaluation of spider silk films as novel carrier for various pharmaceuticals was also part of this work. Ideally, the film preparation process has to be compatible with protein encapsulation and the obtained matrix should be able to release a therapeutic protein for a prolonged time.

Chapter 1 discussed the use of biomaterial in drug delivery and introduced the properties of spider silk proteins, while Chapter 2 presented the material used in this project. In Chapter 3, the preparation of eADF4(C16) films without the use of any organic solvent was demonstrated. Transparent water-based spider silk films with a homogeneous morphology and a smooth surface were obtained. The average thickness of the films was about 30 μm. The film surface resulted to be tight and compact; no visible pores were highlighted by SEM pictures. Films were characterized by a high content of β-sheet protein structures, which led to water insolubility and to a high elastic modulus. It was found that the elongation of films can be increased by adding small hydrophilic plasticizers in the casting formulation. Overall, films cast from a water solution containing glycerol or 2-pyrrolidone were easy to handle and were characterized by a higher elongation than poly(l-lactic acid) films and by a maximal tensile strength comparable with ultra-high-molecular-weight polyethylene films. The film manufacturing method used in this chapter ensured water insolubility. Thus, films did not require to be further treated with methanol as described in the past [143, 146, 147, 152]. Moreover, thermal analysis highlighted the excellent thermal stability of the spider silk films (up to 200°C). This could be relevant for several future technical applications as it allows steam sterilization.

Chapter 4 included the evaluation of spider silk films as drug delivery matrices for both small molecular weight drugs and high molecular weight molecules such as proteins. Films were loaded with a variety of molecules (phenol red, paracetamol, ethacridine-lactate, nipagin, tetracaine hydrochloride, lysozyme, dextran, and albumin–fluorescein isothiocyanate conjugate) exploring two different loading techniques: remote loading and direct loading. The remote loading was found to be feasible for those drugs having a high logP and a strong opposite charge from the spider silk protein. On the contrary, the direct loading was only applicable to those drugs that do not interact with the spider silk protein in solution. Therefore, therapeutic proteins characterized by a similar isoelectric point to spider silk protein are suitable candidates for the direct loading method.

During the investigation of spider silk films as drug delivery matrices, different film designs were prepared creating a drug delivery platform composed by spider silk monolayer, coated monolayer, multilayer (sandwich), and coated multilayer, as shown in Figure 57.

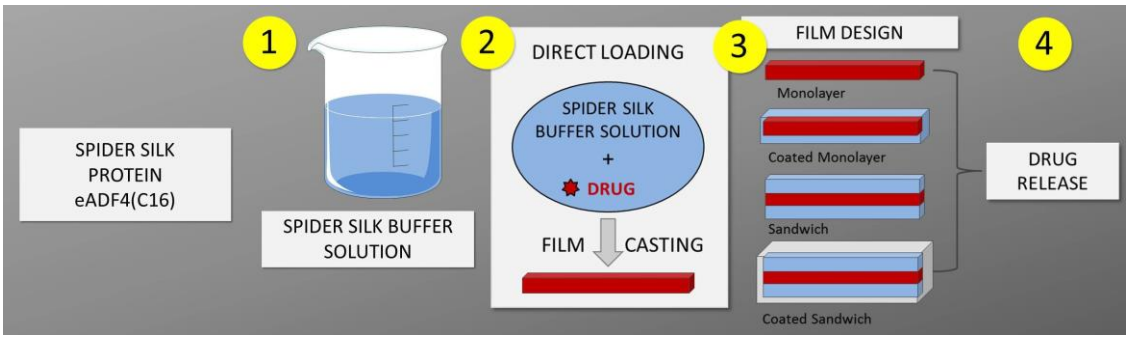

Figure 57: Graphical summary, spider silk films as a platform for drug delivery.

Monolayer water-based spider silk films can be used to achieve a prolonged release for large molecules (>30 kDa). The *in vitro* release profile was characterized by around 30% burst on day 1, and after that spider silk films released the protein BSA in a constant amount per day. Improvements in the film's mechanical properties incorporating glycerol in the film matrix led to higher elongation but also accelerated the release of the model protein BSA. On the

contrary, the use of 2-pyrrolidone as a plasticizer resulted in a burst of approximately 20% and a steady release of the protein over 30 days.

To further reduce the burst release occurring at day one, the monolayer films were coated with concentrated spider silk solution obtaining coated monolayers. On the one hand, this resulted in a decrease of the burst release of BSA (from 50% to 21%) and in a prolonged release of the model protein to over 90 days for films containing glycerol. On the other hand, the *in vitro* release profile of BSA from coated films containing 2-pyrrolidone was not affected.

For the third film design a new method to prepare multilayer films was developed. In this manufacturing process, it was possible to produce sandwich format films by compressing different spider silk layers with the middle layer containing glycerol. The *in vitro* release of BSA from a multi-layer system resulted to be much faster than the one recorded for a monolayer film without plasticizer, and it did not bring additional value over the first two designs.

By coating the multilayer films, an *in vitro* release profile close to a zero order kinetic was achieved. The coating completely eliminated the burst release and the release of BSA was slowed down neutralizing the glycerol effect obtaining a release of the protein for over 40 days. In general, the production of multilayer films could be advantageous in cases where the quantity of the drug loaded in one monolayer is not sufficient to obtain a therapeutic effect, or when it is necessary to load different drugs in different layers.

In conclusion, the monolayer system containing 2-pyrrolidone as plasticizer was evaluated to be the best drug delivery option due to the ease of preparation, good mechanical properties and sustained release of a protein over 90 days.

Finally, in Chapter 4 the biodegradation *in vitro* of spider silk films containing 2-pyrrolidone was considered. The enzymatic degradation of films took place in presence of elastase. In future, relevant *in vivo* studies will be necessary to better characterize the biodegradation mechanism of spider silk matrices and its kinetic.

In Chapter 5, water-based spider silk films were produced using an automatic film applicator. These films showed a smoother and more uniform surface, compared

with films cast manually. The analysis of the secondary structure of eADF4(C16) proteins within the film matrix revealed the poor presence of β-sheet structures. This resulted in films which were no longer water insoluble. In order to increase the content in β-sheets and produce water insoluble films, different post-treatments were investigated. Among all the tested treatments (phosphate ions, ethanol, steam sterilization and water vapor), water vapor was the treatment that provided the most promising results. Further, it has been assessed that the incorporation of 2-pyrrolidone in the film matrix can improve the mechanical properties of the spider silk films. These films can also be treated with water vapor in order to achieve water insolubility. In conclusion, the solvent evaporation method presented in Chapter 5 allowed the production of larger spider silk films. The scale-up production of these films could lead to the development of products such as scaffolds for tissue engineering, implantable drug delivery systems, and coatings for implants with improved biocompatibility.

Finally, Chapter 6 considered the loading of two different therapeutic proteins: nerve growth factor and erythropoietin. The first protein was loaded by remote loading, while the second one by direct loading. Since no stability issues were highlighted by the analysis, it was determined that the film casting and loading procedures were compatible with therapeutic proteins.

In conclusion, the results in this thesis indicate that spider silk films are a promising biodegradable protein drug delivery matrix, capable of releasing a model protein over 90 days. Such films could be used for several pharmaceutical and medical purposes, especially when mechanical strength of a drug eluting matrix is of high importance. Additional work would be needed in order to bring a final drug release system made of spider silk to market, however this thesis demonstrates that this rather new biomaterial has the necessary prerequisites to become a benchmarked polymer for medical applications.

8. Curriculum Vitae

Personal Details

Name	Elisa Agostini
Date of birth	07.05.1985
Place of birth	Trento
Nationality	Italian

Professional Experience

04/2015 – Present	Head of Laboratory Pharmaceutical Science Operations, Sanofi Frankfurt

Education

12/2010 – 04/2015	PhD Thesis Department of Pharmacy Pharmaceutical Technology and Biopharmaceutics Ludwig-Maximilians-University Munich Supervisors: Prof. Dr. Gerhard Winter and Julia Engert
11/2010	Italian State Exam, licensed Pharmacist
10/2004 –10/2010	Degree in Pharmaceutical Chemistry and Technology Faculty of Pharmacy at the University of Padua, Italy

9. References

[1] Williams DF. On the nature of biomaterials. Biomaterials. 2009;30:5897-909.

[2] Ratner BD, Bryant SJ. Biomaterials: where we have been and where we are going. Annual review of biomedical engineering. 2004;6:41-75.

[3] Langer RS, Peppas NA. Present and future applications of biomaterials in controlled drug delivery systems. Biomaterials. 1981;2:201-14.

[4] Langer R, Peppas NA. Advances in biomaterials, drug delivery, and bionanotechnology. AIChE Journal. 2003;49:2990-3006.

[5] Kathryn E. Uhrich SMC, Robert S. Langer, Kevin M. Shakesheff. Polymeric Systems for Controlled Drug Release. Chem Rev. 1999;99:3181-98.

[6] Hoffman AS. The origins and evolution of "controlled" drug delivery systems. Journal of Controlled Release. 2008;132:153-63.

[7] Funk S, Miller MM, Mishell Jr DR, Archer DF, Poindexter A, Schmidt J, et al. Safety and efficacy of Implanon™, a single-rod implantable contraceptive containing etonogestrel. Contraception. 2005;71:319-26.

[8] Conley R, Gupta SK, Sathyan G. Clinical spectrum of the osmotic-controlled release oral delivery system (OROS*), an advanced oral delivery form. Current Medical Research and Opinion. 2006;22:1879-92.

[9] Wright JC, Tao Leonard S, Stevenson CL, Beck JC, Chen G, Jao RM, et al. An in vivo/in vitro comparison with a leuprolide osmotic implant for the treatment of prostate cancer. Journal of Controlled Release. 2001;75:1-10.

[10] Vasil'ev AE, Krasnyuk II, Ravikumar S, Tokhmakhchi VN. Transdermal Therapeutic Systems for Controlled Drug Release (A Review). Pharmaceutical Chemistry Journal. 2001;35:613-26.

[11] Williams DF. On the mechanisms of biocompatibility. Biomaterials. 2008;29:2941-53.

[12] Kirkpatrick C, Bittinger F, Wagner M, Köhler H, Van Kooten T, Klein C, et al. Current trends in biocompatibility testing. Proceedings of the Institution of Mechanical Engineers, Part H: Journal of Engineering in Medicine. 1998;212:75-84.

[13] Anderson JM. In vivo biocompatibility of implantable delivery systems and biomaterials. European journal of pharmaceutics and biopharmaceutics. 1994;40:1-8.

[14] 10993 Id. Biological evaluation of medical devices. http://wwwisoorg/iso/home 2012.

[15] Harris AL, Carmichael J, Cantwell BM, Dowsett M. Zoladex: endocrine and therapeutic effects in post-menopausal breast cancer. British Journal of Cancer. 1989;59:97-9.

[16] Dang W, Daviau T, Ying P, Zhao Y, Nowotnik D, Clow CS, et al. Effects of GLIADEL® wafer initial molecular weight on the erosion of wafer and release of BCNU. Journal of Controlled Release. 1996;42:83-92.

[17] Park K. Controlled drug delivery systems: past forward and future back. Journal of Controlled Release. 2014;190:3-8.

[18] Daniel S. Kohane RL. Biocompatibility and drug delivery systems. Chem Sci

2010;1:441-6.

[19] Mohammadi-Samani S, Taghipour B. PLGA micro and nanoparticles in delivery of peptides and proteins; problems and approaches. Pharm Dev Technol. 2015;20:385-93.

[20] Hirenkumar K. Makadia SJS. Poly Lactic-co-Glycolic Acid (PLGA) as Biodegradable Controlled Drug Delivery Carrier. Polymers. 2011;3:1377-97.

[21] Berkland C, Kim K, Pack DW. PLG Microsphere Size Controls Drug Release Rate Through Several Competing Factors. Pharmaceutical Research.20:1055-62.

[22] Berchane NS, Carson KH, Rice-Ficht AC, Andrews MJ. Effect of mean diameter and polydispersity of PLG microspheres on drug release: Experiment and theory. International Journal of Pharmaceutics. 2007;337:118-26.

[23] Fredenberg S, Wahlgren M, Reslow M, Axelsson A. The mechanisms of drug release in poly(lactic-co-glycolic acid)-based drug delivery systems—A review. International Journal of Pharmaceutics. 2011;415:34-52.

[24] Anderson JM, Shive MS. Biodegradation and biocompatibility of PLA and PLGA microspheres. Advanced Drug Delivery Reviews. 2012;64, Supplement:72-82.

[25] Kohane DS, Tse JY, Yeo Y, Padera R, Shubina M, Langer R. Biodegradable polymeric microspheres and nanospheres for drug delivery in the peritoneum. Journal of Biomedical Materials Research Part A. 2006;77A:351-61.

[26] Ramot Y, Zada MH, Domb AJ, Nyska A. Biocompatibility and safety of PLA and its copolymers. Advanced Drug Delivery Reviews. 2016.

[27] Menei P, Daniel V, Montero-Menei C, Brouillard M, Pouplard-Barthelaix A, Benoit J. Biodegradation and brain tissue reaction to poly (D, L-lactide-co-glycolide) microspheres. Biomaterials. 1993;14:470-8.

[28] van de Weert M, Hennink WE, Jiskoot W. Protein instability in poly (lactic-co-glycolic acid) microparticles. Pharm Res. 2000;17:1159-67.

[29] Bittner B, Morlock M, Koll H, Winter G, Kissel T. Recombinant human erythropoietin (rhEPO) loaded poly (lactide-co-glycolide) microspheres: influence of the encapsulation technique and polymer purity on microsphere characteristics. European journal of pharmaceutics and biopharmaceutics. 1998;45:295-305.

[30] Wu F, Jin T. Polymer-based sustained-release dosage forms for protein drugs, challenges, and recent advances. Aaps Pharmscitech. 2008;9:1218-29.

[31] Gander B, Wehrli E, Alder R, Merkle H. Quality improvement of spray-dried, protein-loaded D, L-PLA microspheres by appropriate polymer solvent selection. Journal of microencapsulation. 1995;12:83-97.

[32] Morlock M, Koll H, Winter G, Kissel T. Microencapsulation of rh-erythropoietin, using biodegradable poly (D, L-lactide-co-glycolide): protein stability and the effects of stabilizing excipients. European Journal of pharmaceutics and biopharmaceutics. 1997;43:29-36.

[33] Stefani M, Dobson CM. Protein aggregation and aggregate toxicity: new insights into protein folding, misfolding diseases and biological evolution. Journal of molecular medicine. 2003;81:678-99.

[34] Cleland JL, Powell MF, Shire SJ. The development of stable protein formulations: a close look at protein aggregation, deamidation, and oxidation.

Critical reviews in therapeutic drug carrier systems. 1992;10:307-77.

[35] Kim HK, Park TG. Microencapsulation of human growth hormone within biodegradable polyester microspheres: protein aggregation stability and incomplete release mechanism. Biotechnology and bioengineering. 1999;65:659-67.

[36] Kim HK, Park TG. Comparative study on sustained release of human growth hormone from semi-crystalline poly (L-lactic acid) and amorphous poly (D, L-lactic-co-glycolic acid) microspheres: morphological effect on protein release. Journal of Controlled Release. 2004;98:115-25.

[37] Kim HK, Chung HJ, Park TG. Biodegradable polymeric microspheres with "open/closed" pores for sustained release of human growth hormone. Journal of Controlled Release. 2006;112:167-74.

[38] Yuan W, Wu F, Guo M, Jin T. Development of protein delivery microsphere system by a novel S/O/O/W multi-emulsion. european journal of pharmaceutical sciences. 2009;36:212-8.

[39] Yeo Y, Park K. Control of encapsulation efficiency and initial burst in polymeric microparticle systems. Archives of pharmacal research. 2004;27:1-12.

[40] Feczkó T, Tóth J, Dósa G, Gyenis J. Influence of process conditions on the mean size of PLGA nanoparticles. Chemical Engineering and Processing: Process Intensification. 2011;50:846-53.

[41] Brodbeck KJ, Pushpala S, McHugh AJ. Sustained release of human growth hormone from PLGA solution depots. Pharmaceutical research. 1999;16:1825-9.

[42] Duncan G, Jess TJ, Mohamed F, Price NC, Kelly SM, van der Walle CF. The

influence of protein solubilisation, conformation and size on the burst release from poly (lactide-co-glycolide) microspheres. Journal of controlled release. 2005;110:34-48.

[43] Anderson JM, Rodriguez A, Chang DT. Foreign body reaction to biomaterials. Seminars in Immunology. 2008;20:86-100.

[44] Anderson JM. BIOLOGICAL RESPONSES TO MATERIALS. Annual Review of Materials Research. 2001;31:81-110.

[45] Frokjaer S, Otzen DE. Protein drug stability: a formulation challenge. Nature Reviews Drug Discovery. 2005;4:298-306.

[46] Schacht K, Scheibel T. Processing of recombinant spider silk proteins into tailor-made materials for biomaterials applications. Current Opinion in Biotechnology. 2014;29:62-9.

[47] Brown CP, Rosei F, Traversa E, Licoccia S. Spider silk as a load bearing biomaterial: tailoring mechanical properties via structural modifications. Nanoscale. 2011;3:870-6.

[48] Spiess K, Lammel A, Scheibel T. Recombinant Spider Silk Proteins for Applications in Biomaterials. Macromolecular Bioscience. 2010;10:998-1007.

[49] Vendrely C, Scheibel T. Biotechnological Production of Spider-Silk Proteins Enables New Applications. Macromolecular Bioscience. 2007;7:401-9.

[50] Gosline J, Guerette P, Ortlepp C, Savage K. The mechanical design of spider silks: from fibroin sequence to mechanical function. Journal of Experimental Biology. 1999;202:3295-303.

[51] Altman GH, Diaz F, Jakuba C, Calabro T, Horan RL, Chen J, et al. Silk-based biomaterials. Biomaterials. 2003;24:401-16.

[52] Vollrath F, Barth P, Basedow A, Engström W, List H. Local tolerance to spider silks and protein polymers in vivo. In vivo (Athens, Greece). 2001;16:229-34.

[53] Newman J, Newman C. Oh what a tangled web: the medicinal uses of spider silk. International Journal of Dermatology. 1995;34:290-2.

[54] Bon M. A discourse upon the usefulness of the silk of spiders. By Monsieur Bon, President of the Court of Accounts, Aydes and Finances, and President of the Royal Society of Sciences at Montpellier. Communicated by the author. Philosophical Transactions. 1710;27:2-16.

[55] Hennecke K, Redeker J, Kuhbier JW, Strauss S, Allmeling C, Kasper C, et al. Bundles of spider silk, braided into sutures, resist basic cyclic tests: Potential use for flexor tendon repair. PloS one. 2013;8:e61100.

[56] Kuhbier JW, Reimers K, Kasper C, Allmeling C, Hillmer A, Menger B, et al. First investigation of spider silk as a braided microsurgical suture. J Biomed Mater Res B Appl Biomater. 2011;97:381-7.

[57] Allmeling C, Jokuszies A, Reimers K, Kall S, Choi CY, Brandes G, et al. Spider silk fibres in artificial nerve constructs promote peripheral nerve regeneration. Cell Proliferation. 2008;41:408-20.

[58] Radtke C, Allmeling C, Waldmann K-H, Reimers K, Thies K, Schenk HC, et al. Spider silk constructs enhance axonal regeneration and remyelination in long nerve defects in sheep. PloS one. 2011;6:e16990.

[59] Doblhofer E, Heidebrecht A, Scheibel T. To spin or not to spin: spider silk

fibers and more. Appl Microbiol Biotechnol. 2015;99:9361-80.

[60] Hardy JG, Scheibel TR. Composite materials based on silk proteins. Progress in Polymer Science. 2010;35:1093-115.

[61] Huemmerich D, Helsen CW, Quedzuweit S, Oschmann J, Rudolph R, Scheibel T. Primary Structure Elements of Spider Dragline Silks and Their Contribution to Protein Solubility†. Biochemistry. 2004;43:13604-12.

[62] Schmidt M, Römer L, Strehle M, Scheibel T. Conquering isoleucine auxotrophy of Escherichia coli BLR(DE3) to recombinantly produce spider silk proteins in minimal media. Biotechnol Lett. 2007;29:1741-4.

[63] Heidebrecht A, Scheibel T. Recombinant production of spider silk proteins. Adv Appl Microbiol. 2013;82:115-53.

[64] Numata K, Kaplan DL. Silk-based delivery systems of bioactive molecules. Advanced Drug Delivery Reviews. 2010;62:1497-508.

[65] Lammel A, Schwab M, Hofer M, Winter G, Scheibel T. Recombinant spider silk particles as drug delivery vehicles. Biomaterials. 2011;32:2233-40.

[66] Hofer M. Development of spider silk protein particles for pharmaceutical applications. Dissertation, LMU, 2013.

[67] Hofer M, Winter G, Myschik J. Recombinant spider silk particles for controlled delivery of protein drugs. Biomaterials. 2012;33:1554-62.

[68] Blüm C, Nichtl A, Scheibel T. Spider silk capsules as protective reaction containers for enzymes. Advanced Functional Materials. 2014;24:763-8.

[69] Blüm C, Scheibel T. Control of drug loading and release properties of spider silk sub-microparticles. BioNanoScience. 2012;2:67-74.

[70] Numata K, Reagan MR, Goldstein RH, Rosenblatt M, Kaplan DL. Spider silk-based gene carriers for tumor cell-specific delivery. Bioconjugate chemistry. 2011;22:1605-10.

[71] Zeplin PH, Maksimovikj NC, Jordan MC, Nickel J, Lang G, Leimer AH, et al. Spider Silk Coatings as a Bioshield to Reduce Periprosthetic Fibrous Capsule Formation. Advanced Functional Materials. 2014;24:2658-66.

[72] Müller-Herrmann S, Scheibel T. Enzymatic degradation of films, particles and non-woven meshes made of a recombinant spider silk protein. ACS Biomaterials Science & Engineering. 2015;1:247-59.

[73] Scheibel T. Spider silks: recombinant synthesis, assembly, spinning, and engineering of synthetic proteins. Microbial Cell Factories. 2004;3:14.

[74] Gosline JM, DeMont ME, Denny MW. The structure and properties of spider silk. Endeavour. 1986;10:37-43.

[75] Vollrath F. Spider webs and silks. Scientific American. 1992;266:70-6.

[76] Vollrath F. Strength and structure of spiders' silks. Reviews in Molecular Biotechnology. 2000;74:67-83.

[77] Omenetto FG, Kaplan DL. New Opportunities for an Ancient Material. Science. 2010;329:528-31.

[78] Hardy JG, Scheibel TR. Production and processing of spider silk proteins. Journal of Polymer Science Part A: Polymer Chemistry. 2009;47:3957-63.

[79] Colgin MA, Lewis RV. Spider minor ampullate silk proteins contain new repetitive sequences and highly conserved non-silk-like “spacer regions”. Protein Science. 1998;7:667-72.

[80] Hayashi CY, Lewis RV. Spider flagelliform silk: lessons in protein design, gene structure, and molecular evolution. Bioessays. 2001;23:750-6.

[81] Lewis RV, Hinman M, Kothakota S, Fournier MJ. Expression and purification of a spider silk protein: a new strategy for producing repetitive proteins. Protein expression and purification. 1996;7:400-6.

[82] Simmons A, Ray E, Jelinski LW. Solid-state 13C NMR of Nephila clavipes dragline silk establishes structure and identity of crystalline regions. Macromolecules. 1994;27:5235-7.

[83] Parkhe AD, Seeley SK, Gardner K, Thompson L, Lewis RV. Structural studies of spider silk proteins in the fiber. Journal of Molecular Recognition. 1997;10:1-6.

[84] Hinman MB, Jones JA, Lewis RV. Synthetic spider silk: a modular fiber. Trends in biotechnology. 2000;18:374-9.

[85] Hayashi CY, Shipley NH, Lewis RV. Hypotheses that correlate the sequence, structure, and mechanical properties of spider silk proteins. International Journal of Biological Macromolecules. 1999;24:271-5.

[86] Van Beek J, Hess S, Vollrath F, Meier B. The molecular structure of spider dragline silk: folding and orientation of the protein backbone. Proceedings of the National Academy of Sciences. 2002;99:10266-71.

[87] Bram A, Bränden C, Craig C, Snigireva I, Riekel C. X-ray diffraction from single fibres of spider silk. Journal of applied crystallography. 1997;30:390-2.

[88] Dong Z, Lewis RV, Middaugh CR. Molecular mechanism of spider silk elasticity. Archives of biochemistry and biophysics. 1991;284:53-7.

[89] Fahnestock SR, Yao Z, Bedzyk LA. Microbial production of spider silk proteins. Reviews in Molecular Biotechnology. 2000;74:105-19.

[90] Gatesy J, Hayashi C, Motriuk D, Woods J, Lewis R. Extreme diversity, conservation, and convergence of spider silk fibroin sequences. Science. 2001;291:2603-5.

[91] Winkler S, Kaplan DL. Molecular biology of spider silk. Reviews in Molecular Biotechnology. 2000;74:85-93.

[92] Guerette PA, Ginzinger DG, Weber BH, Gosline JM. Silk properties determined by gland-specific expression of a spider fibroin gene family. Science. 1996;272-112.

[93] Lazaris A, Arcidiacono S, Huang Y, Zhou J-F, Duguay F, Chretien N, et al. Spider silk fibers spun from soluble recombinant silk produced in mammalian cells. science. 2002;295:472-6.

[94] Huemmerich D, Helsen CW, Quedzuweit S, Oschmann J, Rudolph R, Scheibel T. Primary Structure Elements of Spider Dragline Silks and Their Contribution to Protein Solubility. Biochemistry. 2004;43:13604-12.

[95] Heim M, Keerl D, Scheibel T. Spider silk: from soluble protein to extraordinary fiber. Angewandte Chemie International Edition. 2009;48:3584-96.

[96] Hagn F, Eisoldt L, Hardy JG, Vendrely C, Coles M, Scheibel T, et al. A conserved spider silk domain acts as a molecular switch that controls fibre assembly. Nature. 2010;465:239-42.

[97] Jin H-J, Kaplan DL. Mechanism of silk processing in insects and spiders. Nature. 2003;424:1057-61.

[98] Vollrath F, Knight D, Hu X. Silk production in a spider involves acid bath treatment. Proceedings of the Royal Society of London B: Biological Sciences. 1998;265:817-20.

[99] Dicko C, Kenney JM, Knight D, Vollrath F. Transition to a β-sheet-rich structure in spidroin in vitro: the effects of pH and cations. Biochemistry. 2004;43:14080-7.

[100] Tillinghast EK, Chase S, Townley MA. Water extraction by the major ampullate duct during silk formation in the spider, Argiope aurantia Lucas. Journal of insect physiology. 1984;30:591-6.

[101] Hardy JG, Römer LM, Scheibel TR. Polymeric materials based on silk proteins. Polymer. 2008;49:4309-27.

[102] Rammensee S, Slotta U, Scheibel T, Bausch AR. Assembly mechanism of recombinant spider silk proteins. Proceedings of the National Academy of Sciences. 2008;105:6590-5.

[103] Yucel T, Lovett ML, Kaplan DL. Silk-based biomaterials for sustained drug delivery. Journal of Controlled Release. 2014;190:381-97.

[104] Vendrely C, Scheibel T. Biotechnological Production of Spider-Silk Proteins Enables New Applications. Macromolecular bioscience. 2007;7:401-9.

[105] Scheibel T. Modified spider silk proteins. U.S. Patent Application No. 11/991,037; 2006.

[106] Scheibel T, Huemmerich D, Ackerschott C. Recombinant spider silk proteins. U.S. Patent No. 7,754,851. 13 Jul. 2010; 2010.

[107] Spieß K, Wohlrab S, Scheibel T. Structural characterization and functionalization of engineered spider silk films. Soft Matter. 2010;6:4168-74.

[108] Wohlrab S, Müller S, Schmidt A, Neubauer S, Kessler H, Leal-Egaña A, et al. Cell adhesion and proliferation on RGD-modified recombinant spider silk proteins. Biomaterials. 2012;33:6650-9.

[109] Leal-Egaña A, Lang G, Mauerer C, Wickinghoff J, Weber M, Geimer S, et al. Interactions of fibroblasts with different morphologies made of an engineered spider silk protein. Advanced Engineering Materials. 2012;14:B67-B75.

[110] Bini E, Foo CWP, Huang J, Karageorgiou V, Kitchel B, Kaplan DL. RGD-functionalized bioengineered spider dragline silk biomaterial. Biomacromolecules. 2006;7:3139-45.

[111] Leal-Egaña A, Scheibel T. Interactions of cells with silk surfaces. Journal of Materials Chemistry. 2012;22:14330-6.

[112] Gomes S, Gallego-Llamas J, Leonor IB, Mano JF, Reis RL, Kaplan DL. Biological responses to spider silk-antibiotic fusion protein. Journal of tissue engineering and regenerative medicine. 2012;6:356-68.

[113] Gomes SC, Leonor IB, Mano JF, Reis RL, Kaplan DL. Antimicrobial functionalized genetically engineered spider silk. Biomaterials. 2011;32:4255-66.

[114] Currie HA, Deschaume O, Naik RR, Perry CC, Kaplan DL. Genetically engineered chimeric silk–silver binding proteins. Advanced functional materials. 2011;21:2889-95.

[115] Hermanson KD, Huemmerich D, Scheibel T, Bausch AR. Engineered microcapsules fabricated from reconstituted spider silk. Advanced Materials. 2007;19:1810-5.

[116] Schacht K, Vogt J, Scheibel T. Foams made of engineered recombinant spider silk proteins as 3D scaffolds for cell growth. ACS Biomaterials Science & Engineering. 2016;2:517-25.

[117] Schacht K, Scheibel T. Processing of recombinant spider silk proteins into tailor-made materials for biomaterials applications. Current opinion in biotechnology. 2014;29:62-9.

[118] Schacht K, Scheibel T. Controlled hydrogel formation of a recombinant spider silk protein. Biomacromolecules. 2011;12:2488-95.

[119] DeSimone E, Schacht K, Scheibel T. Cations influence the cross-linking of hydrogels made of recombinant, polyanionic spider silk proteins. Materials Letters. 2016;183:101-4.

[120] Slotta UK, Rammensee S, Gorb S, Scheibel T. An engineered spider silk protein forms microspheres. Angewandte Chemie International Edition. 2008;47:4592-4.

[121] Widhe M, Bysell H, Nystedt S, Schenning I, Malmsten M, Johansson J, et al. Recombinant spider silk as matrices for cell culture. Biomaterials. 2010;31:9575-85.

[122] Humenik M, Smith AM, Arndt S, Scheibel T. Ion and seed dependent fibril assembly of a spidroin core domain. Journal of Structural Biology. 2015;191:130-8.

[123] Humenik M, Magdeburg M, Scheibel T. Influence of repeat numbers on self-assembly rates of repetitive recombinant spider silk proteins. Journal of structural biology. 2014;186:431-7.

[124] Humenik M, Scheibel T. Nanomaterial building blocks based on spider silk–oligonucleotide conjugates. ACS nano. 2014;8:1342-9.

[125] Borkner CB, Elsner MB, Scheibel T. Coatings and Films Made of Silk Proteins. ACS Applied Materials & Interfaces. 2014;6:15611-25.

[126] Junghans F, Morawietz M, Conrad U, Scheibel T, Heilmann A, Spohn U. Preparation and mechanical properties of layers made of recombinant spider silk proteins and silk from silk worm. Appl Phys A. 2006;82:253-60.

[127] Kristina Spieß SWaTS. Structural characterization and functionalization of engineered spider silk film. Soft Matter. 2010;6:4168-74.

[128] Greving I, Cai M, Vollrath F, Schniepp HC. Shear-Induced Self-Assembly of Native Silk Proteins into Fibrils Studied by Atomic Force Microscopy. Biomacromolecules. 2012;13:676-82.

[129] Decher G. Fuzzy nanoassemblies: toward layered polymeric multicomposites. science. 1997;277:1232-7.

[130] Zasadzinski J, Viswanathan R, Madsen L, Garnaes J, Schwartz D. Langmuir-blodgett films. Science. 1994;263:1726-33.

[131] Agarwal VK. Langmuir-Blodgett Films. Physics Today. 1988;41:40-6.

[132] Greiner A, Wendorff JH. Electrospinning: a fascinating method for the preparation of ultrathin fibers. Angewandte Chemie International Edition.

2007;46:5670-703.

[133] Zhang F, Zuo B, Fan Z, Xie Z, Lu Q, Zhang X, et al. Mechanisms and control of silk-based electrospinning. Biomacromolecules. 2012;13:798-804.

[134] Zhang X, Reagan MR, Kaplan DL. Electrospun silk biomaterial scaffolds for regenerative medicine. Advanced drug delivery reviews. 2009;61:988-1006.

[135] Zhu J, Shao H, Hu X. Morphology and structure of electrospun mats from regenerated silk fibroin aqueous solutions with adjusting pH. International journal of biological macromolecules. 2007;41:469-74.

[136] Zhou S, Peng H, Yu X, Zheng X, Cui W, Zhang Z, et al. Preparation and characterization of a novel electrospun spider silk fibroin/poly (D, L-lactide) composite fiber. The Journal of Physical Chemistry B. 2008;112:11209-16.

[137] Park WH, Jeong L, Yoo DI, Hudson S. Effect of chitosan on morphology and conformation of electrospun silk fibroin nanofibers. Polymer. 2004;45:7151-7.

[138] Boccaccini A, Keim S, Ma R, Li Y, Zhitomirsky I. Electrophoretic deposition of biomaterials. Journal of the Royal Society Interface. 2010;7:S581-S613.

[139] Zhang Z, Jiang T, Ma K, Cai X, Zhou Y, Wang Y. Low temperature electrophoretic deposition of porous chitosan/silk fibroin composite coating for titanium biofunctionalization. Journal of Materials Chemistry. 2011;21:7705-13.

[140] Maniglio D, Bonani W, Bortoluzzi G, Servoli E, Motta A, Migliaresi C. Electrodeposition of silk fibroin on metal substrates. Journal of Bioactive and Compatible Polymers. 2010;25:441-54.

[141] del Campo A, Arzt E. Fabrication Approaches for Generating Complex Micro-

and Nanopatterns on Polymeric Surfaces. Chemical Reviews. 2008;108:911-45.

[142] Tawfick S, De Volder M, Copic D, Park SJ, Oliver CR, Polsen ES, et al. Engineering of Micro- and Nanostructured Surfaces with Anisotropic Geometries and Properties. Advanced Materials. 2012;24:1628-74.

[143] Hardy JG, Leal-Egaña A, Scheibel TR. Engineered Spider Silk Protein-Based Composites for Drug Delivery. Macromolecular Bioscience. 2013;13:1431-7.

[144] Agostini E, Winter G, Engert J. Water-based preparation of spider silk films as drug delivery matrices. Journal of Controlled Release. 2015;213:134-41.

[145] Kristina Spiess RE, Caroline D. Keenan, Jürgen Senker, Friedrich Kremer and Thomas Scheibel Impact of initial solvent on thermal stability and mechanical properties of recombinant spider silk films. J Mater Chem 2011;21:13594-604.

[146] Metwalli E, Slotta U, Darko C, Roth SV, Scheibel T, Papadakis CM. Structural changes of thin films from recombinant spider silk proteins upon post-treatment. Applied Physics A. 2007;89:655-61.

[147] Slotta U, Tammer M, Kremer F, Koelsch P, Scheibel T. Structural Analysis of Spider Silk Films. Supramolecular Chemistry. 2006;18:465-71.

[148] Chen X, Knight DP, Shao Z, Vollrath F. Conformation transition in silk protein films monitored by time-resolved Fourier transform infrared spectroscopy: effect of potassium ions on Nephila spidroin films. Biochemistry. 2002;41:14944-50.

[149] Stephens JS, Fahnestock SR, Farmer RS, Kiick KL, Chase DB, Rabolt JF. Effects of electrospinning and solution casting protocols on the secondary structure of a genetically engineered dragline spider silk analogue investigated via Fourier transform Raman spectroscopy. Biomacromolecules. 2005;6:1405-13.

[150] Young SL, Gupta M, Hanske C, Fery A, Scheibel T, Tsukruk VV. Utilizing conformational changes for patterning thin films of recombinant spider silk proteins. Biomacromolecules. 2012;13:3189-99.

[151] Wohlrab S, Spieß K, Scheibel T. Varying surface hydrophobicities of coatings made of recombinant spider silk proteins. Journal of Materials Chemistry. 2012;22:22050-4.

[152] Huemmerich D, Slotta U, Scheibel T. Processing and modification of films made from recombinant spider silk proteins. Appl Phys A. 2006;82:219-22.

[153] Hardy JG, Torres-Rendon JG, Leal-Egaña A, Walther A, Schlaad H, Cölfen H, et al. Biomineralization of engineered spider silk protein-based composite materials for bone tissue engineering. Materials. 2016;1:13-560.

[154] Borkner CB, Wohlrab S, Möller E, Lang G, Scheibel T. Surface modification of polymeric biomaterials using recombinant spider silk proteins. ACS Biomaterials Science & Engineering. 2016 (article ASAP).

[155] Technologies L. SilverXpress® Silver Staining Kit Protocol. 2012;Catalog number LC6100

[156] Winston PW, Bates DH. Saturated Solutions For the Control of Humidity in Biological Research. Ecology. 1960;41:232-7.

[157] Martin P. Neubauer CB, Elisa Agostini, Julia Engert, Thomas Scheibel and Andreas Fery. Micromechanical characterization of spider silk particles. Biomaterials Science. 2013; 1160:1165-1.

[158] Lucke M, Winter G, Engert J. The effect of steam sterilization on recombinant spider silk particles. International Journal of Pharmaceutics. 2015;481:125-31.

[159] Kevin D. Hermansona MBH, Thomas Scheibel and Andreas R. Bausch. Permeability of silk microcapsules made by the interfacial adsorption of protein. Physical Chemistry Chemical Physics. 2007;9:6442-6.

[160] Hofmann S, Wong Po Foo CT, Rossetti F, Textor M, Vunjak-Novakovic G, Kaplan DL, et al. Silk fibroin as an organic polymer for controlled drug delivery. Journal of Controlled Release. 2006;111:219-27.

[161] Hines DJ, Kaplan DL. Mechanisms of controlled release from silk fibroin films. Biomacromolecules. 2011;12:804-12.

[162] Lu S, Wang X, Lu Q, Zhang X, Kluge JA, Uppal N, et al. Insoluble and flexible silk films containing glycerol. Biomacromolecules. 2010;11:143-50.

[163] Wilson D, Valluzzi R, Kaplan D. Conformational Transitions in Model Silk Peptides. Biophysical Journal.78:2690-701.

[164] Park K. Controlled drug delivery systems: Past forward and future back. Journal of Controlled Release. 2014;190:3-8.

[165] Higuchi T. Mechanism of sustained-action medication. Theoretical analysis of rate of release of solid drugs dispersed in solid matrices. Journal of Pharmaceutical Sciences. 1963;52:1145-9.

[166] Peppas NA, Narasimhan B. Mathematical models in drug delivery: How modeling has shaped the way we design new drug delivery systems. Journal of Controlled Release. 2014;190:75-81.

[167] Fu K, Pack DW, Klibanov AM, Langer R. Visual Evidence of Acidic Environment Within Degrading Poly(lactic-co-glycolic acid) (PLGA) Microspheres. Pharm Res. 2000;17:100-6.

[168] Schwendeman SP, Shah RB, Bailey BA, Schwendeman AS. Injectable controlled release depots for large molecules. Journal of Controlled Release. 2014;190:240-53.

[169] Nair LS, Laurencin CT. Biodegradable polymers as biomaterials. Progress in Polymer Science. 2007;32:762-98.

[170] Franz S, Rammelt S, Scharnweber D, Simon JC. Immune responses to implants – A review of the implications for the design of immunomodulatory biomaterials. Biomaterials. 2011;32:6692-709.

[171] Pamula E, Menaszek E. In vitro and in vivo degradation of poly(l-lactide-co-glycolide) films and scaffolds. Journal of Materials Science: Materials in Medicine. 2008;19:2063-70.

[172] Lu L, Peter SJ, D. Lyman M, Lai H-L, Leite SM, Tamada JA, et al. In vitro and in vivo degradation of porous poly(dl-lactic-co-glycolic acid) foams. Biomaterials. 2000;21:1837-45.

[173] Jin HJ, Park J, Karageorgiou V, Kim UJ, Valluzzi R, Cebe P, et al. Water-Stable Silk Films with Reduced β-Sheet Content. Advanced Functional Materials. 2005;15:1241-7.

[174] Lawrence BD, Wharram S, Kluge JA, Leisk GG, Omenetto FG, Rosenblatt MI, et al. Effect of Hydration on Silk Film Material Properties. Macromolecular Bioscience. 2010;10:393-403.

[175] Lammel AS, Hu X, Park S-H, Kaplan DL, Scheibel TR. Controlling silk fibroin particle features for drug delivery. Biomaterials. 2010;31:4583-91.

[176] Lammel A, Schwab M, Slotta U, Winter G, Scheibel T. Processing Conditions

for the Formation of Spider Silk Microspheres. ChemSusChem. 2008;1:413-6.

[177] Lu Q, Wang X, Hu X, Cebe P, Omenetto F, Kaplan DL. Stabilization and Release of Enzymes from Silk Films. Macromolecular Bioscience. 2010;10:359-68.

[178] Wenk E, Wandrey AJ, Merkle HP, Meinel L. Silk fibroin spheres as a platform for controlled drug delivery. Journal of Controlled Release. 2008;132:26-34.

[179] Taketani I, Nakayama S, Nagare S, Senna M. The secondary structure control of silk fibroin thin films by post treatment. Applied Surface Science. 2005;244:623-6.

[180] Nogueira GM, Rodas ACD, Leite CAP, Giles C, Higa OZ, Polakiewicz B, et al. Preparation and characterization of ethanol-treated silk fibroin dense membranes for biomaterials application using waste silk fibers as raw material. Bioresource Technology. 2010;101:8446-51.

[181] Chen X, Shao Z, Knight DP, Vollrath F. Conformation transition kinetics of Bombyx mori silk protein. Proteins: Structure, Function, and Bioinformatics. 2007;68:223-31.

[182] EMA. Decision tree for the selection of sterilization methods (CPMP/QWP/054/98). 2000.

[183] Menzen T, Friess W, Niessner R, Haisch C. Laser-induced breakdown detection of temperature-ramp generated aggregates of therapeutic monoclonal antibody. European Journal of Pharmaceutics and Biopharmaceutics. 2015;94:463-7.

[184] Menzen T, Friess W. Temperature-Ramped Studies on the Aggregation, Unfolding, and Interaction of a Therapeutic Monoclonal Antibody. Journal of

Pharmaceutical Sciences. 2014;103:445-55.

[185] Menzen T, Friess W. High-throughput melting-temperature analysis of a monoclonal antibody by differential scanning fluorimetry in the presence of surfactants. Journal of Pharmaceutical Sciences. 2013;102:415-28.

[186] Hino T, Tanimoto M, Shimabayashi S. Change in secondary structure of silk fibroin during preparation of its microspheres by spray-drying and exposure to humid atmosphere. Journal of Colloid and Interface Science. 2003;266:68-73.

[187] Hu X, Shmelev K, Sun L, Gil E-S, Park S-H, Cebe P, et al. Regulation of Silk Material Structure by Temperature-Controlled Water Vapor Annealing. Biomacromolecules. 2011;12:1686-96.

[188] Rattenholl A, Lilie H, Grossmann A, Stern A, Schwarz E, Rudolph R. The pro-sequence facilitates folding of human nerve growth factor from Escherichia coli inclusion bodies. European Journal of Biochemistry. 2001;268:3296-303.

[189] Lai P, Everett R, Wang F-F, Arakawa T, Goldwasser E. Structural characterization of human erythropoietin. Journal of Biological Chemistry. 1986;261:3116-21.

[190] Greene L, Shooter E. The nerve growth factor: biochemistry, synthesis, and mechanism of action. Annual review of neuroscience. 1980;3:353-402.

[191] Lee AC, Yu VM, Lowe JB, Brenner MJ, Hunter DA, Mackinnon SE, et al. Controlled release of nerve growth factor enhances sciatic nerve regeneration. Experimental neurology. 2003;184:295-303.

[192] Micera A, Vigneti E, Pickholtz D, Reich R, Pappo O, Bonini S, et al. Nerve growth factor displays stimulatory effects on human skin and lung fibroblasts,

demonstrating a direct role for this factor in tissue repair. Proceedings of the National Academy of Sciences. 2001;98:6162-7.

[193] Jorgensen L, Bennedsen P, Hoffmann SV, Krogh RL, Pinholt C, Groenning M, et al. Adsorption of insulin with varying self-association profiles to a solid Teflon surface—Influence on protein structure, fibrillation tendency and thermal stability. European Journal of Pharmaceutical Sciences. 2011;42:509-16.

[194] Vermeer AWP, Giacomelli CE, Norde W. Adsorption of IgG onto hydrophobic teflon. Differences between the Fab and Fc domains. Biochimica et Biophysica Acta (BBA) - General Subjects. 2001;1526:61-9.

[195] Bee JS, Randolph TW, Carpenter JF, Bishop SM, Dimitrova MN. Effects of surfaces and leachables on the stability of biopharmaceuticals. Journal of Pharmaceutical Sciences. 2011;100:4158-70.

[196] Bittner B, Morlock M, Koll H, Winter G, Kissel T. Recombinant human erythropoietin (rhEPO) loaded poly(lactide-co-glycolide) microspheres: influence of the encapsulation technique and polymer purity on microsphere characteristics. European Journal of Pharmaceutics and Biopharmaceutics. 1998;45:295-305.

[197] Morlock M, Kissel T, Li YX, Koll H, Winter G. Erythropoietin loaded microspheres prepared from biodegradable LPLG–PEO–LPLG triblock copolymers: protein stabilization and in-vitro release properties. Journal of Controlled Release. 1998;56:105-15.

[198] Morlock M, Koll H, Winter G, Kissel T. Microencapsulation of rh-erythropoietin, using biodegradable poly(d,l-lactide-co-glycolide): protein stability and the effects of stabilizing excipients. European Journal of Pharmaceutics and Biopharmaceutics. 1997;43:29-36.

[199] Siepmann J, Peppas NA. Higuchi equation: Derivation, applications, use and misuse. International Journal of Pharmaceutics. 2011;418:6-12.